


GEOLOGI FOR SAMFUNNET

GEOLOGY FOR SOCIETY



Rapport nr.: 2014.035		ISSN 0800-3416	Gradering: Åpen
Tittel: Hydrochemical data report from sampling of polymetallic mines in Zabaikalskii Krai, eastern Siberia, Russian Federation			
Forfatter: Banks, D., Karnachuk, O.V., Kadnikov, V.V., Watts, M., Boyce, A., Ivashenko, D.A., Filenko, R.A., Danilova, E.V., Pimenov, N.V., Gundersen, P.		Oppdragsgiver: Tomsk State University (Russia), University of Glasgow (UK), D Banks Geoenvironmental Services (UK), British Geological Survey (UK)	
Fylke: Russian Federation		Kommune: Zabaikalskii Krai	
Kartblad (M=1:250.000)		Kartbladnr. og -navn (M=1:50.000)	
Forekomstens navn og koordinater: Sherlovaya Gora, Akatui, Balei, Zhireken		Sidetall: 102	Pris: 200
Feltarbeid utført: August 2014	Rapportdato: 27/11/2015	Prosjektnr.: 346000	Ansvarlig: 
Sammendrag: This report documents the hydrochemical and stable isotope (^{18}O , ^2H , $^{34}\text{SO}_4^-$) analyses performed on water samples and stable isotope analyses (^{34}S and $^{34}\text{SO}_4^-$) performed on mineral samples, all collected during a field expedition during July / August 2014 to several metal sulphide mining sites in the Zabaikalsk polymetallic province of south-eastern Siberia. Water samples collected from the Sherlovaya Gora (Schorl Mountain) polymetallic/greisen deposit (rich in Be, F, B, W, Sn, Bi, Mo, Fe, As, Pb, Zn, Cu and S) exhibited field pH values as low as 2.5. The waters were all extremely impacted by sulphide oxidation processes, containing between 3 and 16 g/L sulphate, up to 0.47 g/L Al, 1.9 g/L Fe, 0.75 g/L Mn, 3.6 g/L Zn. Waters also contained up to 80 mg/L Cu, 49 mg/L As, 38 mg/L Cd, 2.5 mg/L Th and 2.3 mg/L U. Beryllium concentrations reach several hundred $\mu\text{g/L}$ and exceed 0.5 mg/L in one borehole. Conversely, tungsten and tin remain below analytical detection limits in the waters. The variation in concentrations of some elements (chloride, uranium) suggests that the water in the opencast pit lake and (especially) the tailings area pond, have been strongly concentrated by evaporation in the extreme summer heat. This interpretation is supported by ^{18}O and ^2H trajectories. At Novii Akatui Pb-Zn(-Ag) mine, water emerges at pH 7.15 and a temperature of 2.8°C from flooded underground workings. The water contains extremely low chloride concentrations (0.6 to 0.9 mg/L) characteristic of continental Central Asia. It also contains some 223 mg/L sulphate and 2.7 mg/L Zn. Iron concentrations are modest at 0.14 mg/L. It is likely that interaction with carbonate-rich host-rocks has maintained the mine water at a high pH and alkalinity (3.6 meq/L) and suppressed iron solubility. As the mine water traverses the large tailings areas it gradually acquires sulphate and the alkalinity decreases, suggesting that leachate from the tailings are adding acid sulphide weathering products to the water (and pyrite is visible in the tailings). Arsenic concentrations in the Akatui water vary from 53 to 246 $\mu\text{g/L}$. Samples from Balei (gold) and Zhireken (molybdenite) mines are also documented, as is a CO_2 -effervescent water from Bazanovskii borehole, near Akatui.			
Emneord: Geokjemi	Hydrogeologi	Borebrønn	
Grunnvannskvalitet	Stabile isotoper	Sur gruveavrenning	
Malm	Sulfidisotoper		

CONTENTS

1	INTRODUCTION.....	5
1.1	PREVIOUS STUDIES AND SAMPLING ACTIVITIES	5
1.2	SAMPLING ACTIVITIES - AUGUST 2014.....	6
2	SAMPLING AND ANALYSIS ROUTINES: YEAR 2014	10
2.1	MINE WATER AND GROUNDWATER SAMPLING	10
2.2	FIELD MEASUREMENTS	11
2.3	ANALYSIS AT BRITISH GEOLOGICAL SURVEY	11
3	SHERLOVAYA GORA (ШЕРЛОВАЯ ГОРА)	12
3.1	LOCATION AND DESCRIPTION	12
3.2	SAMPLES	15
3.3	FIELD MEASUREMENTS	17
3.4	RESULTS: LABORATORY CHEMICAL ANALYSIS OF WATER SAMPLES	20
3.5	RESULTS: LABORATORY STABLE ISOTOPE ANALYSIS OF WATER SAMPLES.....	21
3.6	RESULTS: LABORATORY SULPHUR ISOTOPE ANALYSIS OF MINERAL SAMPLES	23
3.7	RESULTS: LABORATORY SULPHUR ISOTOPE ANALYSIS OF WATER SAMPLES	23
3.8	SOURCES OF INFORMATION:	24
4	NOVII AKATUI (НОВИЙ АКАТУЙ).....	29
4.1	LOCATION AND DESCRIPTION	29
4.2	SAMPLES	31
4.3	FIELD MEASUREMENTS	36
4.4	RESULTS: LABORATORY CHEMICAL ANALYSIS OF WATER SAMPLES	39
4.5	RESULTS: LABORATORY STABLE ISOTOPE ANALYSIS OF WATER SAMPLES.....	42
4.6	RESULTS: LABORATORY SULPHUR ISOTOPE ANALYSIS OF MINERAL SAMPLES	42
4.7	SOURCES OF INFORMATION:	43
5	BAZANOVSKII (БАЗАНОВСКИЙ) BOREHOLE.....	44
5.1	LOCATION AND DESCRIPTION	44
5.2	SAMPLES	44
5.3	FIELD MEASUREMENTS	45
5.4	RESULTS: LABORATORY CHEMICAL ANALYSIS OF WATER SAMPLES	46
5.5	RESULTS: LABORATORY STABLE ISOTOPE ANALYSIS OF WATER SAMPLES.....	47
5.6	SOURCES OF INFORMATION:	47
6	BALEI (БАЛЕЙ)	49
6.1	LOCATION AND DESCRIPTION	49
6.2	SAMPLES	50
6.3	FIELD MEASUREMENTS	53
6.4	RESULTS: LABORATORY CHEMICAL ANALYSIS OF WATER SAMPLES	54
6.5	RESULTS: LABORATORY SULPHUR ISOTOPE ANALYSIS OF SULPHATE SAMPLES.....	55
6.6	SOURCES OF INFORMATION:	55
7	ZHIREKEN (ЖИРЕКЕН).....	56
7.1	LOCATION AND DESCRIPTION	56
7.2	SAMPLES	57

7.3	FIELD MEASUREMENTS	58
7.4	RESULTS: LABORATORY CHEMICAL ANALYSIS OF WATER SAMPLES	58
7.5	RESULTS: LABORATORY SULPHUR ISOTOPE ANALYSIS OF MINERAL SAMPLES	59
7.6	SOURCES OF INFORMATION:	60
8	SUMMARY	61
8.1	SULPHUR ISOTOPES	62
9	REFERENCES.....	64
10	APPENDIX A: REPORT BY D.A. IVASENKO ON SAMPLING AND ANALYSIS (BY TOMSK STATE UNIVERSITY) BY ICP-MS, SCANNING ELECTRON MICROSCOPE / ENERGY DISPERSIVE X-RAY SPECTROSCOPY (SEM-EDS) AND X-RAY DIFFRACTION (XRD) METHODS	67

1 INTRODUCTION

1.1 Previous studies and sampling activities

Tomsk State University (TGU) has long enjoyed informal yet fruitful collaboration in the field of hydrochemistry with Norges geologiske undersøkelse (NGU) and Holymoer Consultancy (UK), now trading as D Banks Geoenvironmental Services. This collaboration initially supported a joint project between TGU and the Khakassian State Committee for Environmental Protection (SCEP) to produce the geological section of an "Environmental Atlas of Khakassia". This period of collaboration resulted in the following publications:

- Parnachev, V.P., Banks, D. & Berezovsky, A.Y. (1997).** The anionic composition of groundwaters in extensional tectonic environments: the Shira Region, Khakassia, southern Siberia. *Norges geologiske undersøkelse Bulletin* 433, 62-63.
- Parnachev, V.P., Khromikh, V.C., Kopilova, Y.G., Tanzibaev, M.G., Polozhii, A.V., Kurbatskii, V.I., Makarenko, N.A., Vidrina, S.N., Zarubina, R.F., Kallas, E.V., Kulizhskii, S.P., Naumova, E.G., Smetanina, I.V., Solovyeva, T.P. (1998a).** *Otsenka sostoyaniya prirodnykh resursov i sozdanie ekologicheskogo atlasa territorii Respubliki Khakassia (Otchet ob itogakh vipolneniya khozdogovornikh rabot po teme No. 277 za 1997 god)*. TGU/Tomsk 1998, 129 pp.
- Parnachev, V.P., Khromikh, V.C., Kopilova, Y.G., Tanzibaev, M.G., Kurbatskii, V.I., Makarenko, N.A., Zarubina, R.F., Kulizhskii, S.P., Petrov, A.I., Smetanina, I.V., Panteleev, M.M., Sai, M.V., Arkhipov, A.L., Polekh, N.V. (1998b).** *Otsenka sostoyaniya prirodnykh resursov i sozdanie ekologicheskogo atlasa territorii Respubliki Khakassia (Otchet ob itogakh vipolneniya khozdogovornikh rabot po teme No. 277 za pervoe polugodie 1998 goda)*. TGU/Tomsk 1998, 120 pp.
- Parnachev, V.P., Banks, D., Berezovsky, A.Y. & Garbe-Schönberg, D. (1999).** Hydrochemical evolution of Na-SO₄-Cl groundwaters in a cold, semi-arid region of southern Siberia. *Hydrogeology Journal*, 7, 546-560.
- Parnachev, V.P., Makarenko, N.A., Kopilova, Y.G., Tanzibaev, M.G., Kulizhskii, S.P., Petrov, A.I., Zarubina, R.F., Smetanina, I.V., Arkhipov, A.L., Arkhipova, N.V. (2000).** *Otsenka sostoyaniya prirodnykh resursov i sozdanie ekologicheskogo atlasa territorii Respubliki Khakassia (Otchet ob itogakh vipolneniya khozdogovornikh rabot. po teme No. 277 za 1999 god)*. TGU/Tomsk 2000, 142 pp.
- Banks, D., Parnachev, V.P., Frengstad, B., Holden, W., Karnachuk, O.V. & Vedernikov, A.A. (2004).** The evolution of alkaline, saline ground- and surface waters in the southern Siberian steppes. *Applied Geochemistry* 19, 1905-1926.

and the following NGU Reports

- Banks, D., Parnachev, V.P., Berezovsky, A.Y., & Garbe-Schönberg, D. (1998).** The hydrochemistry of the Shira region, Republic of Khakassia, southern Siberia, Russian Federation - data report. **Nor. Geol. Unders. report** 98.090.
- Banks, D., Parnachev, V.P., Frengstad, B., Holden, W., Karnachuk, O.V. & Vedernikov, A.A. (2001).** The hydrogeochemistry of the Altaiskii, Askizskii, Beiskii, Bogradskii, Shirinskii, Tashtipskii & Ust' Abakanskii Regions, Republic of Khakassia, Southern Siberia, Russian Federation, data report. **Nor. Geol. Unders. report** 2001.006, 45 pp. + appendices.
- Banks, D., Parnachev, V.P., Frengstad, B., & Karnachuk, O.V. (2008).** Hydrogeochemical data report: the sampling of selected locations in the Republic of Khakassia, Kuznetsk Alatau oblast' and Kemerovo oblast', Southern Siberia, Russian Federation. **Nor. Geol. Unders. report** 2008.013, 60 pp. + appendices.

In more recent years, the focus has been transferred to new projects: in particular, (i) a series of projects involving the characterisation of microbial communities in mine waters, mine wastes and oil boreholes, managed by Prof. Olga V. Karnachuk (Dept. of Plant Physiology and Biotechnology, Tomsk State University), and (ii) a project between Professor Valerii P. Parnachev (Department of Dynamic Geology, TGU) and the Tomsk Oblast' Committee for Ecology, to produce an atlas and characterisation of water quality in Tomsk Oblast'. Results of this period of work have been presented in the following NGU Reports and publications:

- Banks, D., Parnachev, V.P., Frengstad, B., & Karnachuk, O.V. (2008).** Hydrogeochemical data report: the sampling of selected locations in the Republic of Khakassia, Kuznetsk Alatau oblast' and Kemerovo oblast', Southern Siberia, Russian Federation. **Nor. Geol. Unders. report** 2008.013, 60 pp. + appendices.
- Karnachuk, O.V., Gerasimchuk, A.L., Banks, D., Frengstad, B., Stykon, G.A., Tikhonova, Z.L., Kaksonen, A., Puhakka, J., Yanenko, A.S. & Pimenov, N.V. (2009).** Bacteria of the sulfur cycle in the sediments of gold mine tailings, Kuznetsk Basin, Russia (Бактерий цикла серы в осадках хвостохранилища добычи золота в кузбассе). **Microbiology** 78 (4), 483–491. Published in Russian in *Mikrobiologiya*, 78 (4), 535–544.
- Banks, D., Parnachev, V.P., Karnachuk, O.V., Arkhipov, A.L., Gundersen, P. & Davis, J. (2011).** Hydrogeochemical data report: the sampling of selected localities in Kemerovo oblast' and Tomsk oblast', Siberia, Russian Federation. **Nor. Geol. Unders. report** 2011.054, 69 pp. + appendices.
- Banks, D., Frank, Y.A., Kadnikov, V.V., Karnachuk, O.V., Watts, M., Boyce, A. & Frengstad, B.S. (2014).** Hydrochemical data report from sampling of two deep abandoned hydrocarbon exploration wells: Byelii Yar and Parabel', Tomsk oblast', western Siberia, Russian Federation. **Nor. Geol. Unders. report** 2014.034, 44 pp.

1.2 Sampling activities - August 2014

This report documents the most recent round of field work, in the period 27th July - 1st August 2014, carried out by:

- Prof. Olga V. Karnachuk and Prof. Marc Solioz (Dept. of Plant Physiology and Biotechnology, Tomsk State University).
- Dr Vitalii V. Kadnikov (Bioengineering Centre of the Russian Academy of Sciences, Moscow),
- David Banks (University of Glasgow and D Banks Geoenvironmental Services, UK),
- Dr Nikolai V. Pimenov (Vinogradsky Institute of Microbiology, Russian Academy of Sciences, Moscow).
- Denis A. Ivasenko (Dept. of Plant Physiology and Biotechnology, Tomsk State University)
- Roman A. Filenko (Institute of Natural Resources, Ecology and Cryology, Siberian Branch, Russian Academy of Sciences, Chita, Russia)
- Erzhena V. Danilova (Institute of General and Experimental Biology, Siberian Branch, Russian Academy of Sciences, Ulan-Ude, Russia).

Sampling was carried out of mine waters at four mining sites in Zabaikalsk Krai in eastern Siberia (Figure 1.1):

- The Sherlovaya Gora [Шерловая Гора] polymetallic opencast mine and tailings area, an area historically worked also for topaz, beryl (aquamarine and heliodor) and tourmaline. The name translates as Schorl Mountain and is located around 25 km NW of the town of Borzya and 250 km SE of the city of Chita.
- The Novii Akatui [Новый Акатуй] underground mine and tailings area, located around 18 km NW of Aleksandrovskii Zavod and 310 km ESE of Chita.
- The mines of Balei [Балей] and their tailings areas, located around 46 km S of Nerchinsk and 220 km ESE of Chita.
- The opencast molybdenite (MoS_2) mine and tailings area of Zhireken [Жирекен], located around 110 km NE of Nerchinsk and 280 km ENE of Chita.

The TGU Department of Plant Physiology and Biotechnology is currently engaged in a research project to characterise the microbiota able to tolerate the extreme conditions encountered in some of these mine waters. Additionally, groundwater samples were also taken from

- a borehole at Bazanovskii, some 15 km WNW of Aleksandrovskii Zavod and 13 km SSW of Novii Akatui. The water here overflowed under artesian pressure, was extremely cold and effervesced with carbon dioxide.

During the sampling of July/August 2014, alkalinity, pH, temperature and (where meaningful) Eh were measured in the field at all sites.

Field-filtered (0.45 µm) samples of water were returned to the United Kingdom for analysis by:

- Inductively Coupled Plasma Mass Spectrometry (ICP-MS) at the British Geological Survey, Keyworth, Nottinghamshire.
- Ion Chromatography (IC) methods at the British Geological Survey, Keyworth, Nottinghamshire.
- ¹⁸O and ²H stable isotopic determinations at the laboratory of NERC Isotope Community Support Facility, Scottish Universities' Environmental Research Centre (SUERC), Rankine Avenue, East Kilbride, G75 0QF.

Solid samples of:

- Mineral phases, especially primary sulphide or secondary sulphate phases
- Barium sulphate precipitate, derived from adding barium chloride solution to sulphate-rich mine waters

were also returned to the NERC isotope facility of SUERC for stable isotopic determinations of ³⁴S.

Dr Michael Watts and his staff at the British Geological Survey and Professor Adrian Boyce of SUERC / University of Glasgow are gratefully thanked for providing these analyses.

In addition, Tomsk State University collected samples of water and precipitates from the various sample locations for analysis by ICP-MS, SEM-EDS and XRD methods. These results are documented separately in a report by D.A. Ivasenko, forming Appendix A of this report.

This report is intended to document the raw data produced during the study, together with a limited degree of interpretation. This raw data report will form the documentation basis for scientific papers interpreting the data collected during the study.



Figure 1.1. Map of Zabaikalskii Krai, by Nzeemin [CC-BY-SA-3.0 (<http://creativecommons.org/licenses/by-sa/3.0>)], via Wikimedia Commons. Sampling locations are shown.

2 SAMPLING AND ANALYSIS ROUTINES: YEAR 2014

The sites sampled in July / August 2014 are detailed in Sections 3 to 7 of this Report.

2.1 Mine Water and Groundwater Sampling

Groundwater samples were taken at the wellhead of the Bazanovskii flowing artesian borehole. The borehole overflows continuously, so no “purging” was required. Field measurements were made in a container continuously being replenished by the overflowing water.

Groundwater / minewater samples were taken from shallow boreholes (most likely aborted blasting boreholes, or possibly exploration boreholes) in a bench of the opencast quarry at Sherlovaya Gora. The water in these boreholes may represent a mixture of (a) groundwater contaminated by the oxidation products of sulphide minerals and (b) surface water run-in to the boreholes. The replenishment rate of the boreholes was so low that they could not realistically be purged. The water samples thus represent the water found in the boreholes on arrival. The water was extracted using a bailer comprising a cut-off bottled water flask on a cable. Field measurements were made in the bailer immediately on removal from the borehole.

The other minewater samples were collected either from pit lakes and tailings ponds, or from flowing minewater. In all cases, water samples were collected from a short distance (c. 5 cm) below the water surface, and field measurements were also made by submerging the relevant probes to a depth of c. 10 cm.

Water samples for analysis in the UK were filtered on site using a 0.45 µm filter capsule, mounted on a polypropylene hand-held syringe.

For each sample, the following aliquots were taken:

- 1 x 30 ml and 1 x 15 mL polyethene flasks, of water filtered at 0.45 µm, using a Millipore filter capsule and hand-held polypropene syringe. No acidification was carried out in the field. These samples were carried in baggage to the UK and delivered to the British Geological Survey. Except during periods of transport, samples were stored in the dark at c. 4°C. The 30 mL flask was used for ion chromatography analysis and the 15 mL flask for ICP-MS.
- 1 x 15 ml polyethene flask, completely filled with water, filtered at 0.45 µm, using a Millipore filter capsule and hand-held polypropene syringe. Sample flask sealed

additionally at neck with “Parafilm[®]” to hinder any leakage or evaporative losses. These samples were carried in baggage to the UK and delivered to SUERC. Except during periods of transport, samples were stored in the dark at c. 4°C.

- In some cases, a selection of samples for bacteriological analysis at TGU and additional chemical analysis at Russian organisations.

2.2 Field Measurements

Field determinations included:

- determination of alkalinity (by average of multiple determinations, typically three determinations) using a standard solution of 0.05 N HCl, prepared by TGU’s Department for Plant Physiology and Biotechnology, an indicator comprising Hach bromocresol green / methyl red powder portioned in foil pillows (with an end point, in the region 4.3 to 4.6, depending on the alkalinity value, giving a measure of t-alkalinity), and a sampling syringe / container from the AquaMerck 11109 alkalinity test kit. This arrangement was due to strict air carriage regulations prohibiting carriage of acid and indicators in flammable organic solutions by aircraft from the UK.
- pH, Eh and temperature (T) using TGU Department for Plant Physiology and Biotechnology’s Hanna Instruments HI8314 pH meter, regularly calibrated against solutions of known pH around 4, 7 or 10 as appropriate. Measurements were manually corrected for drift (assumed to be linear with time) on the basis of daily calibrations. The pH value was automatically temperature-compensated by the meter.

2.3 Analysis at British Geological Survey

Samples (for each sample 1 x 15 mL and 1 x 30 mL aliquot of filtered water) were transported by David Banks to the laboratory of the British Geological Survey at Keyworth, Nottingham. Prior to analysis, samples were stored in a refrigerator at around +4°C, except for brief periods of transport.

Analytical procedures at the British Geological Survey. are broadly identical to those documented in **NGU Report 2014.034** (Banks et al. 2014).

The 15 mL flasks were used for ICP-MS analysis. The samples were acidified with 1% v/v HNO₃ and 0.5% v/v HCl prior to analysis. The highly concentrated mine water samples were diluted, as appropriate, prior to analysis. These dilution factors are reflected in the cited detection limits.

The 30 mL samples were used, following appropriate dilution, dependent on total dissolved solids, for the ion chromatography determination.

3 SHERLOVAYA GORA (ШЕРЛОВАЯ ГОРА)

3.1 Location and Description

The name Sherlovaya Gora translates as “Schorl Mountain” and is located around 24 km NW of the town of Borzya and 250 km SE of the city of Chita. The deposit is located in association with a Jurassic (Kozlov, 2009) pegmatitic granite inlier, forming a cluster of low hills (up to c. 1000 m asl), surrounded by the plains of the Onon and Borzya Rivers. The inlier is surrounded by clastic and volcanoclastic rocks (slates/shales and sandstones) of Lower Carboniferous age.

The mining area can be subdivided into two sub-areas:

- (i) the original gemstone mining area, a greisen deposit, associated with a dome leucogranite in the hills of the western part of the area. This is also associated with tungsten and bismuth mineralisation. The granite is regarded by Kozlov (2009) as being associated with the Jurassic Kukul’bei Complex (although other sources - Webmineral, 2014 - rather dubiously cite a Palaeozoic age for the granite).
- (ii) the eastern area, associated with eruptive and subvolcanic quartz and felsite porphyries (ongonites¹), hosting the main cassiterite and polymetallic sulphide ore bodies, and recently worked via a large opencast. The eruptive/subvolcanic phase is believed to be later than the granite intrusion: Webmineral (2014) suggests that it is of Early Cretaceous age.

The sampling activity described in this report focussed on the latter, eastern polymetallic area.

The western Aquamarine-Topaz Greisen area

The Sherlovaya Gora gemstone deposit is associated with a greisenised² granite dome, and was first mentioned in records in 1721-1723 (Kozlov, 2009), but was probably known about long before that (Kokunin, 2006). Initially, the Sherlovaya Gora greisen deposit was worked on the southern slopes of the hill, from the 18th Century, for semi-precious stones such as:

- aquamarine and heliodor - blue and yellow varieties of beryl ($\text{Be}_3\text{Al}_2(\text{SiO}_3)_6$), respectively. High grade aquamarine was the most sought-after gem.
- topaz - $\text{Al}_2\text{SiO}_4(\text{F},\text{OH})_2$
- smoky quartz

¹ an ongonite is a topaz-rich quartz keratophyre; the subvolcanic equivalent of REE-, Li and F-rich granites

² a greisen is a -highly self-altered endoskarn granite or pegmatite, characterised by an abundance of hydrothermal minerals, e.g. tourmaline, beryl, topaz, fluorite etc.

- tourmaline, a crystalline borocyclosilicate, of which schorl is one variety: $(\text{Ca,K,Na})(\text{Al,Fe,Li,Mg,Mn})_3(\text{Al,Cr,Fe,V})_6(\text{BO}_3)_3(\text{Si,Al,B})_6\text{O}_{18}(\text{OH,F})_4$

According to Klopotow & Kantor (2014) and Webmineral (2014), the mineralised veins are enriched in W, F, B, Be and As and are also associated with pneumatolytic mineralisation such as:

- wolframite - $(\text{Fe,Mn})\text{WO}_4$, which is reported to have been worked from 1915-16, according to Klopotow & Kantor (2014).
- cassiterite - SnO_2 . According to Wikipedia (2014), cassiterite mining commenced at Sherlovaya Gora from 1928-32. Kozlov (2009) reports that rich cassiterite placers were being worked in the 1940s and 1950s within the dome area.
- molybdenite - MoS_2
- native bismuth and bismuthite - $\text{Bi}_2\text{CO}_3(\text{OH})_4$, which was also worked, from a later date than the wolframite.
- fluorite - CaF_2
- siderite and siderophyllite - $\text{KFe}^{\text{II}}_2\text{Al}(\text{Al}_2\text{Si}_2)\text{O}_{10}(\text{F,OH})_2$

Local inhabitants still sporadically work the shallow underground mine workings in the original Sherlovaya Gora gemstone deposit.

The eastern Polymetallic Ore area

According to Kozlov (2006), the Academician S.S. Smirnov discovered a large cassiterite-polymetallic sulphide ore body in the quartz porphyry (ongonite) zone in the 1930s. In the upper part of the ore body, oxidised ores predominate, including cassiterite (SnO_2) and iron oxyhydroxides, yielding a reddish hue. At greater depth, the polymetallic sulphide ores occur, exploited via progressively deeper opencasting since the 1970s.

Among the sulphide minerals associated with Sherlovaya Gora are:

- pyrites, FeS_2 , pyrrhotite, $\text{Fe}_{(1-x)}\text{S}$ ($x = 0$ to 0.2) and arsenopyrite (FeAsS)
- galena (PbS)
- sphalerite (ZnS),
- chalcopyrite (CuFeS_2)

According to Webmineral (2014), the polymetallic ores are associated with quartz, tourmaline, muscovite, chlorite, feldspar and also fluorite, native bismuth, bismuthinite (Bi_2S_3) and cosalite ($\text{Pb}_2\text{Bi}_2\text{S}_5$). The opencast metal mine was closed in c.1995.

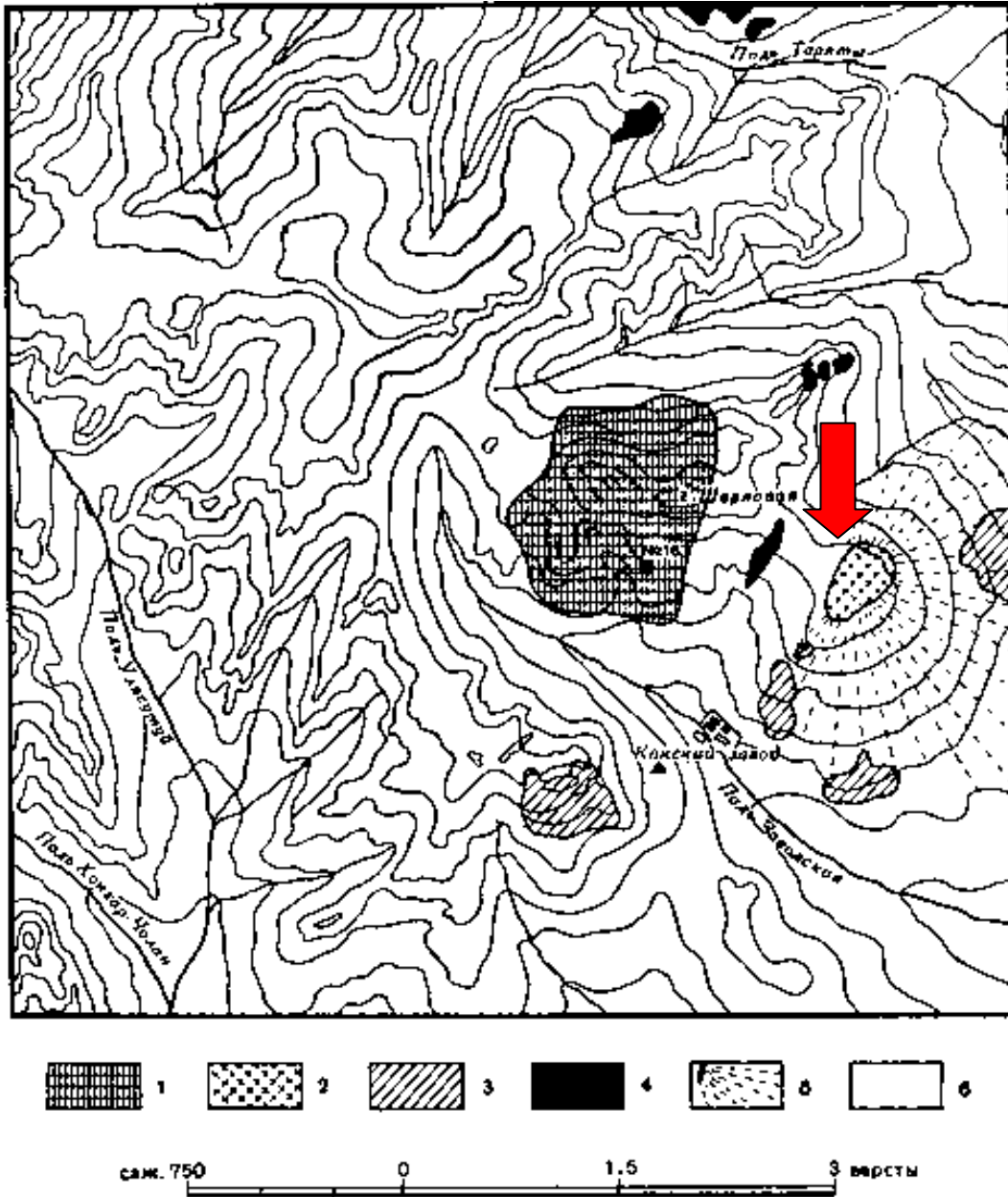


Figure 3.1. Geological map of Sherlovaya Gora (after P.P. Sushinskii, 1915), from the website of Klopotow & Kantor (2014). 1 = granite, 2 = quartz porphyry, 3 = felsitic porphyry, 4 = aplite, 5 = deposits/placers of quartz / felsite porphyry and eruptive breccia, 6 = slate/shale. No. 16 = the Millionaire Mine. The scale is in versts (1 verst = c. 1.067 km). Today's major opencast is in the porphyry area (indicated by red arrow) to the east of the beryl/topaz/tourmaline greisen/granite deposit.

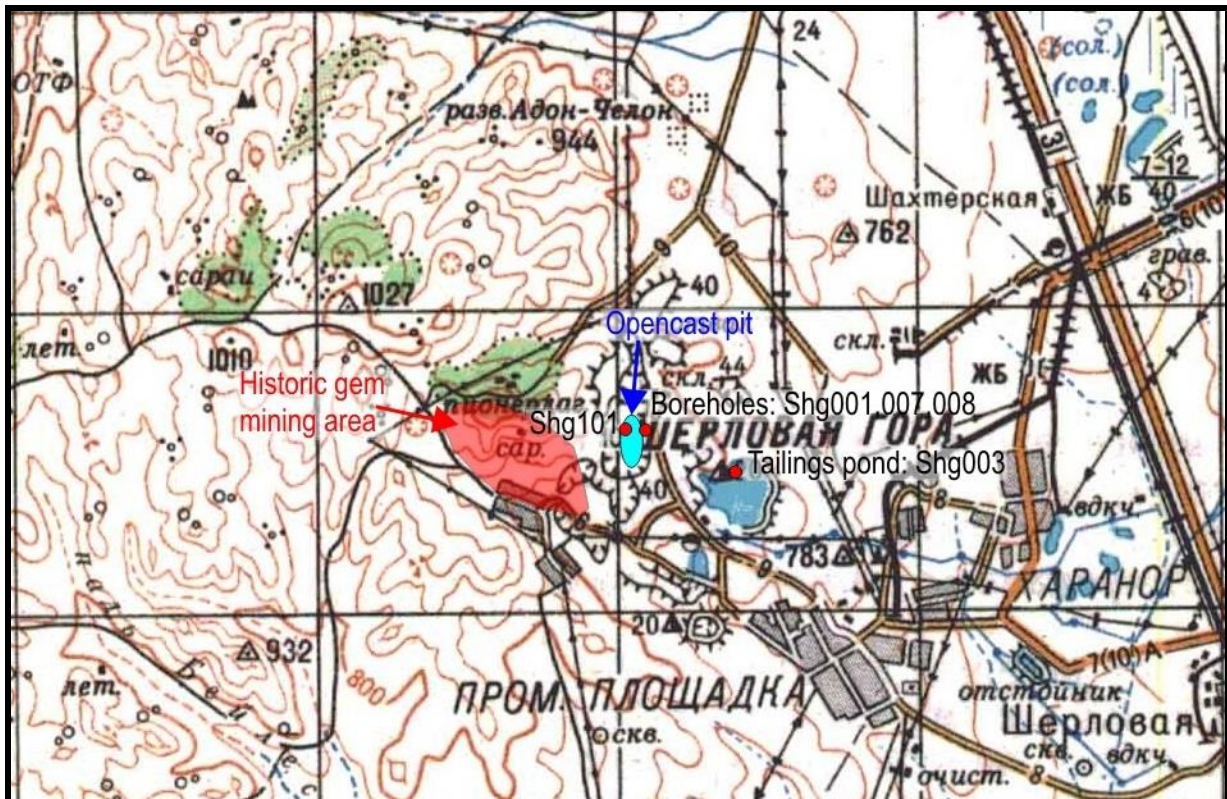


Figure 3.2. Extract of 1:200,000 map of Sherlovaya Gora (m-50-XV dated 1983). Each square is 4 km, north is vertically up the page. The pale blue ellipse shows the opencast pit lake. Shg101 is the sample of the pit lake water; Shg001, 007 and 008 are from boreholes drilled into an opencast bench; while Shg003 is a sample from a shallow area of ponded water in the tailings area.

3.2 Samples

Boreholes on Opencast Bench

The majority of the sampling activity took place on a bench of the opencast quarry, on the eastern side of the pit, where a number of shallow (c. 10 m) boreholes had been drilled into the floor of the bench. It is unclear whether these were drilled as exploration boreholes, or as unused shot holes for bench blasting.

Some of these boreholes were dry, while some contained a few metres of water, typically of pale yellow to orange colour and containing the products of sulphide oxidation. Surface water could be observed to run into several of the boreholes from the bench surface, and it is thought likely that, while a component of the water in the boreholes could be groundwater or interflow, a significant component could represent run-in from the contaminated (with sulphide oxidation minerals etc.) surface of the rock bench.

Water was extracted from the boreholes using an improvised bailer, comprising a plastic water bottle on the end of a rope. There was insufficient replenishment of water in the boreholes to realistically “purge” the boreholes, thus the samples should be regarded as water “as found” in the bores. pH, temperature and Eh were determined on the water samples immediately on extracting the water with the bailer, while water samples (filtered at 0.45µm) were taken from 3 of the boreholes.

- Sample Shg-01F from borehole 1 at 11.15 am on 27/7/14
- Sample Shg-01Fdup, duplicate sample from borehole 1 at 13.30 pm on 27/7/14
- Sample Shg-07F from borehole 6 on 30/7/14
- Sample Shg-08F from borehole 7 on 30/7/14

Aliquots (filtered) for ^2H and ^{18}O analysis were taken for Shg-01F (borehole 1) and Shg-07F (borehole 6).

A larger quantity of water was taken from borehole 1 for addition of barium chloride solution, for precipitation of aqueous sulphate as BaSO_4 and isotopic analysis of sulphate ^{34}S .

The sampled boreholes (1, 6 and 7) were among those exhibiting the lowest pH and most intense orange water colour. The numbering system for the boreholes was arbitrary.

The samples contained significant quantities of fine particulates / flocculates, necessitating the use of several filters at some boreholes.

Opencast Pit Lake

The water quality in the main opencast pit lake has also been measured at a sampling point on the NW shore. A single set of samples (Shg-101F) was taken of filtered water from just below the water surface around 1 m from the shore, comprising several aliquots.

An aliquot of water (filtered) for ^2H and ^{18}O analysis was also taken for Shg-101F, as was a larger quantity of water for addition of barium chloride solution, precipitation of aqueous sulphate as BaSO_4 and isotopic analysis of sulphate ^{34}S .

Ponded Water in Tailings Area

To the ESE of the main opencast is a large, now mainly dry, area where tailings have historically been deposited. An area of ponded water exists in one part of this area, and this was also subject to sampling.

A single set of samples (Shg-03F) was taken of filtered water from just below the water surface around 1 m from the shore, comprising several aliquots.

An aliquot of water (filtered) for ^2H and ^{18}O analysis was also taken for Shg-03F, as was a larger quantity of water for addition of barium chloride solution, precipitation of aqueous sulphate as BaSO_4 and isotopic analysis of sulphate ^{34}S .

Mineral samples

The following mineral samples were taken for sulphide ^{34}S isotopic analysis

- Shg-A: Near drilled bench in Sherlovaya Gora opencast. Primary sulphide (possibly arsenopyrite with some galena) mineralization. 27/07/2014
- Shg-B Near drilled bench in Sherlovaya Gora opencast. Primary sulphide mineralization. 27/07/2014
- Shg-C Sherlovaya Gora opencast. Primary sulphide (probably sphalerite) mineralisation. 27/07/2014

and the following mineral samples were taken for sulphate ^{34}S isotopic analysis

- SG-14-1-4 Near drilled bench, Sherlovaya Gora opencast. Secondary sulphate mineral - possibly epsomite, maybe gypsum. 27/07/2014

3.3 Field Measurements

The full set of field measurements is shown in Table 3.1. It will be seen that the pH of the borehole water was in the range 2.47 (borehole 1) to 4.03 (borehole 2). The waters were highly oxidised and the colour intensity of the water was inversely related to pH in most cases. The fact that the pH varied somewhat when boreholes were resampled on later dates suggests that the water is influenced by surface run-in, rather than just being a stable groundwater quality.

The ponded water in the tailings area had a consistent pH of just over 3.7, but its temperature was in the mid-20s°C when sampled, reflecting the very hot summer weather and intense sunshine during the sampling period. The water was relatively clear and colourless.

The water in the opencast pit lake also had a stable pH of around 2.9 and was also clear and colourless. The high temperature also reflects solar warming of the water surface.

Sample	Location	Date	pH	Eh	Temp.	t-alkalinity	Description
				mV	°C	meq/L	
Shg-01F	Sherlovaya Gora Borehole 1	27/07/2014 11.15 am	2.58	+494	6.6	0	Dark orange colour. Some Fe retained on filter.
Shg-01F dup	Sherlovaya Gora Borehole 1	27/07/2014 13.30 pm					Dark orange colour and more turbid. Some Fe and particulates retained on filter.
	Sherlovaya Gora Borehole 1	28/07/2014	2.47	+480	5.1		
	Sherlovaya Gora Borehole 2	27/07/2014	4.03	+436	6.4		Very slight yellow colour
	Sherlovaya Gora Borehole 3	27/07/2014	2.92	+453	6.0		Medium orange colour
	Sherlovaya Gora Borehole 4	27/07/2014	2.58	+548	6.9		Medium orange colour
	Sherlovaya Gora Borehole 5	27/07/2014	3.66	+431	6.8		Less orange colour
	Sherlovaya Gora Borehole 6	27/07/2014	3.34	+362	5.1		Little colour
Shg-07F	Sherlovaya Gora Borehole 6	30/07/2014	3.19	+365	4.4	0	Medium orange colour in bulk, but clear and colourless after filtration. Orange flocs retained on filter.
	Sherlovaya Gora Borehole 7	27/07/2014	3.66	+475	6.3		Fairly colourless
Shg-08F	Sherlovaya Gora Borehole 7	30/07/2014	2.65	+447	6.5	0	Pale yellow colour in bulk, but clear and v. pale yellow after filtration. Orange flocs retained on filter.
	Sherlovaya Gora Borehole 8	27/07/2014					Colourless
	Sherlovaya Gora Borehole 9	27/07/2014					Colourless
	Sherlovaya Gora Borehole 10	27/07/2014					Very pale yellow colour
	Sherlovaya Gora Borehole 11	27/07/2014					Colourless
Shg-03F	Sherlovaya Gora tailings pond	28/07/2014	3.73	+430	22.0	0	Clear colourless water. Small amount of precipitate on filter
Shg-03F	Sherlovaya Gora tailings pond	30/07/2014	3.75	+384	26.3		Clear colourless water. Little or no precipitate on filter
Shg-101-F	Opencast pit lake, Sherlovaya Gora	27/07/2014	2.90	+556	23.1	0	Water clear colourless. Iron precipitation on lake bed near shore
Shg-101-F	Opencast pit lake, Sherlovaya Gora	30/07/2014	2.90	+555	23.1	0	Water clear colourless. No precipitate on filter

Table 3.1. Summary of field measurements taken at the Sherlovaya Gora site. Note that the samples Shg-101F and Shg-03F for water chemical analysis were taken on 27th and 28th July respectively, while those for oxygen, hydrogen and sulphate isotope determination were taken on 30/7/14.

LIMS Code			13444-0001	13444-0002	13444-0007	13444-0008	13444-0011	13444-0003
Sample Code			Shg-01F	Shg-01F dup	Shg-07F	Shg-08F	Shg-101-F	Shg-03F
Date			27/7/14	27/7/14	30/7/14	30/7/14	27/7/14	28/7/14
		Detection limit	Borehole 1	Borehole 1	Borehole 6	Borehole 7	Opencast pit	Tailings pond
Field Measurements								
pH			2.58	2.58	3.19	2.65	2.90	3.73
Eh	mV		494	494	365	447	556	430
Temp	°C		6.6	6.6	4.4	6.5	23.1	22.0
Alkalinity	meq l ⁻¹		0.0	0.0	0.0	0.0	0.0	0.0
Anions								
Cl ⁻	mg l ⁻¹	<0.05	<50	<50	<20	<12.5	5.3	30
SO ₄ ²⁻	mg l ⁻¹	<0.05	15990	16352	6522	3631	2708	6288
NO ₃ ⁻	mg l ⁻¹	<0.03	<30	<30	<12	<7.5	<3.0	<7.5
Br ⁻	mg l ⁻¹	<0.01	<10	<10	<4.0	<2.5	<1.0	<2.5
HPO ₄ ²⁻	mg l ⁻¹	<0.01	11	<10	<4.0	<2.5	<1.0	<2.5
F ⁻	mg l ⁻¹	<0.01	13	14	<2.0	4.6	14	105
Cations and main metals								
Ca	mg/l	<855	<855	<855	<855	<855	<855	<855
Mg	mg/l	<65	381	380	391	151	214	477
Na	mg/l	<1000	<1000	<1000	<1000	<1000	<1000	<1000
K	mg/l	<135	<135	<135	<135	<135	<135	<135
Al	mg/l	<2.2	471	471	24.6	170	34.2	137
Fe	mg/l	<2.845	1898	1891	342	434	31.4	<2.845
Mn	mg/l	<0.435	734	751	584	48.7	91.1	275
Cu	mg/l	<0.325	80.9	79.4	0.668	6.67	3.81	14.3
Zn	mg/l	<0.6	3597	3621	1868	787	457	1394
S, Si & P								
P	mg/l	<13	13	14	<13	<13	<13	<13
S	mg/l	<4045	4410	4451	<4045	<4045	<4045	<4045
Si	mg/l	<63.3	<63.3	<63.3	<63.3	<63.3	<63.3	<63.3
Minor and Trace Elements								
Ag	µg/l	<225	<225	<225	<225	<225	<225	<225
As	µg/l	<60	48282	48698	121	3922	<60	81
B	µg/l	<32500	<32500	<32500	<32500	<32500	<32500	<32500
Ba	µg/l	<100	<100	<100	<100	<100	120	<100
Be	µg/l	<15	563	592	250	101	170	264
Cd	µg/l	<70	16023	16092	7131	34622	3328	38404
Cr	µg/l	<105	120	110	<105	204	<105	<105
Co	µg/l	<42	2596	2672	2766	1161	931	3744
Cs	µg/l	<6	10	14	23	9	24	20
Ga	µg/l	<665	<665	<665	<665	<665	<665	<665
Hf	µg/l	<5	7	7	<5	<5	<5	<5
Li	µg/l	<7250	<7250	<7250	<7250	<7250	<7250	<7250
Mo	µg/l	<18	229	74	<18	<18	<18	30
Nb	µg/l	<5	<5	<5	<5	<5	<5	<5
Ni	µg/l	<80	3467	3522	3121	1974	2776	13543
Pb	µg/l	<30	349	276	328	436	534	2399
Rb	µg/l	<16	32	28	196	<16	92	133
Sb	µg/l	<13	13	15	<13	<13	<13	<13
Se	µg/l	<330	<330	<330	<330	<330	<330	<330
Sn	µg/l	<280	<280	<280	<280	<280	<280	<280
Sr	µg/l	<135	666	562	1917	<135	1828	1036
Ta	µg/l	<4	<4	<4	<4	<4	<4	<4
Ti	µg/l	<150	<150	<150	<150	<150	<150	<150

Th	µg/l	<50	2328	2536	113	212	66	145
Tl	µg/l	<22	<22	<22	<22	<22	<22	<22
U	µg/l	<29	2287	2306	257	1286	148	805
V	µg/l	<1210	<1210	<1210	<1210	<1210	<1210	<1210
W	µg/l	<175	<175	<175	<175	<175	<175	<175
Zr	µg/l	<176	437	354	206	<176	<176	465
REE								
Y	µg/l	<6	6499	6518	1746	3849	619	4197
La	µg/l	<5	2694	2739	265	262	73	369
Ce	µg/l	<5	6177	6172	660	651	180	1118
Pr	µg/l	<4	752	743	78	92	26	218
Nd	µg/l	<80	2728	2645	284	394	<80	908
Sm	µg/l	<10	668	657	84	180	45	431
Eu	µg/l	<4	87	75	16	14	6	10
Tb	µg/l	<7	144	151	31	79	17	125
Gd	µg/l	<6	790	832	139	342	81	609
Dy	µg/l	<5	910	932	194	569	99	723
Ho	µg/l	<4	205	210	47	118	20	142
Er	µg/l	<5	634	628	143	359	54	414
Tm	µg/l	<4	87	90	19	51	9	59
Yb	µg/l	<5	589	592	107	314	47	305
Lu	µg/l	<3	82	86	18	44	7	45

Table 3.2. Laboratory chemical determinations (British Geological Survey) of water samples (filtered in the field at 0.45 µm) from Sherlovaya Gora. Anions (Cl⁻, SO₄²⁻, NO₃⁻, Br⁻, HPO₄²⁻, F⁻) analysed by ion chromatography, all other elements by ICP-MS. Field measurements included in uppermost rows for comparison. All samples were laboratory-diluted by a factor of 60000 prior to analysis by ICP-MS, hence the very high detection limits.

3.4 Results: Laboratory Chemical Analysis of Water Samples

The results of the laboratory chemical analyses performed by BGS are shown in Table 3.2. All samples were laboratory-diluted by a factor of 60000 prior to analysis by ICP-MS, hence the very high detection limits. The following should be noted:

- The duplicate samples from Borehole 1 show very good reproducibility, despite the fact that they are extracted by bailing 2 hours apart from each other.
- Chloride concentrations are generally low. This is presumed to reflect low chloride concentrations in precipitation in this extreme inland location.
- Chloride concentrations are six times higher in the very shallow tailings pond (30 mg/L) than in the opencast pit lake (5.3 mg/L). This may represent evapoconcentration of soluble salts in both open water bodies in the extremely hot summer climate. One might estimate that the shallow waters of the tailings pond are around 6x more evapoconcentrated than the deeper pit lake waters.
- It is noteworthy that a number of other elements show a similar evapoconcentration factor between the pit lake and the tailings pond (such as some of the REEs, uranium).
- The anion composition is dominated by sulphate, ranging from 3.6 to 16 g/L in the borehole waters, and 2.7 g/L and 6.3 g/L in the pit lake and tailings pond respectively.

This, together with the acid nature of the waters and extreme metal concentrations, illustrates the overwhelming dominance of sulphide oxidation processes in determining the chemical nature of the water.

- Extreme aluminium concentrations of several tens to several hundred mg/L of aluminium are observed, reflecting aluminosilicate hydrolysis in the extremely acidic environment, and the solubility of Al at low pH. The highest concentration is 471 mg/L in the lowest pH waters of Borehole 1.
- Extreme concentrations of many metals are also observed. The highest contents are typically observed in the low pH water of Borehole 1: for example; 1.9 g/L iron (although Fe is below detection limit in the higher pH waters of the tailings pond), 750 mg/L manganese; 80 mg/L copper, 3.6 g/L zinc, 2.3 mg/L uranium and a massive 2.5 mg/L thorium. 16 mg/L cadmium is observed in borehole 1 and almost 35 mg/L Cd in borehole 7.
- Despite its higher pH, the tailings pond exhibits elevated concentrations of some heavy metals, presumably reflecting evapoconcentrative processes: e.g. 2.4 mg/L lead (Pb), 13.5 mg/L nickel (Ni), 3.7 mg/L cobalt (Co), 38.4 mg/L cadmium (Cd).
- Arsenic is present in extreme quantities in borehole 1, of 48-49 mg/L.
- Other elements associated with the greisen mineralization are present in elevated quantities, including fluoride at 13-14 mg/L in borehole 1 and the pit lake and at 105 mg/L in the evapoconcentrated waters of the tailings pond; beryllium at several hundred µg/L and exceeding 0.5 mg/L in borehole 1.
- On the other hand, both tin and tungsten are generally below analytical detection limit in all samples, despite their known abundance in the ore mineralization. Tin has a generally very low environmental aqueous solubility, while tungsten is generally soluble at higher pH values (Frengstad et al. 2001).

3.5 Results: Laboratory Stable Isotope Analysis of Water Samples

Sample	Location	Sample date	$\delta^{18}\text{O}_{\text{smow}}$	$\delta^2\text{H}_{\text{smow}}$
Shg-01F	Sherlovaya Gora Borehole 1. 11.15 am	27/7/14	-13.1 ‰	-87.9 ‰
Shg-07F	Sherlovaya Gora Borehole 6	30/7/14	-12.8 ‰	-93.0 ‰
Shg-101F	Opencast pit lake, Sherlovaya Gora	30/7/14	-6.5 ‰	-69.8 ‰
Shg-03F	Sherlovaya Gora tailings pond	30/7/14	-2.0 ‰	-43.5 ‰

Table 3.3. Laboratory ^2H and ^{18}O determinations (SUERC) of water samples (filtered in the field at 0.45 µm) from Sherlovaya Gora. Job number 14-38-TOMSKOH.

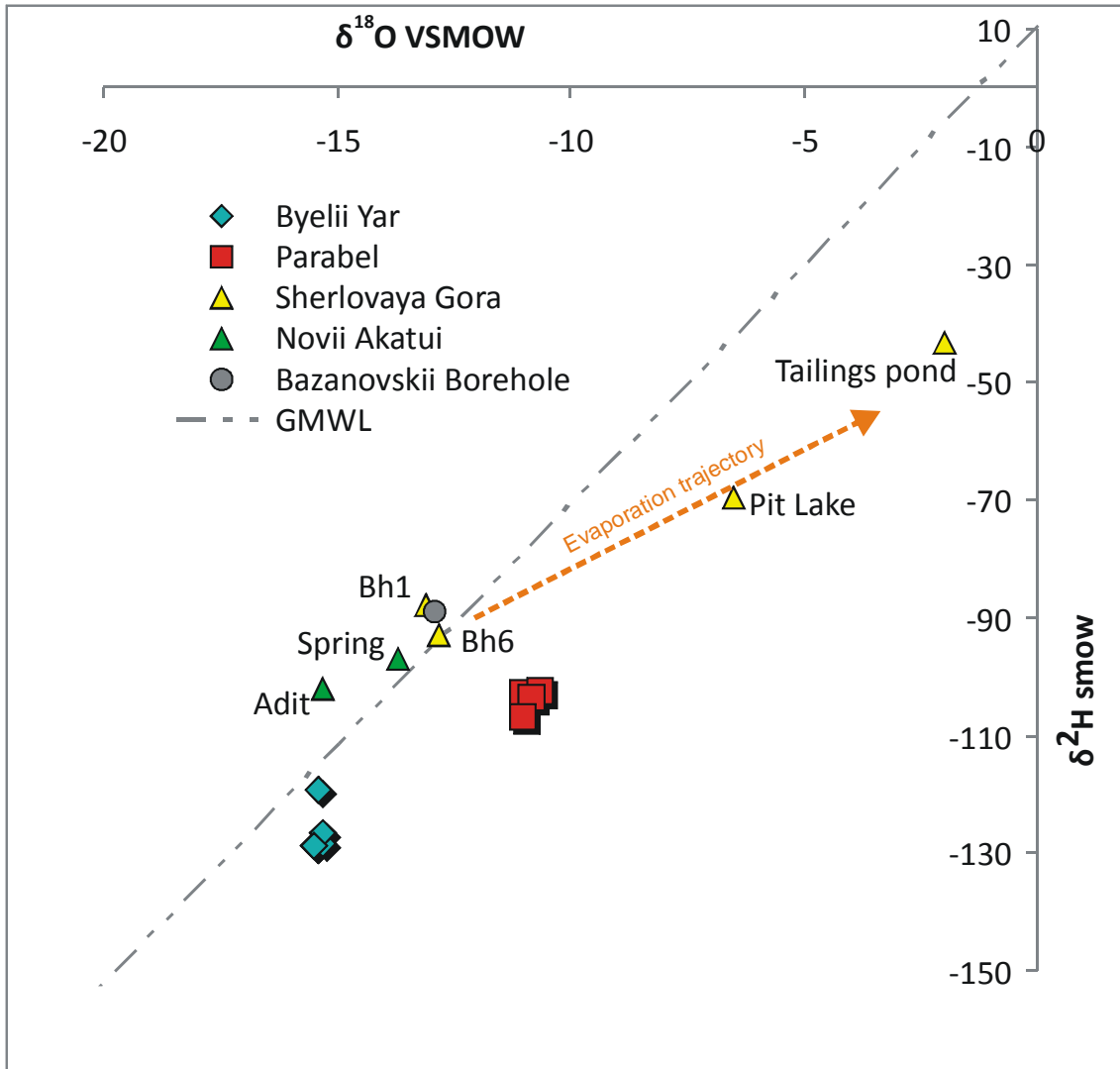


Figure 3.3. $\delta^{18}\text{O}$ vs $\delta^2\text{H}$ plot of water samples from this study, compared with deep borehole samples from Tomsk oblast' (Banks et al. 2014 - NGU report 2014-034). All values are in ‰. The Global Meteoric Water Line (GMWL) is defined as $\delta^2\text{H} = 8.13 * \delta^{18}\text{O} + 10.8$, after Clark & Fritz (1997).

The results of the laboratory ^2H and ^{18}O analyses performed by BGS are shown in Table 3.3 and are plotted on Figure 3.3. The following should be noted:

- The two borehole samples plot very close to the global meteoric water line (GMWL) as defined by the equation

$$\delta^2\text{H} = (8.13 * \delta^{18}\text{O}) + 10.8 \quad (\text{Clark \& Fritz 1997})$$

effectively confirming that they are derived from precipitation. The fact that most of the Zabaikalsk samples lie a little above the GMWL suggests that there is a local (arid zone) meteoric water line (LMWL) slightly enriched in ^2H relative to the GMWL (Banks, 2014; SAHRA, 2014).

- The pit lake and the tailings pond lie below the GMWL, but above and to the right of the borehole samples. This enrichment in both heavy isotopes, but preferentially in ^{18}O , is strongly indicative of evaporative upconcentration.

3.6 Results: Laboratory Sulphur Isotope Analysis of Mineral Samples

The following sulphur isotope results were obtained from SUERC for analysis of primary sulphide and sulphate minerals (Table 3.4):

Sample	Description	$\delta^{34}\text{S}_{\text{V-CDT}}$ (‰)
Sulphide mineralization		
Shg-A	Near drilled bench. Sherlovaya Gora opencast. Sulphide (possibly arsenopyrite with some galena) mineralisation	-2.1
Shg-B	Near drilled bench. Sherlovaya Gora opencast. Sulphide mineralisation	-1.9
Shg-C	Sherlovaya Gora opencast. Probably sphalerite mineralisation	-2.2
Sulphate mineralization		
SG14-1-4	Near drilled bench. Sherlovaya Gora opencast. Secondary sulphate mineral. Possibly epsomite, maybe gypsum	-8.4

Table 3.4. Laboratory ^{34}S determinations (SUERC) of primary sulphide and secondary(?) sulphate mineral samples from Sherlovaya Gora. Job number: 14-53-Banks.

The values of around -2‰ in the sulphides are compatible with a magmatic origin, but cannot be regarded as exclusively indicative of such an origin (Frietsch et al., 1995; Seal, 2006).

The sulphate mineralization has a much lower $\delta^{34}\text{S}$ value of -8.4‰.

3.7 Results: Laboratory Sulphur Isotope Analysis of Water Samples

Table 3.5 documents the sulphur isotope composition of the barium sulphate precipitated from the water samples.

Sample	Description	$\delta^{34}\text{S}_{\text{V-CDT}}$ (‰)
Shg-01	Water from Sherlovaya Gora borehole 1	-0.4
Shg-03	Ponded water, tailings area, Sherlovaya Gora	-2.2
Shg-101	Open cast pit lake, Sherlovaya Gora	-5.8

Table 3.5. Laboratory ^{34}S determinations (SUERC) of on barium sulphate precipitates derived from addition of excess barium chloride to water samples from Sherlovaya Gora. Job number: 14-53-Banks.

3.8 Sources of information:

- Wikipedia (2014). *Шерловая Гора*. Available at https://ru.wikipedia.org/wiki/Шерловая_Гора. Accessed November 2014.
- Klopotow, K.I. & Kantor, B.Z. (2014). *Шерлова гора*. Website: Минералы России. Available at http://klopotow.narod.ru/mindata/locathn/Chit_obl/zabaik/sherlov/fersman.htm, accessed November 2014.
- Kokunin M.V. [Кокунин М.В.] (2006). *История геологического изучения Шерловогорского месторождения берилла и топаза*. Website: Цветные камни Трансбайкальского региона. Available at <http://lavrovit.narod.ru/history/sherlovagora.htm>. Accessed November 2014.
- Kozlov, V.D. (2009). Rare-earth elements as indicators of ore sources and the degree of differentiation and ore potential of rare-metal granite intrusions (eastern Transbaikalia). *Russian Geology and Geophysics* **50**: 29-42. doi: 10.1016/j.rgg.2008.06.015.
- Webmineral (2014). *Шерловогорское месторождение, Борзинский район, Забайкальский край, Забайкалье, Россия*. Available at <http://webmineral.ru/deposits/item.php?id=1204>, accessed November 2014.



Figure 3.4. Sherlovaya Gora host rocks - porphyritic effusives (Photo by David Banks)



Figure 3.5. The polymetallic opencast at Sherlovaya Gora, seen from the north (Photo by David Banks)



Figure 3.6. Bench of the polymetallic opencast at Sherlovaya Gora, into which shallow boreholes had been drilled, and which were sampled for water (Photo by David Banks)



Figure 3.7. Borehole in bench of the polymetallic opencast at Sherlovaya Gora (Photo by David Banks)

Figure 3.8 (below) Sampling the ponded water at the tailings area (Shg-03) (Photo by David Banks).





Figure 3.8 (above). Filtering mine water samples to obtain microbiological samples (Photo by David Banks).



Figure 3.9 (left) Addition of barium chloride solution to Sherlovaya Gora opencast pit lake water (Shg-101) produces a white barium sulphate precipitate (Photo by David Banks).



Figure 3.10. The polymetallic opencast at Sherlovaya Gora, seen from sampling point for Shg-101, looking east. The red arrow indicates the bench into which the sampled boreholes were drilled. Note the iron oxyhydroxide staining of the lake bed near the shore (Photo by David Banks)

4 NOVII AKATUI (НОВИЙ АКАТУЙ)

4.1 Location and Description

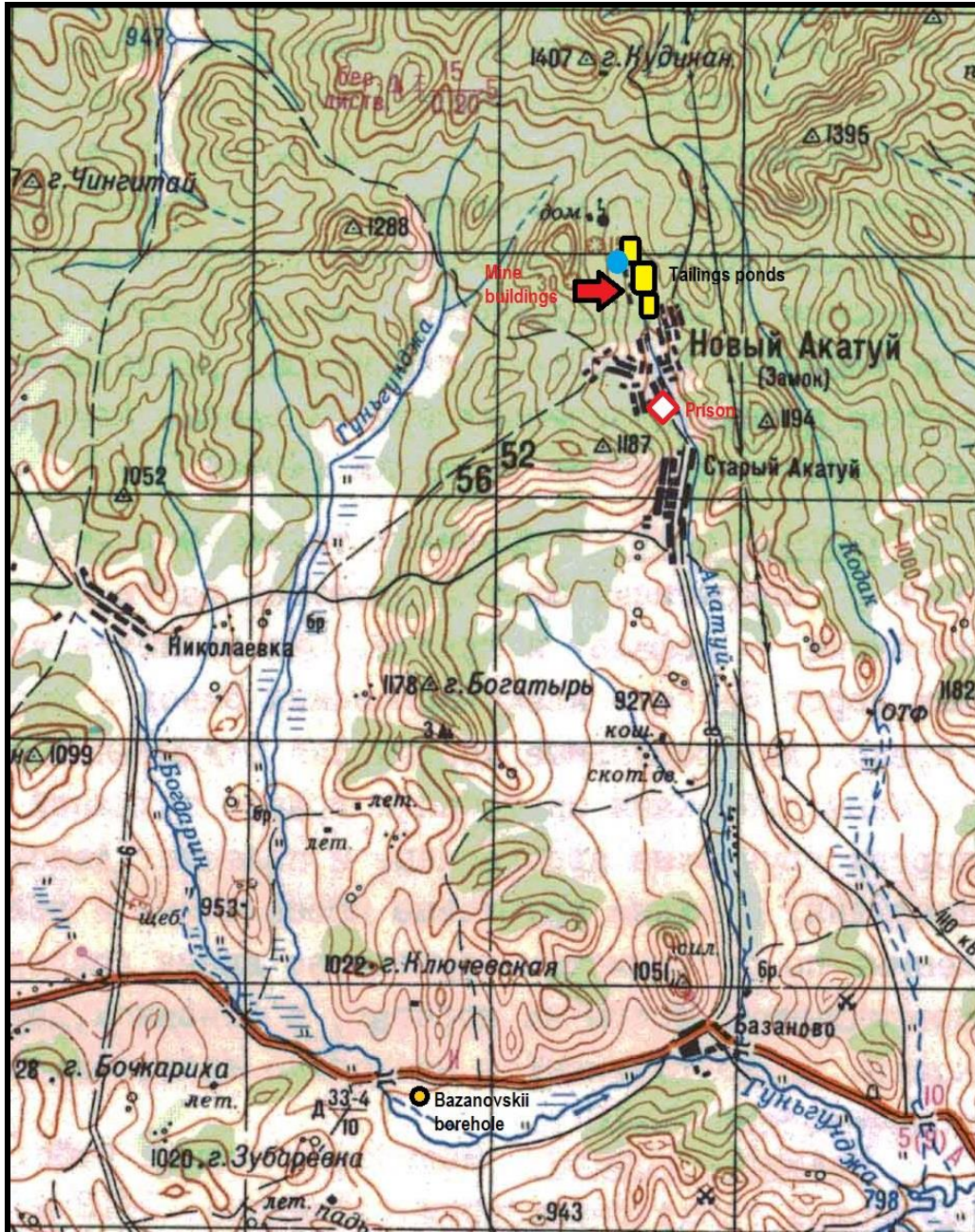


Figure 4.1. Extract of 1:200,000 map of Akatui (m-50-X dated 1989). Each square is 4 km, north is vertically up the page. The blue circle shows the approximate location of the mine water adit. The tailings areas are approximately indicated in yellow. The prison is shown as a red/white diamond, and the mine buildings by a red arrow. The Bazanovskii borehole (Chapter 5) is shown as a black/orange circle.

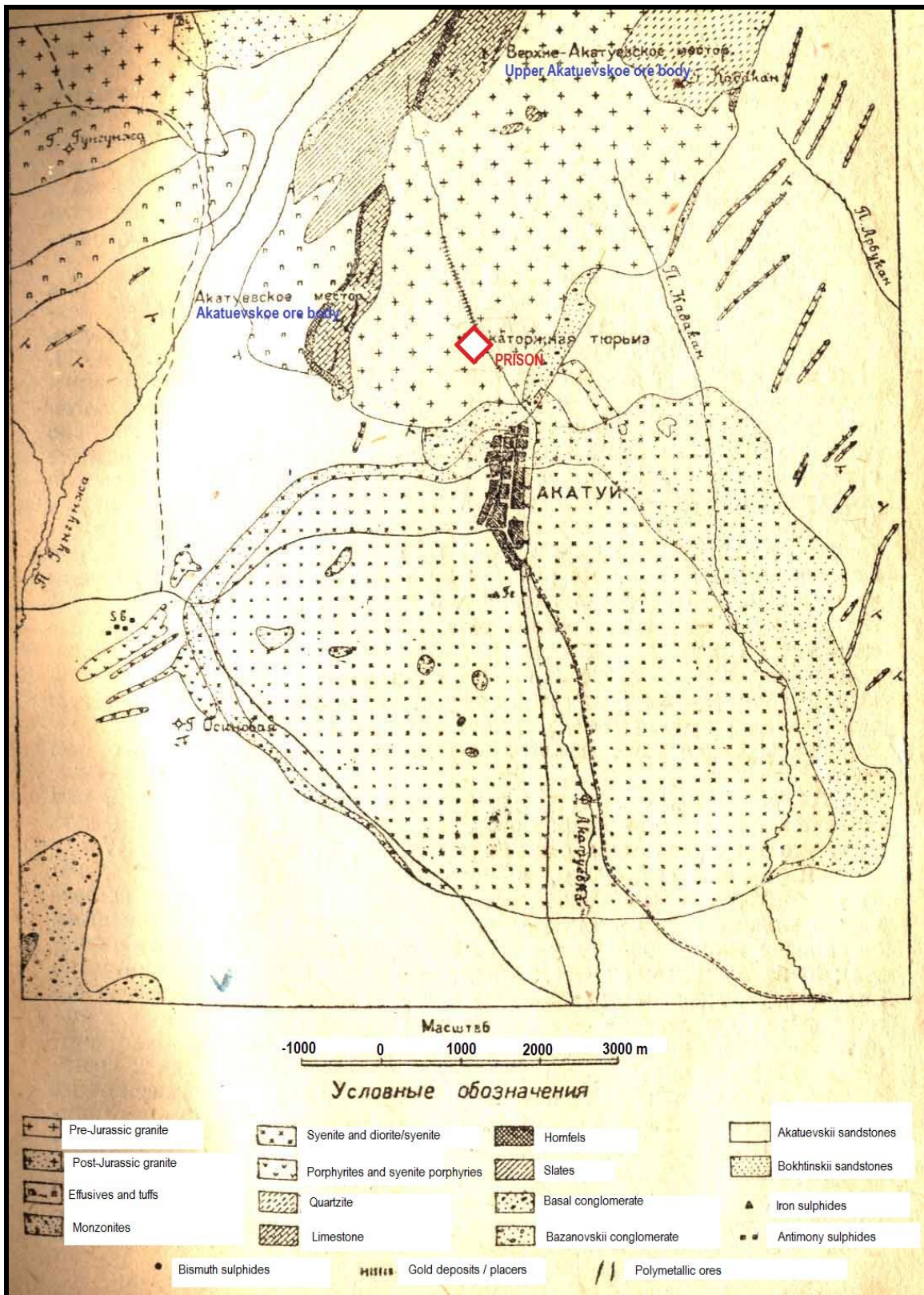


Figure 4.2. Historic geological map of Akatui (believed to be after S.S. Smirnov and downloaded from <http://lavrovit.narod.ru/maps/Rudnik.html>). The prison is shown as a red/white diamond while the sampled Novii Akatui mine is located in the area marked as Upper Akatuevskoe ore body.

According to Wikipedia (2014), a silver-lead sulphide ore was discovered at Akatui in 1815. From 1832 to 1917, the tsarist regime operated the Akatuiszkaya prison, which provided labour in the mines.

More recently, the skarn deposits associated with the contact zone between a granite intrusion and the carbonate country rocks have been exploited for Pb-Zn (sphalerite-galena) ores via underground mining. The deposit is associated with other sulphide minerals such as pyrite (which is found in high concentrations in the tailings) and chvilevite ($\text{Na}(\text{Cu,Fe,Zn})_2\text{S}_2$) (Dobrovolskaya 1996). The Novii (New) or Severo-(North) Akatui mine kept working until 1994 (Webmineral 2014). At present, the underground workings are flooded and overflow via a horizontal tunnel (adit) into the tailings area.

According to Zabaikalskii Krai (2014), the regional geology comprises Lower Palaeozoic (Cambrian) sedimentary and metamorphic rocks, intruded by lower Palaeozoic gabbros and diabases, late Palaeozoic granites and overlain by Lower Jurassic clastic sediments and later Jurassic volcanoclastic and effusive rocks. Widespread small Jurassic age intrusions also occur. The mineralisations largely occur along a strip 0.6 - 1.2 km in width extending SW-NE in carbonates and shales. The main ores are referred to as the Akatuevskoe and Upper / North Akatuevskoe ores and lie along the NW limb of an anticlinal structure, falling at around 60°. The ore deposits reported to be strongly oxidised to a depth of 100-240 m. The minerals present are:

- anglesite (PbSO_4)
- cerussite (PbCO_3)
- galena (PbS)
- sphalerite (ZnS)
- smithsonite (ZnCO_3)
- pyrite, arsenopyrite, pyrrhotite and boulangerite ($\text{Pb}_5\text{Sb}_4\text{S}_{11}$).
- the deposit also contains significant contents of Mn, As, Cd, In, Bi, Ag (up to 243 g/t) and Au (up to c. 2 g/t).

4.2 Samples

Water samples

The Novii Akatui site comprises three main levels of tailings deposits descending southwards along the head of the valley of the Akatui River, each with a retaining dam or embankment at its southern end. The upper tailings area was not observed to have any major flows of surface water across it when visited in July 2014, but was occupied by a lake of standing water.

A flow of mine water emerges from a major mine tunnel, dated 1959, from the west side of the valley, near the junction between the upper and middle tailings levels. Samples **Shg-05F** were taken from the mouth of the adit.



Figure 4.3. The flowing 1959 mine adit, from which samples Shg-05F were taken (Photo by David Banks)



Figure 4.4. The middle tailings level at Novii Akatui (Photo by David Banks)



Figure 4.5. Mine water flowing over the lower tailings level at Novii Akatui (sample Shg-06F). The dam at the foot of the middle level can be seen to the left (Photo by David Banks)



Figure 4.6. Poned mine water on the lower tailings level at Novii Akatui, looking north. The dam at the foot of the middle level can be seen at the rear of the pond (Photo by David Banks)



Figure 4.7. Seepage of water from foot of dam at base of lower tailings level at Novii Akatui (pH 6.7, +289 mV). (Photo by David Banks)



Figure 4.7. Spring at eastern end of foot of dam at base of lower tailings level at Novii Akatui (pH 6.7, +258 mV, samples Shg-04F). (Photo by David Banks)

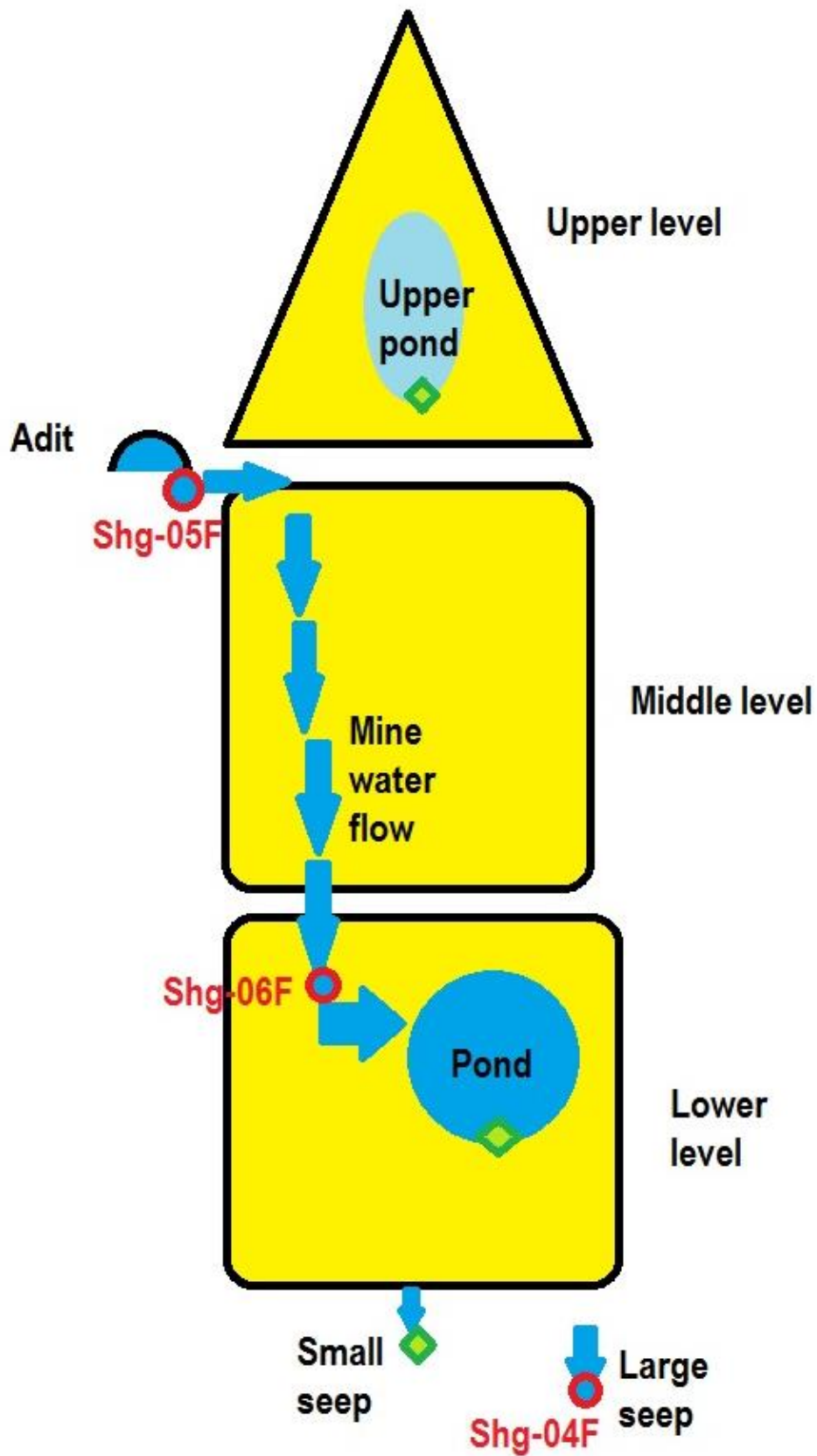


Figure 4.8. Schematic of the three tailings areas (yellow) at Novii Akatui. The red circles show sample locations, the green diamonds show locations of other field measurements. North is up the page.

The mine water flows down the embankment and across the middle level of tailings. It then flows down the embankment of the middle tailings level to the lowest tailings level. Here, samples **Shg-06F** were taken from the flowing mine water. At this location, where minerals had been sorted by the flowing water, the very high pyritiferous content of the tailings was clear to observe.

The minewater then ponded on the lower tailings level, with no surface water outlet. It is thus assumed that the minewater infiltrates vertically downward into the lower tailings body. Below the foot of the lowest tailings dam, a few seepages of water emerge, the largest of which was sampled (**Shg-04F**).

Mineral samples

Two samples of primary sulphide were collected from Novii Akatui:

- Shg-Ei Pyrite/chalcopyrite from tailings area. 29/07/2014
- Shg-Eii Sphalerite with small crystals of pyrite. 29/07/2014

4.3 Field Measurements

The full set of field measurements is shown in Table 4.1.

The water in the lake (“upper pond” in Figure 4.8) on the upper level of the tailings area shows little sign of contamination by acid rock drainage. The pH is elevated (almost 7.7) and the Eh is not excessively high.

The minewater itself is clear, colourless, very cold (2.8°C), has a slightly alkaline pH and a high content of bicarbonate (3.6 meq/L). This likely reflects the carbonate nature of the host rocks which would buffer and neutralise any acidity generated by sulphide oxidation and would suppress the solubility of ferric iron and manganese.

As the mine water flows down over the lower tailings area (possibly mixing with leachate from the tailings?), its temperature rises in the hot summer weather, while the Eh initially rises and then falls.

The water seeping from the base of the lower tailings dam has a lower pH than the mine water and a lower Eh than the lower pond, possibly reflecting the dissolution of sulphide oxidation products during seepage through the tailings. The temperature is also much lower than the pond, as the water picks up stored “coolth” from the tailings mass during its passage through them.

Sample	Location	Date	pH	Eh	Temp.	t-alkalinity	Description
				mV	°C	meq/L	
	Novii Akatui, upper tailings lake	29/07/2014	7.69	+178	24.5		Ponded water. Brownish coloured lake with little vegetation
Shg-05F	Novii Akatui. Minewater flow from 1959 adit at c. 10 L/s.	29/07/2014	7.15	+210	2.8	3.6 (3.6,3.6,3.7)	Flowing mine water. Clear colourless water. No precipitate on filter.
Shg-06F	Novii Akatui, stream running over lower tailings area	29/07/2014	6.50	+435	16.9	3.6 (3.7,3.5,3.6)	Flowing water derived from mine adit. Clear colourless water. Grey/buff residue on filter
	Novii Akatui lower tailings pond	29/07/2014	7.20	+345	22.1		Very slight bluish colouration in bulk
	Novii Akatui. Seepage at foot of retaining dam of lower tailings area	29/07/2014	6.7	+289	7.3		Iron hydroxide precipitation in area
Shg-04F	Novii Akatui, spring at eastern foot of retaining dam of lower tailings area	29/07/2014	6.7	+258	9.7	2.6 (2.5,2.7,2.6)	Clear colourless water. No precipitate on filter. Eh is -40 mV in sediments and sulphate reduction is apparent. Some iron hydroxide precipitate in stream bed

Table 4.1. Summary of field measurements taken at the Novii Akatui site, sorted in descending order through the site, from north to south.

The column marked t-alkalinity shows the average of three titrations, followed (in parentheses) by the three titration results.

LIMS Code			13444-0005	13444-0006	13444-0004	13444-0012	13444-0009	13444-0010
Sample Code			Shg-05F	Shg-06F	Shg-04F	Shg-102-F	Shg-09F	Shg-10F
Date			29/7/14	29/7/14	29/7/14	29/7/14	31/7/14	1/8/14
		Detection limit	Akatui mine	Akatui stream	Akatui seep	Bazanovskii bore	Balei	Zhireken
Field Measurements								
pH			7.15	6.50	6.7	6.36	3.40	5.6
Eh	mV		+210	+435	+258	+41	+468	+446
Temp	°C		2.8	16.9	9.7	0.8	25.2	17.5
Alkalinity	meq l ⁻¹		3.6	3.6	2.6	33.2	0.0	1.2
Anions								
Cl ⁻	mg l ⁻¹	<0.05	0.57	0.93	0.76	5.1	13	3.2
SO ₄ ²⁻	mg l ⁻¹	<0.05	223	298	400	0.06	1447	403
NO ₃ ⁻	mg l ⁻¹	<0.03	1.4	6.3	7.9	<0.03	7.8	46
Br ⁻	mg l ⁻¹	<0.01	<0.01	0.02	<0.01	0.03	0.01	0.01
HPO ₄ ²⁻	mg l ⁻¹	<0.01	<0.01	<0.01	<0.01	<0.01	<0.01	1.8
F ⁻	mg l ⁻¹	<0.01	0.39	0.47	0.64	0.08	0.45	0.22
Cations and main metals								
Ca	mg/l	<0.8	135.8	170.9	188.0	259.3	248.8	141.9
Mg	mg/l	<0.06	33.64	35.10	33.05	108.37	212.31	33.90
Na	mg/l	<0.9	2.9	6.4	4.7	417.8	41.1	24.9
K	mg/l	<0.2	1.0	1.4	2.2	4.9	15.5	3.4
Al	µg/l	<2	5	4	<2	3	1891	2
Fe	µg/l	<3	141	27	78	8621	2952	5
Mn	µg/l	<0.4	178.4	181.5	220.0	555.1	1339.3	2.9
Cu	µg/l	<0.4	0.6	2.5	1.1	<0.4	3.5	8.5
Zn	µg/l	<0.5	2723.2	1388.7	533.9	15.0	145.3	10.7
S, Si & P								
P	mg/l	<0.01	<0.01	<0.01	<0.01	<0.01	<0.01	<0.01
S	mg/l	<4	90	120	150	<4	548	140
Si	µg/l	<53	7754	8372	7380	10609	642	1000
Minor and Trace Elements								
Ag	µg/l	<0.2	<0.2	<0.2	<0.2	0.5	<0.2	<0.2
As	µg/l	<0.05	52.78	245.91	59.08	3.13	4.95	1.30
B	µg/l	<28	64	72	83	53	<28	<28
Ba	µg/l	<0.1	8.4	17.2	29.9	10764	13.8	25.9
Be	µg/l	<0.02	0.08	<0.02	<0.02	0.32	0.69	<0.02
Cd	µg/l	<0.06	3.96	4.05	1.97	<0.06	0.22	0.42
Cr	µg/l	<0.09	<0.09	<0.09	<0.09	0.16	0.26	<0.09
Co	µg/l	<0.04	0.81	0.44	0.05	<0.04	19.83	0.15
Cs	µg/l	<0.005	0.672	0.629	0.247	5.389	2.719	0.459
Ga	µg/l	<0.6	<0.6	<0.6	<0.6	<0.6	<0.6	<0.6
Hf	µg/l	<0.01	<0.01	<0.01	<0.01	0.92	0.01	0.02
Li	µg/l	<7	13	15	13	1194	149	18
Mo	µg/l	<0.03	1.93	2.45	5.43	0.08	<0.03	882.18
Nb	µg/l	<0.02	<0.02	<0.02	<0.02	0.03	<0.02	<0.02
Ni	µg/l	<0.1	7.2	4.5	1.4	0.2	28.4	2.4
Pb	µg/l	<0.03	0.70	15.99	0.42	0.38	0.21	<0.03
Rb	µg/l	<0.02	2.74	3.51	2.66	7.22	11.64	9.50
Sb	µg/l	<0.02	5.42	7.11	3.17	0.04	0.19	12.31
Se	µg/l	<0.3	2.5	1.7	0.3	<0.3	<0.3	5.1
Sn	µg/l	<0.3	<0.3	<0.3	<0.3	<0.3	<0.3	<0.3
Sr	µg/l	<0.2	508	661	812	23016	3438	2141
Ta	µg/l	<0.02	<0.02	<0.02	<0.02	<0.02	<0.02	<0.02
Ti	µg/l	<0.2	<0.2	<0.2	<0.2	8.7	<0.2	0.8
Th	µg/l	<0.05	<0.05	<0.05	<0.05	0.40	0.39	<0.05
Tl	µg/l	<0.02	0.02	0.05	<0.02	<0.02	0.11	<0.02

U	µg/l	<0.03	3.76	6.27	8.81	0.08	2.33	58.41
V	µg/l	<2	<2	<2	<2	<2	<2	<2
W	µg/l	<0.2	<0.2	<0.2	<0.2	<0.2	<0.2	<0.2
Zr	µg/l	<0.2	<0.2	<0.2	<0.2	208.9	<0.2	4.6
REE								
Y	µg/l	<0.005	0.605	0.213	0.310	4.500	13.709	0.035
La	µg/l	<0.004	0.091	0.027	0.189	0.776	4.785	0.012
Ce	µg/l	<0.004	0.186	0.041	0.022	1.147	12.727	0.013
Pr	µg/l	<0.004	0.022	0.005	0.017	0.152	1.792	<0.004
Nd	µg/l	<0.07	0.08	<0.07	<0.07	0.66	7.78	<0.07
Sm	µg/l	<0.009	0.028	0.012	0.009	0.223	2.300	<0.009
Eu	µg/l	<0.003	0.007	<0.003	0.005	0.085	0.562	<0.003
Tb	µg/l	<0.006	0.009	<0.006	<0.006	0.046	0.445	<0.006
Gd	µg/l	<0.005	0.052	0.010	0.018	0.260	2.909	<0.005
Dy	µg/l	<0.005	0.063	0.021	0.020	0.332	2.406	<0.005
Ho	µg/l	<0.003	0.017	0.009	0.006	0.092	0.476	<0.003
Er	µg/l	<0.005	0.046	0.044	0.022	0.306	1.293	<0.005
Tm	µg/l	<0.003	0.008	0.009	0.005	0.048	0.178	<0.003
Yb	µg/l	<0.004	0.041	0.085	0.032	0.343	1.002	<0.004
Lu	µg/l	<0.002	0.007	0.021	0.007	0.075	0.148	<0.002

Table 4.2. Laboratory chemical determinations (British Geological Survey) of water samples (filtered in the field at 0.45 µm) from Novii Akatui, Bazanovskii, Balei and Zhireken. Anions (Cl⁻, SO₄²⁻, NO₃⁻, Br⁻, HPO₄²⁻, F⁻) analysed by ion chromatography, all other elements by ICP-MS. Field measurements included in uppermost rows for comparison. All samples were laboratory-diluted by a factor of 5 prior to analysis by ICP-MS, hence the slightly higher than normal detection limits.

4.4 Results: Laboratory Chemical Analysis of Water Samples

The results of the laboratory chemical analyses performed by BGS are shown in Table 4.2. All samples were laboratory-diluted by a factor of 5 prior to analysis by ICP-MS. The major cations and anions have been converted to meq/L in Table 4.3 and are shown as pie diagrams in Figure 4.9.

It will be noted that the ion balance errors for the Novii Akatui samples range from 5-8%, which is relatively high. Table 4.3 suggests, however, that when alkalinity is low or negligible, the ion balance errors are low, but that the errors increase as alkalinity increases. This suggests that the source of ion balance error is likely to be the field alkalinity titration (which used “home-prepared acid”), which is likely to slightly underestimate the true alkalinity.

The following should be noted from the analyses:

		Shg-05F	Shg-06F	Shg-04F	Shg-102-F	Shg-09F	Shg-10F
		Akatui mine	Akatui stream	Akatui seep	Bazanovskii bore	Balei	Zhireken
Ca	meq/L	6.77	8.53	9.38	12.94	12.41	7.08
Mg	meq/L	2.77	2.89	2.72	8.92	17.47	2.79
Na	meq/L	0.13	0.28	0.20	18.17	1.79	1.08
K	meq/L	0.03	0.04	0.06	0.13	0.40	0.09
Cl ⁻	meq/L	0.02	0.03	0.02	0.14	0.36	0.09
SO ₄ ⁼	meq/L	4.64	6.20	8.33	0.00	30.13	8.38

Alkalinity	meq/L	3.6	3.6	2.6	33.2	0.0	1.2
NO ₃ ⁻	meq/L	0.02	0.10	0.13		0.13	0.74
F ⁻	meq/L	0.02	0.02	0.03	0.00	0.02	0.01
Sum cations	meq/L	9.69	11.73	12.36	40.15	32.07	11.04
Sum anions	meq/L	8.30	9.95	11.11	33.38	30.63	10.42
IBE	%	7.74	8.21	5.32	9.21	2.29	2.88

Table 4.3. Laboratory chemical determinations (British Geological Survey) of water samples (filtered in the field at 0.45 µm) from Novii Akatui, Bazanovskii, Balei and Zhireken, converted to meq/L. IBE = calculated ion balance error.

- All three water samples from Akatui, while not identical, are broadly hydrochemically similar, suggesting that mine water is the major component in all, possibly modified by tailings leachate (in Shg-04F and Shg-06F), or by admixture with natural groundwater in Shg-04F.
- Chloride concentrations are very modest (0.6 to 0.9 mg/L), which likely reflect the very low chloride concentrations in precipitation (due to distance from the sea and the low content of marine salts). These concentrations are not dissimilar to those found elsewhere in Central Asia (e.g. Afghanistan, Banks 2014).
- Sulphate is the major anion at 220 to 400 mg/L. Thus, although the mine water contains only modest concentrations of dissolved metals and is slightly alkaline, it does bear the hydrochemical fingerprint of sulphide oxidation. The sulphate content increases “downstream” through the tailings area, suggesting that sulphate is being acquired through contact with the tailings and seepage through them. The decrease in alkalinity between the second and third sampling points may also reflect acquisition of acidity from the tailings.
- The mine water type is Ca-(Mg)-SO₄, suggesting that acid, generated by sulphide oxidation, is being neutralised by Ca-(Mg) carbonates in the host rocks.
- The content of several other ions increases downstream, e.g. Ca, K, F, Mn. It is possible that these are being acquired through dissolution of secondary salts in the tailings area.
- The iron concentration of 141 µg/L in the minewater is relatively modest and does not increase downstream, despite the pyrite content of the tailings. The iron concentration is related to redox conditions - as Eh increases, iron decreases - suggesting iron in the minewater is largely in ferrous (Fe⁺⁺) form and is precipitated out by oxidation to ferric iron.

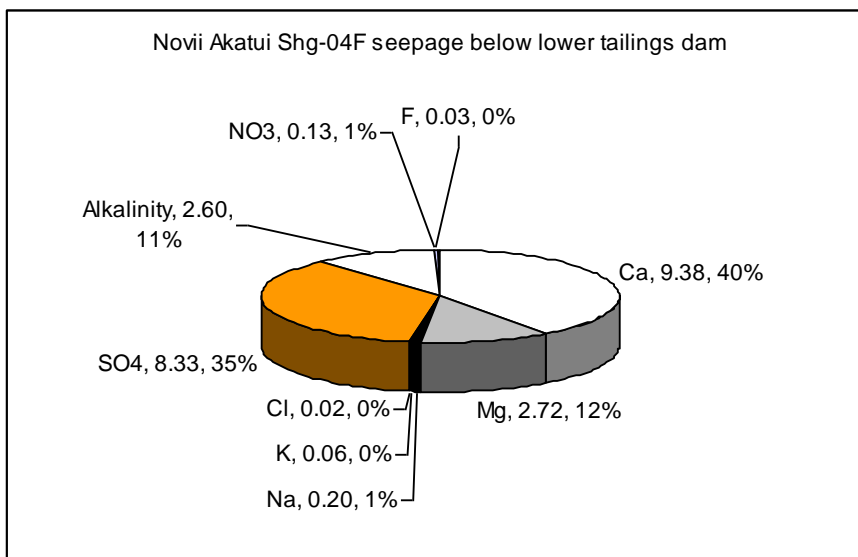
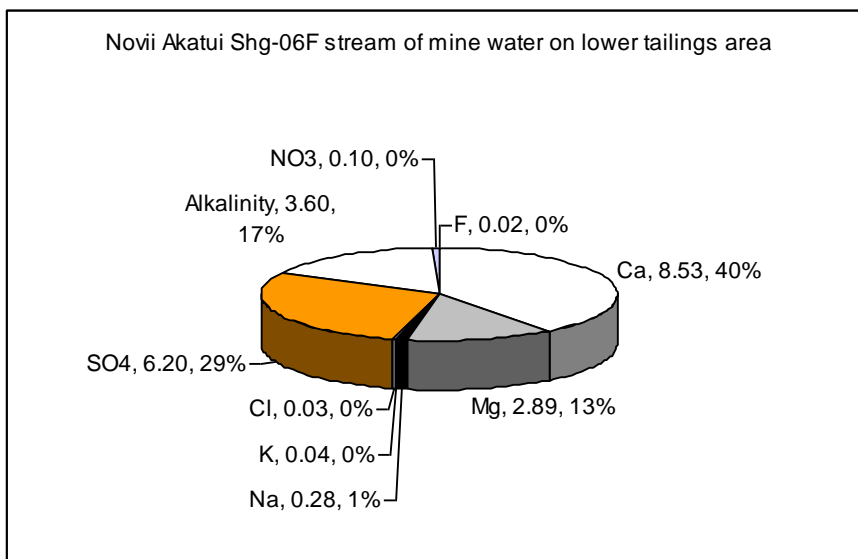
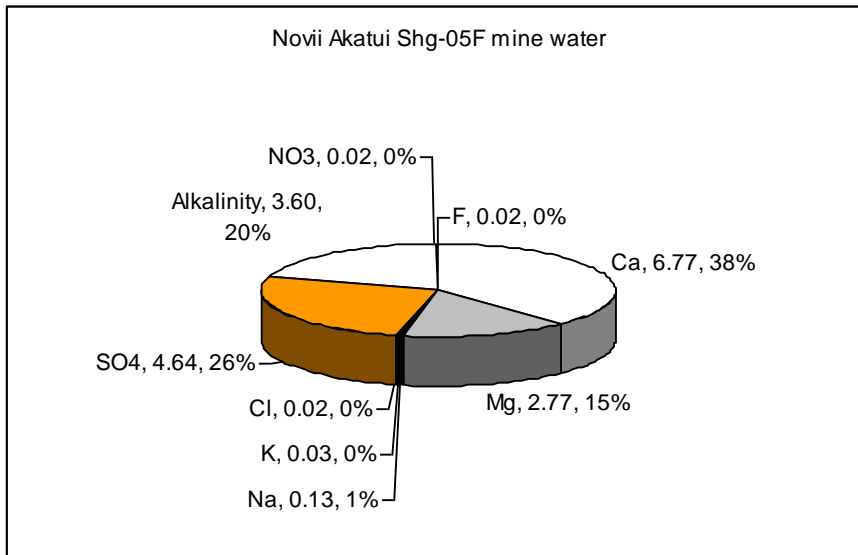


Figure 4.9. The analyses for Novii Akatui shown as pie diagrams. For each parameter, the first figure is the meq/L concentration, the second figure the percentage of the ion total in meq/L.

- The minewater contains modestly elevated concentrations of several other sulphide-related metals and metalloids - Zn at 2.7 mg/L, Cd at 4 µg/L and As at 53 µg/L. Both Zn and As are soluble in high-pH environments.
- Zn appears to be removed downstream in the system, possibly due to precipitation as a carbonate phase.
- Pb is only present at <1 µg/L in the mine water (solubility suppressed in a high pH environment), but increases to 16 µg/L in the stream of the lower tailings area. Arsenic increases to 246 µg/L.

4.5 Results: Laboratory Stable Isotope Analysis of Water Samples

Sample	Location	Sample date	$\delta^{18}\text{O}_{\text{smow}}$	$\delta^2\text{H}_{\text{smow}}$
Shg-05F	Novii Akatui. Minewater flow from 1959 adit at c. 10 L/s.	29/7/14	-15.3 ‰	-102.3 ‰
Shg-04F	Novii Akatui, spring at foot of retaining dam of lower tailings area	29/7/14	-13.7 ‰	-96.9 ‰

Table 4.4. Laboratory ^2H and ^{18}O determinations (SUERC) of water samples (filtered in the field at 0.45 µm) from Novii Akatui. Job number 14-38-TOMSKOH.

The results of the laboratory ^2H and ^{18}O analyses performed by BGS are shown in Table 4.4 and are plotted on Figure 3.3. The following should be noted:

The samples plot very close to the global meteoric water line (GMWL) and also very close to the groundwater from the nearby Bazanovskii borehole. This effectively confirms that the samples are derived from precipitation.

4.6 Results: Laboratory Sulphur Isotope Analysis of Mineral Samples

The following sulphur isotope results were obtained from SUERC for analysis of primary sulphide minerals:

Sample	Description	$\delta^{34}\text{S}_{\text{V-CDT}}$ (‰)
Shg-Ei	Pyrite/chalcopyrite from tailings area	+3.4
Shg-Eii	Sphalerite with small crystals of pyrite	+1.2

Table 4.5. Laboratory ^{34}S determinations (SUERC) of primary sulphide mineral samples from Novii Akatui. Job number Job: 14-53-Banks.

The values of around +1-3‰ are compatible with a magmatic origin, but cannot be regarded as exclusively indicative of such an origin (Frietsch et al. 1995, Seal 2006).

4.7 Sources of information:

Dobrovolskaya, M.G. (1996). Geochemistry of alkali metals in sulfides. *Abstract 133, 6th V.M. Goldschmidt Conference, Heidelberg, March/April 1996*. Available at <http://www.the-conference.com/JConfAbs/1/133.html>, accessed July 2015.

Webmineral (2014). *Акатуй месторождение, Александрово-Заводский район, Забайкальский край, Забайкалье, Россия*. Available at <http://webmineral.ru/deposits/item.php?id=412>, accessed December 2014.

Wikipedia (2014). *Новый Акатуй*. Available at https://ru.wikipedia.org/wiki/Новый_Акатуй, accessed December 2014.

Zabaikalskii Krai (2014). *Порядок и условия проведения аукциона. на право пользования недрами с целью разведки и добычи свинца, цинка, серебра, золота, кадмия и попутных компонентов на участке недр Акатуевское рудное поле в Александрово-Заводском районе Забайкальского края. Приложение 1 к приказу Центрсибнедра от 05.05.2014 № 104*. Available at <http://geo.chita.ru/documents/download/532>.

5 BAZANOVSKII (БАЗАНОВСКИЙ) BOREHOLE

5.1 Location and Description

This artesian borehole is located just south of the road from Borzuya to Aleksandrovskii Zavod, around 13 km SSW of Novii Akatui and 15 km west of Aleksandrovskii Zavod. The borehole is drilled in the valley bottom on the flood plain of the Gun'gundzha River (Figure 4.1).

The depth of the borehole is not known, but its temperature suggests it is not of any great depth. Indeed, a document by GIPROGOR & NIPETERPLAN (2010) states that the depths of the aquifer horizons are only 25-50 to 60-70 metres. The water is effervescent, degassing bubbles of CO₂ on emergence from the continuously flowing discharge pipe from the well head. The borehole is used as a source of drinking water by local residents who come to collect water in containers.

5.2 Samples

A single sample (Shg-102F, field filtered at 0.45 µm) was taken directly from the well-head on 29/7/14, where field measurements were also taken. The artesian discharge rate was estimated as 0.5 L/s.



Figure 5.1 Bazanovskii borehole well head. The discharge pipe passes through the rear wall. (Photo by David Banks)



Figure 5.2. Bazanovskii borehole discharge pipe (photo by David Banks).

5.3 Field Measurements

The full set of field measurements is shown in Table 5.1. The appearance of the water was clear and colourless and effervescing with bubbles of (presumed) CO₂.

Date	29/07/2014
pH	6.36
Eh	+41 mV
Temperature	0.8°C
Average t-alkalinity in meq/L (individual titration results in parentheses)	33.2 (33.4, 32.9, 33.4)

Table 5.1. Summary of field measurements taken at the Bazanovskii borehole. The column marked t-alkalinity shows the average of three titrations, followed (in parentheses) by the three titration results.

It will be noted that the water is extremely cold, only just above 0°C. The water's pH is low, although not negative and the pH is slightly acidic, likely reflecting the high content of dissolved CO₂. The alkalinity is, however, high. Use of PHREEQC Interactive suggests that (a) the water is saturated with respect to calcite and (b) the partial pressure (fugacity) of CO₂ in the water is as high as 10^{-0.24} atmospheres, compared with typical partial pressures of up to 10^{-1.5} atm. in the soil zone. This is suggestive of either:

- of an unusual source of CO₂, which has partially reacted with basic minerals to generate a high alkalinity
- or a source of other (proton) acidity, that has reacted with carbonate minerals to release an excess of alkalinity.

5.4 Results: Laboratory Chemical Analysis of Water Samples

The results of the laboratory chemical analyses performed by BGS are shown in Table 4.2. All samples were laboratory-diluted by a factor of 5 prior to analysis by ICP-MS. The major cations and anions have been converted to meq/L in Table 4.3 and are shown as a pie diagram in Figure 5.3.

It will be noted that the ion balance errors for the Bazanovskii sample is rather high at c. 9%. Table 4.3 suggests, however, that when alkalinity is low or negligible than ion balance errors are low, but that the errors increase as alkalinity increases. This suggests that the source of ion balance error is likely to be the field alkalinity titration (which used “home-prepared acid”), which is likely to slightly underestimate the true alkalinity.

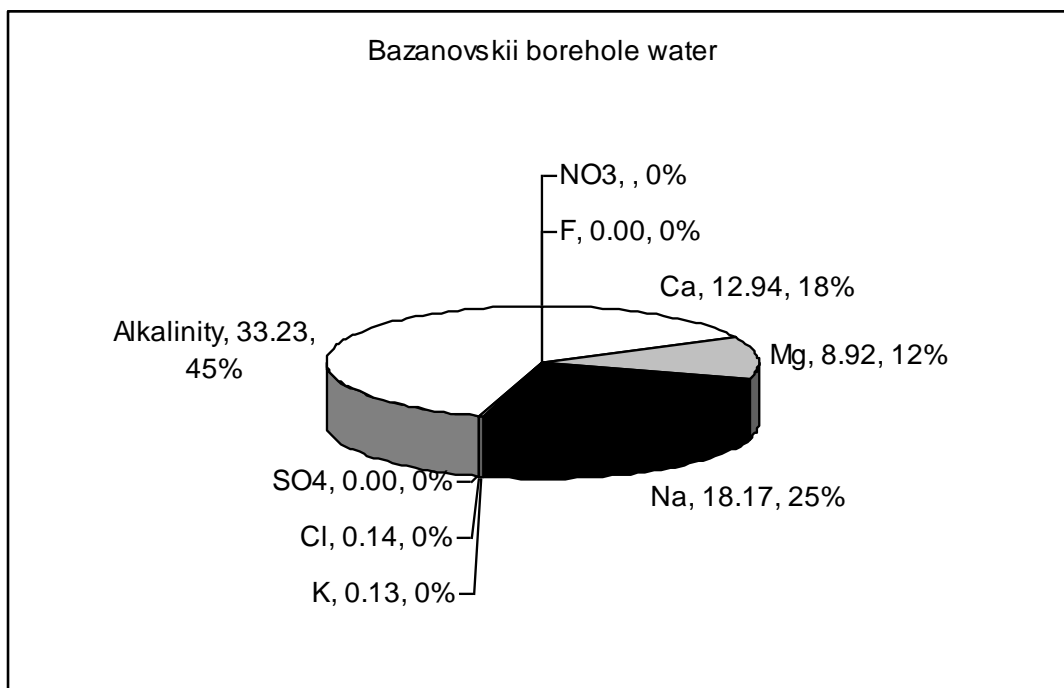


Figure 5.3. The analysis for Bazanovskii borehole shown as a pie diagram. For each parameter, the first figure is the meq/L concentration, the second figure the percentage of the ion total in meq/L.

The following should be noted from the analyses:

- The water is a Na-(Ca-Mg)-HCO₃ water. There is a significant excess of Na over Cl, which is indicative of intensive mineral hydrolysis.

- Nitrate is not detectable in the water and sulphate is almost absent. This indicative of reducing conditions in the water. The high barium concentration (10.8 mg/L) is only possible due to the absence of sulphate and thus of a barite saturation ceiling. This is strongly indicative of sulphate reduction processes occurring.
- The elevated dissolved iron (8.6 mg/L) and manganese (0.56 mg/L) concentrations are also indicative of reducing conditions.
- The fact that uranium concentrations (0.08 µg/L) are lower than thorium (0.4 µg/L) is another indicator of a generally reducing environment.
- Concentrations of Si are higher than would be expected, at 10.6 mg/L, another indicator of intense hydrolysis of silicate minerals by CO₂.
- The concentration of lithium is remarkably high at 1.2 mg/L, as is strontium at 23 mg/L. Both are indicators of intense and/or prolonged water-rock interaction.
- Zirconium and titanium concentrations are elevated at 209 µg/L and 9 µg/L respectively.

The water has been analysed previously, as reported by GIPROGOR & NIPETERPLAN (2010): here the water is described as rich in carbon dioxide (3.4 to 3.6 g/L), rather modestly mineralised (3.3 to 3.5 g/L) and of HCO₃⁻-Mg-Ca-Na type, with 13.4 to 22.3 mg/L iron. The temperature is confirmed as only 0.3°C.

5.5 Results: Laboratory Stable Isotope Analysis of Water Samples

Sample	Location	Sample date	δ ¹⁸ Osmow	δ ² Hsmow
Shg-102F	Sparkling (CO ₂) mineral water, overflowing at c. 0.5 L/s. Clear colourless	29/7/14	-12.9	-89.0

Table 5.2. Laboratory ²H and ¹⁸O determinations (SUERC) of water samples (filtered in the field at 0.45 µm) from Bazanovskii borehole. Job number 14-38-TOMSKOH.

The results of the laboratory ²H and ¹⁸O analyses performed by BGS are shown in Table 5.2 and are plotted on Figure 3.3. The sample plots very close to the global meteoric water line (GMWL) and also very close to the waters from the nearby Akatui mine. This effectively confirms that the samples are derived from precipitation.

5.6 Sources of information:

GIPROGOR & NIPETERPLAN (2010). «Стратегия территориального планирования и градостроительного развития Забайкальского края с учётом условий особого периода 2009-2012 гг.»; Этап 2 «Схема территориального планирования Забайкальского края»; Том 2 Материалы по обоснованию проекта Книга 1 Современное состояние территории [*Strategy for the areal planning and urban development of Zabaikalsk Krai 2009-2012*]. ОАО «Российский Государственный Институт Градостроительства и

Инвестиционного Развития «ГИПРОГОР» & ООО «Научно– Исследовательский и Проектный Институт Территориального Планирования и Управления». Moscow-Chita 2010.

6 БАЛЕЙ (БАЛЕЙ)

6.1 Location and Description

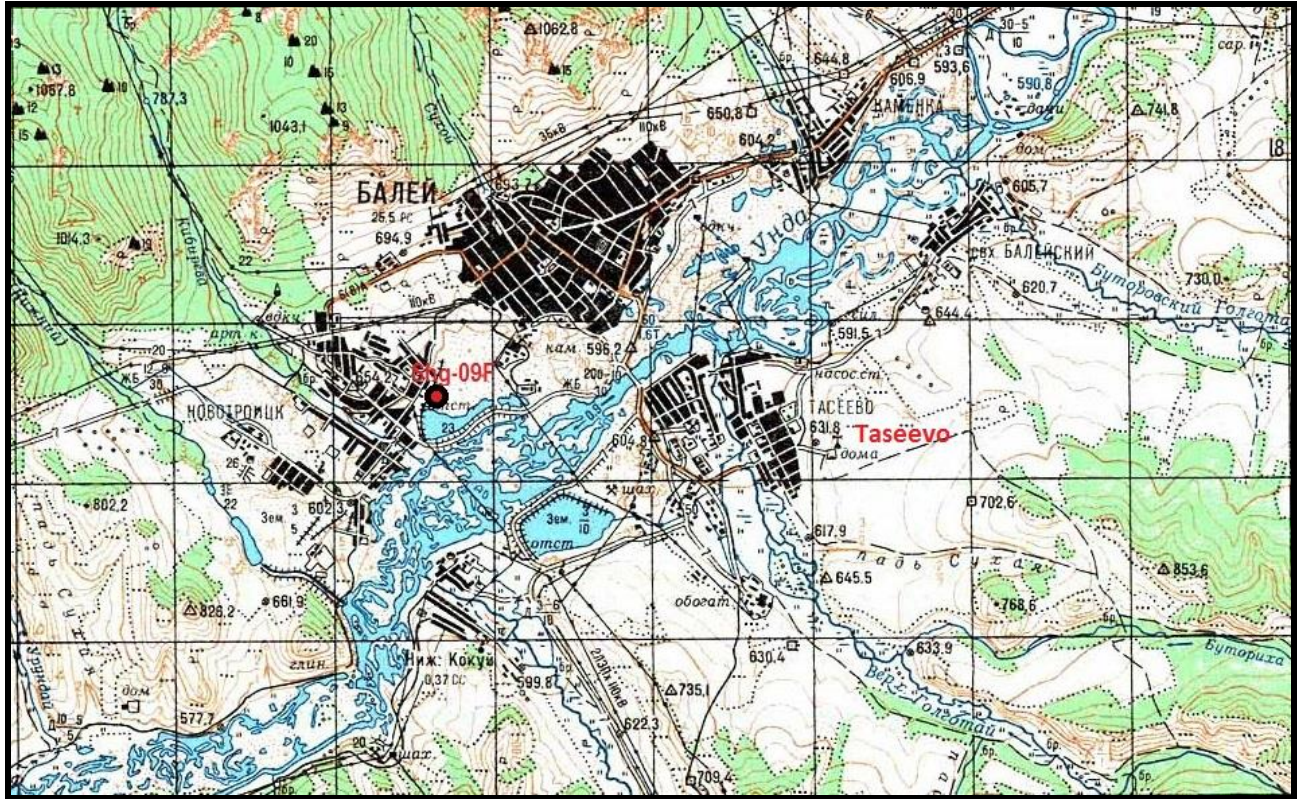


Figure 6.1. Extract of 1:100,000 map of Balei (m-50-018 dated 1988). Each square is 2 km, north is vertically up the page. The red/black circle shows the approximate location of the sampled ponded water within the tailings area (sample Shg-09F). The Taseevo mining area is also shown.

Prokof'ev et al. (2006) regard the gold-bearing epithermal quartz-sulphide-adularia veins of Balei as being of Early Cretaceous age (114-120 Ma). The veins are also associated with phyllosilicates, carbonates, pyrite, marcasite, sulphosalts of antimony, stibnite and arsenopyrite. The gold deposit is associated with a Mesozoic-Recent ENE-WSW graben-like structure, termed the Unda Valley Rift (Ross 2005). The ore veins are partly located in Palaeozoic granitoids and also in Cretaceous conglomerates and sandstones which fill the rift basins. Working has been both by opencasting and underground working and both flotation and cyanide leaching have been used in ore concentration (Ross 2005, Mining Encyclopedia 2014). During Soviet times, the Balei area represented the largest gold deposit in Chita district (Prokof'ev et al. 2006). In situ oxidation and sulphatisation is believed to have taken place in some parts of the ore, such that large crystals of gypsum can be found in the tailings.

Alluvial gold had been worked around Balei from the second half of the 19th Century (Wikipedia 2014) before a quartz-gold deposit was discovered in 1928, which came into production within a few years of discovery. At the Balei epithermal Au-Ag deposit, underground mining was carried

out from the 1920s, while opencast mining was carried out from 2nd World War to the 1970s (Ross 2005).

Around 2 km south of the original Balei deposit is the more modern location of extraction at Taseevo (Figure 6.1), while other lodes are registered at Sverdlovskoe and Srednegolybtaiskoe (Jensen et al. 1983). The Taseevo deposit has been worked by underground methods from 1946 till 1992, down to depths in excess of 300 m, producing a total of 195 tons Au with an average content of 13.6 g Au/t of ore. In the 1980s opencast mining of the deposit was also introduced, reaching c. 100 m depth (Ross 2005).

Tailings have been dumped in large areas in the immediate vicinity of the town. The current project team sampled ponded water within one of the largest tailings areas, north of the river Unda at the western end of Balei (Figure 6.1). The water was ponded at the foot of a tailings embankment (which, according to the map in Figure 6.1 was probably a railway embankment).

6.2 Samples

A single sample of water was taken from ponded water standing on the tailings area at the foot of the former (presumed) railway embankment on the east of the major mine tailings area to the north of the river. The embankment also appeared to be largely constructed (or at least faced with) tailings material. The sample was taken c. 30 cm from the edge of the ponded area, from about 5 cm below the water surface. It was designated **Shg-09F** (filtered at 0.45 µm).

Within the tailings material, abundant secondary mineralisation could be observed, tentatively identified as yellowish jarosite (or similar hydroxysulphate mineral).

Large crystals of transparent gypsum were also found amongst the tailings and spoil: these are thought to represent in-situ oxidation, alteration and sulphatisation of the ore body and not recent alteration products within the tailings. A single sample of this gypsum mineral was taken for sulphur isotope analysis, designated **Sample Shg-G**.



Figure 6.2. Mine tailings area at Balei, looking approximately north, with embankment on left. (Photo by Dave Banks)



Figure 6.3. Ponded water at foot of tailings area embankment at Balei. (Photo by Dave Banks).



Figure 6.4. Sampling ponded water at foot of tailings area embankment at Balei. (Photo by Dave Banks).



Figure 6.5. Presumed jarosite mineralisation with tailings area embankment at Balei. (Photo by Dave Banks).



Figure 6.6. Gypsum mineralisation found within tailings material at Balei. (Photo by Dave Banks).

6.3 Field Measurements

The full set of field measurements is shown in Table 6.1. The appearance of the water was clear and colourless but left a pale yellow-orange residue (jarosite/ iron oxyhydroxide?) on the 0.45 μm filter on filtration.

Date	31/07/2014
pH	3.40
Eh	+468 mV
Temperature	25.2°C
t-Alkalinity (meq/L)	0

Table 6.1. Summary of field measurements taken in the water ponded at the Balei tailings area.

It will be noted that the water is relatively acidic, oxidising and has been warmed up by the intense solar radiation and summer heat of the fieldwork period to over 25°C.

6.4 Results: Laboratory Chemical Analysis of Water Samples

The results of the laboratory chemical analyses performed by BGS are shown in Table 4.2. All samples were laboratory-diluted by a factor of 5 prior to analysis by ICP-MS. The major cations and anions have been converted to meq/L in Table 4.3 and are shown as pie diagrams in Figure 6.7.

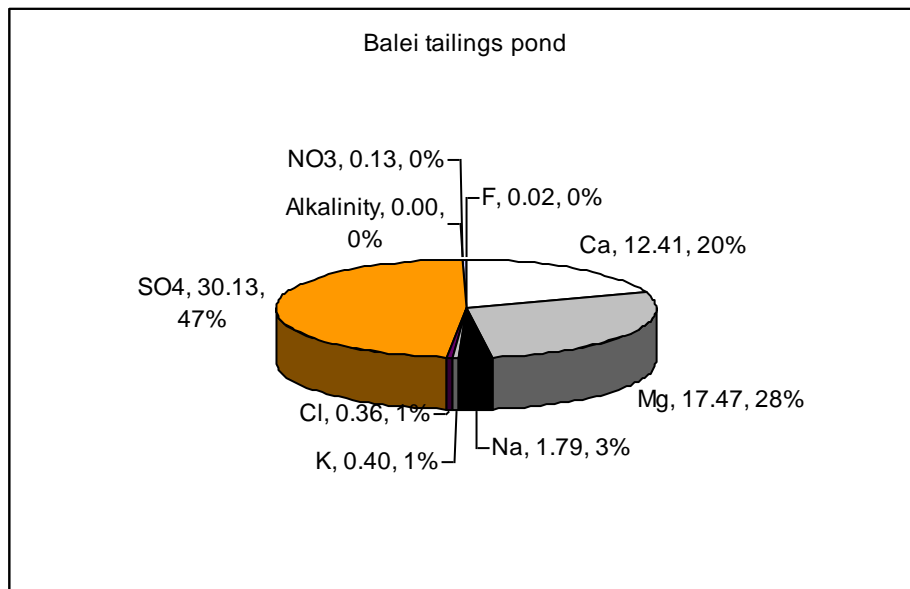


Figure 6.6. The analysis for water from the Balei tailings area shown as a pie diagram. For each parameter, the first figure is the meq/L concentration, the second figure the percentage of the ion total in meq/L.

It will be noted that the ion balance errors for the Balei sample is rather good at only c. 2%. The water is dominated by sulphate as an anion and magnesium, followed by calcium, as cations. Chloride is 13 mg/L, probably representing evaporatively up-concentrated chloride in rainfall. Sulphate is 1447 mg/L, which, together with the low pH, indicates acid-generating sulphide oxidation, possibly also with dissolution of gypsum. The water is by no means as “concentrated” as the waters from Sherlovaya Gora (Chapter 3), however. The following additional points should also be noted:

- aluminium, iron and manganese are all significantly elevated in this low pH environment, a 1.9, 3.0 and 1.3 mg/L respectively.
- other sulphide-related elements are surprisingly low, with Cu at only 3 µg/L and Zn at a rather modest 145 µg/L.
- Silicon concentration is very low at 0.64 mg/L, suggesting rather little hydrolysis of silicate minerals in the water on top of the tailings area. It is thus possible, that the standing water simply receives the readily soluble products of sulphide oxidation or sulphate dissolution from a superficial layer of the tailings.
- For an area which has been subject to so much speculation regarding high levels of uranium/thorium-related environmental radioactivity (Jones 1997, Orttung et al. 2000), the uranium concentration in the tailing water samples very modest at c. 2 µg/L.

6.5 Results: Laboratory Sulphur Isotope Analysis of Sulphate Samples

The following sulphur isotope results were obtained from SUERC for analysis of a large sulphate (gypsum) crystal derived from the Balei tailings area (Sample Shg-G)

Sample	Description	$\delta^{34}\text{S}_{\text{V-CDT}}$ (‰)
Shg-G	Gypsum crystal from Balei tailings area	-0.2

Table 7.2. Laboratory ^{34}S determinations (SUERC) of gypsum mineralisation from Balei spoil/tailings. Job number Job: 14-53-Banks.

6.6 Sources of information:

- Jensen, R.G., Shabad, T. & Wright, A.W. (1983). *Soviet Natural Resources in the World Economy*. University of Chicago Press, 700 pp.
- Jones, L. (1997). Radioactive cement sickens town. *The Moscow Times*, 24/7/97. Available at <http://www.themoscowtimes.com/sitemap/free/1997/7/article/radioactive-cement-sickens-town/303751.html>.
- Mining Encyclopedia (2014). *Балейское месторождение*. At Website Горная энциклопедия, available at <http://www.mining-enc.ru/b/balijskoe-mestorozhdenie/>. Accessed December 2014.
- Orttung, R.W., Lussier, D.N. & Paretskaya, A. (2000). *The Republics and Regions of the Russian Federation: a guide to politics, policies and leaders*. East-West Institute and M.E. Sharpe Inc.
- Prokof'ev, V.Y., Baksheev, I.A., Zorina, L.D., Belyatskii, B.V. & Bortnikov, N.S. (2006). First estimate of the age of gold ores of the Darasun Deposit (Eastern Transbaikal Region) by the Sm–Nd method. *Doklady Earth Sciences* **409A(6)**: 963–966. doi: 10.1134/S1028334X06060298.
- Ross, A.F. (2005). *Highland Gold Mining Limited: Taseevskoye Resource Estimate Update*. Project No. V381. Report prepared by Snowden Mining Industry Consultants, February 2005.
- Wikipedia (2014). *Балей*. Available at <https://ru.wikipedia.org/wiki/Балей>, accessed December 2014.

7 ZHIREKEN (ЖИРЕКЕН)

7.1 Location and Description

The molybdenum deposit at Zhireken was discovered in 1954 (Wikipedia 2014). The deposit is a Mo-Cu deposit, occurring in Upper Jurassic (c. 160 Ma) felsic porphyries, within the Bushulei granitic/granodiorite/granosyenite pluton. It occurs along the so-called Mongolo-Okhotsk volcano-plutonic belt, related to the Mesozoic subduction of the Mongolo-Okhotsk oceanic plate beneath Siberia and the eventual collision between the Siberia and Mongolo-Chinese plates in the mid-late Jurassic (Berzina & Sotnikov 2010).



Figure 7.1. The tailings pond, Zhireken. (Photo by David Banks)

The mineralized stockwork occupies an area of some 0.12 km² associated with a fault junction. It incorporates a pipe-like breccia extending to some 600 m depth. The deposit contains molybdenite (MoS₂) chalcopyrite (CuFeS₂), chalcocite (Cu₂S), scheelite (CaWO₄) and also high contents of palladium (Pd) and platinum (Pt) - (Berzina & Sotnikov, 2010). The terminal ore stage is represented by quartz- pyrite-sphalerite-galena veinlets in sericitised zones (Berzina et al. 2005). The ore is mined by a single deep opencast pit.

In 2013, the falling global molybdenum prices led to a halt in production and the Zhireken opencast being “mothballed”

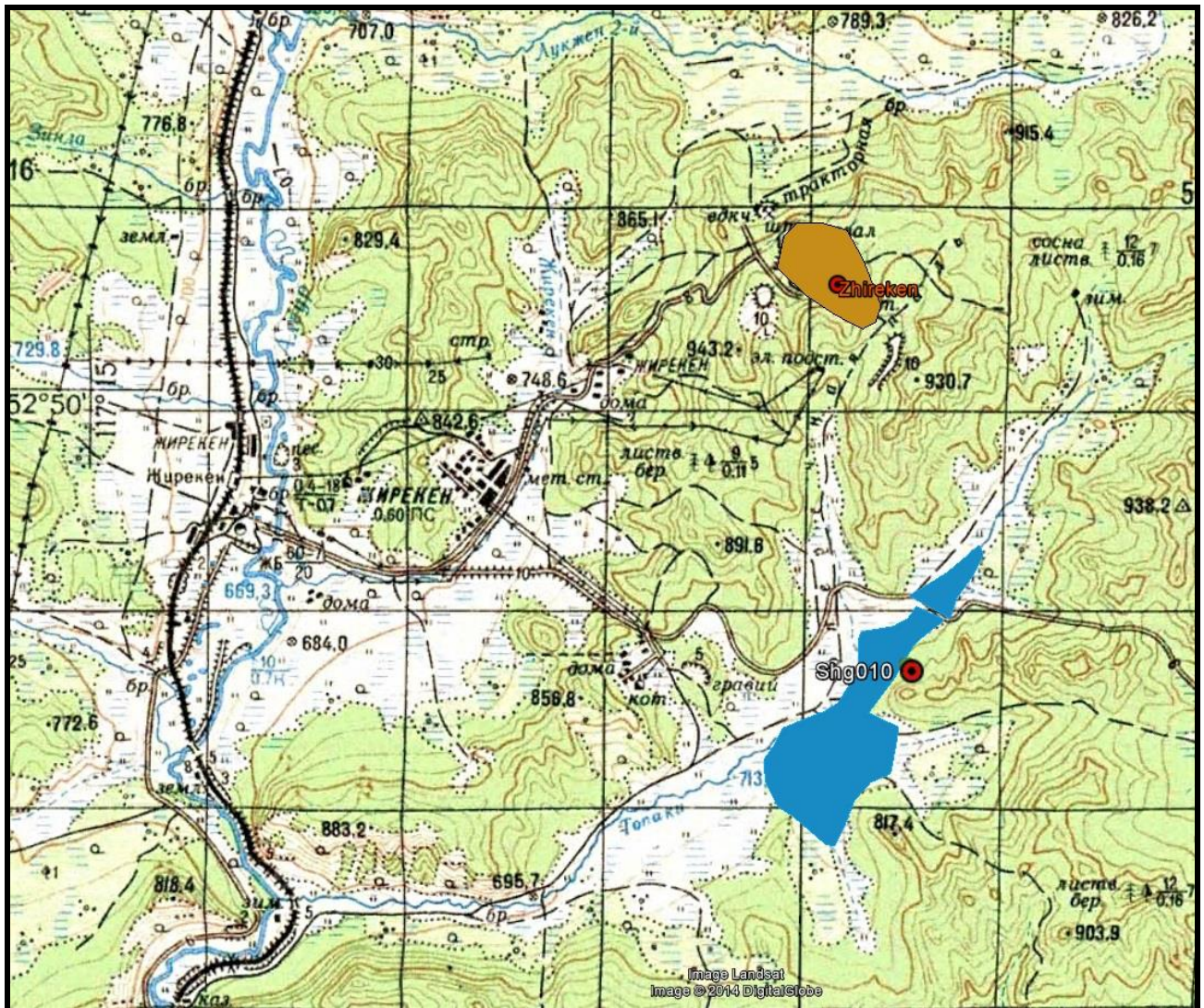


Figure 7.2. Extract of 1:100,000 map of Zhireken (m-50-115 dated 1985). Each square is 2 km, north is vertically up the page. The red/black circle labelled Shg010 shows the approximate location of the sampled ponded water near the tailings area (sample Shg-10F). Blue shading shows the tailings lakes, orange/brown shows the approximate open-cast area.

7.2 Samples

Water sample Shg-10F: The main tailings pond (Figure 7.1) was not sampled, as the pH was relatively high and the water was not deemed to be of interest to Tomsk State University in their quest for acid- and metal-tolerant extremophile micro-organisms.

Instead, a smaller area of water, ponded against the dirt road, on the SE side of the tailings area, was sampled. It showed some evidence of elevated iron concentrations, depressed pH and ochre precipitation. The water samples were filtered at 0.45 μm and designated Shg-10F.

Sulphide sample Shg-H: A single sample of primary sulphide: molybdenum sulphide (MoS₂), with some chalcopyrite, was collected from the opencast pit area. This was designated **Shg-H** and submitted for sulphur isotope determination.

7.3 Field Measurements

The full set of field measurements is shown in Table 7.1. The water in bulk had a slight orange-brown hue and there was some evidence of minor ochre precipitation in the ponded area. After filtration, the samples were clear and colourless, however.

Date	1/8/2014
pH	5.6
Eh	+446 mV
Temperature	17.5°C
t-Alkalinity (meq/L)	1.2 (1.0 to 1.3, 1.2, 1.0 to 1.3)

Table 7.1. Summary of field measurements taken in the water ponded near the Zhireken tailings area. The row marked t-alkalinity shows the average of three titrations, followed (in parentheses) by the three titration results.

7.4 Results: Laboratory Chemical Analysis of Water Samples

The results of the laboratory chemical analyses performed by BGS are shown in Table 4.2. All samples were laboratory-diluted by a factor of 5 prior to analysis by ICP-MS. The major cations and anions have been converted to meq/L in Table 4.3 and are shown as pie diagrams in Figure 7.3.

It will be noted that the ion balance error for the Zhireken sample is rather good at only c. 3%. The water is dominated by sulphate as an anion and calcium as a cation. Chloride is only 3 mg/L, probably representing slightly evaporatively upconcentrated chloride in rainfall. Sulphate is rather high at 403 mg/L, presumably as a result of sulphide oxidation reactions. The water is by no means as “concentrated” as the waters from Sherlovaya Gora (Chapter 3), however. The following additional points should also be noted:

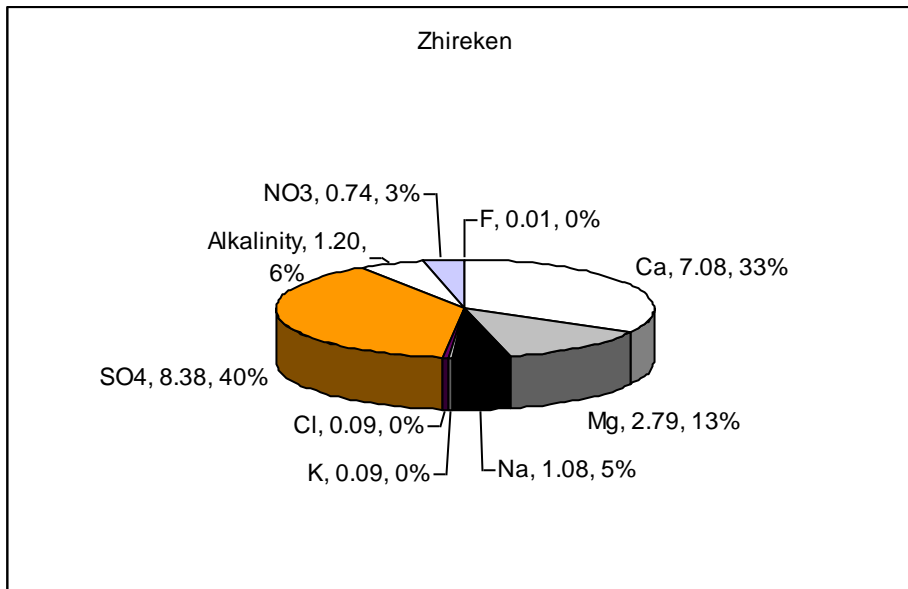


Figure 6.6. The analysis for water from the Zhireken water shown as a pie diagram. For each parameter, the first figure is the meq/L concentration, the second figure the percentage of the ion total in meq/L.

- the pH is relatively high at 5.6, suggesting either that the main sulphide oxidation reactions are not sulphide generating, or that any protons generated by sulphide oxidation have been largely neutralised by basic minerals.
- Concentrations of Al, Fe and Mn are very low, all < 5 µg/L, probably reflecting the high pH and oxidising environment. Any iron present in the water (slight orange coloration) is probably present as flocs or particles of oxyhydroxide and hence not in the filtered sample.
- Silicon concentration is rather low at 1 mg/L, suggesting that the ponded water is largely of surficial nature, having experienced rather little hydrolysis of silicate minerals.
- Concentrations of most sulphide-related elements are modest, with the exception of very high molybdenum concentrations (882 µg/L) and slightly elevated concentrations of antimony (12 µg/L) and selenium (5 µg/L).
- Uranium is present at a relatively high concentration of 58 µg/L.
- Nitrate is present at 46 mg/L. There is no obvious source of organic waste or fertiliser to the water. Nitrate may possibly be derived from explosives residues from the opencast quarry.

7.5 Results: Laboratory Sulphur Isotope Analysis of Mineral Samples

The following sulphur isotope results were obtained from SUERC for analysis of primary sulphide minerals:

Sample	Description	$\delta^{34}\text{S}_{\text{V.CDT}}$ (‰)
Shg-H	Molybdenum sulphide with some chalcopyrite, from opencast area	+3.2

Table 7.2. Laboratory ³⁴S determinations (SUERC) of primary sulphide mineral samples from Novii Akatui. Job number Job: 14-53-Banks.

The value of around +3.2‰ is compatible with a magmatic origin, but cannot be regarded as exclusively diagnostic of such an origin (Frietsch et al. 1995, Seal 2006). Previous sulphide $\delta^{34}\text{S}$ determinations, cited by Berzina & Sotnikov (2010) range from +0.6 to +4.1‰.

7.6 Sources of information:

Berzina, A.N., Sotnikov, V.I., Economou-Eliopoulos, M. & Eliopoulos, D.G. (2005). Distribution of rhenium in molybdenite from porphyry Cu-Mo and Mo-Cu deposits of Russia (Siberia) and Mongolia. *Ore Geology Reviews* **26**: 91-113. doi: 10.1016/j.oregeorev.2004.12.002.

Berzina, A.N. & Sotnikov, V.I. (2010). Contribution from mafic melt to the Zhireken porphyry Mo-Cu Deposit, Eastern Transbaikalia, Russia: Evidence from mafic microgranular enclaves. *International Journal of Economic & Environmental Geology* **1(1)**: 42-45

Wikipedia (2014). *Жирекен*. Available at <https://ru.wikipedia.org/wiki/Жирекен>, accessed December 2014. <https://ru.wikipedia.org/wiki/Жирекен>

8 SUMMARY

This report documents the hydrochemical and stable isotope (^{18}O , ^2H , $^{34}\text{SO}_4^-$) analyses performed on water samples and stable isotope analyses (^{34}S and $^{34}\text{SO}_4^-$) performed on mineral samples, all collected during a field expedition during July / August 2014 to several metal sulphide mining sites in the Zabaikalsk polymetallic province of south-eastern Siberia.

Water samples collected from the Sherlovaya Gora (Schorl Mountain) polymetallic/greisen deposit (rich in Be, F, B, W, Sn, Bi, Mo, Fe, As, Pb, Zn, Cu and S) exhibited field pH values as low as 2.5. The waters were all extremely impacted by sulphide oxidation processes, containing between 3 and 16 g/L sulphate, up to 0.47 g/L Al, 1.9 g/L Fe, 0.75 g/L Mn, 3.6 g/L Zn. Waters also contained up to 80 mg/L Cu, 49 mg/L As, 38 mg/L Cd, 2.5 mg/L Th and 2.3 mg/L U. Beryllium concentrations reach several hundred $\mu\text{g/L}$ and exceed 0.5 mg/L in one borehole. Conversely, tungsten and tin remain below analytical detection limits in the waters. The variation in concentrations of some elements (chloride, uranium) suggests that the water in the opencast pit lake and (especially) the tailings area pond, have been strongly concentrated by evaporation in the extreme summer heat. This interpretation is supported by ^{18}O and ^2H trajectories.

At Novii Akatui Pb-Zn(-Ag) mine, water emerges at pH 7.15 and a temperature of 2.8°C from flooded underground workings. The water contains extremely low chloride concentrations (0.6 to 0.9 mg/L) characteristic of continental Central Asia. It also contains some 223 mg/L sulphate and 2.7 mg/L Zn. Iron concentrations are modest at 0.14 mg/L. It is likely that interaction with carbonate-rich host-rocks has maintained the mine water at a high pH and alkalinity (3.6 meq/L) and suppressed iron solubility. As the mine water traverses the large tailings areas it gradually acquires sulphate and the alkalinity decreases, suggesting that leachate from the tailings are adding acid sulphide weathering products to the water (and pyrite is visible in the tailings). Arsenic concentrations in the Akatui water vary from 53 to 246 $\mu\text{g/L}$.

Samples from Balei (gold) and Zhireken (molybdenite) mines are also documented, as is a CO_2 -effervescent water from Bazanovskii borehole, near Akatui.

The Bazanovskii water is remarkable for its low temperature (0.8°C) and reducing nature, with negligible quantities of nitrate and sulphate, significant dissolved iron and manganese, and a high concentration of 10.8 mg/L Ba, due to the absence of a barite saturation ceiling. Indicators of intense mineral hydrolysis also include elevated Li (1.2 mg/L), Sr (23 mg/L), Si (10.6 mg/L) and a high Na/Cl ratio.

The ponded water from the Balei tailings area contains elevated Al, Fe and Mn (1.9, 3.0 and 1.3 mg/L respectively), sulphate (1447 mg/L) and a low pH of 3.4. The presence of gypsum and jarosite in the tailings and the low concentrations of Si in the water itself, suggests that the ponded

water is dominantly rainfall, containing dissolution products of secondary sulphate mineralisations, rather than of primary mineral hydrolysis.

The Zhireken water is remarkable primarily for its elevated molybdenum concentration (882 µg/L).

8.1 Sulphur Isotopes

A stable isotope of an element is a non-radioactive atomic form of the element, which has the characteristic number of protons normally found in the element's nucleus, but a differing number of neutrons. For example, the most abundant form (95.02% of all sulphur atoms) of sulphur is sulphur-32 (^{32}S), which has an atomic mass of around 32 amu, due to its nucleus containing 16 protons and 16 neutrons. A less abundant isotope, sulphur-34 (^{34}S) comprising 4.21% of sulphur atoms), has an atomic mass of 34 amu (16 protons and 18 neutrons).

The deviation from the "normal" isotopic composition is cited as an enrichment (positive ‰) or depletion (negative ‰) in ^{34}S relative to some arbitrary but easily definable standard. For stable oxygen and hydrogen isotopes (^{18}O and ^2H), this standard is Vienna Standard Mean Ocean Water (VSMOW). For sulphur, the standard is a particular iron sulphide mineral found in a meteorite and verified by the IEA in Vienna - the standard is called the Vienna Canyon Diablo Troilite (VCDT). The isotopic content of any sample is cited as $\delta^{34}\text{S}$ in parts per thousand (‰) deviation, relative to the standard.

$$\delta^{34}\text{S} \text{ ‰} = (R_{\text{sample}}/R_{\text{standard}} - 1)1000$$

where R is the ratio of the heavier isotope to the lighter one (in the case of sulphur-34, this is around 0.044). The higher the $\delta^{34}\text{S}$, the more enriched it is in ^{34}S , relative to ^{32}S (USGS 2004a,b).

The two isotopes ^{32}S and ^{34}S have almost identical chemical behaviours, but small differences (fractionations) can arise due to their differing masses, volatilities etc. It is these small differences that can tell us about the sources of solutes in water and about reaction pathways. For example, igneous rocks derived from the mantle (i.e. similar isotopic composition to the meteorite troilite) have an isotopic signature ($\delta^{34}\text{S}$) around 0‰. Run off derived from oxidation of sulphides in such rocks thus also has an isotopic signature around 0‰. One of the main processes changing the isotopic signature is reduction of sulphate to sulphide by sulphate reducing bacteria. This typically leads to a negative $\delta^{34}\text{S}$ (depletion) in the biogenic sulphide phase and, if extensive enough, a corresponding enrichment in the sulphate phase.

Present day ocean water has a $\delta^{34}\text{S}$ sulphate isotopic signature of +21‰ (although this has ranged from between +10‰ at the start of the Mesozoic to +30‰ at the beginning of the Palaeozoic - USGS 2004b). River run-off from continents has a variable signature (depending on the relative proportions of sulphide and sulphate weathering in the catchment), but is often in the range 0 to +10‰. As regards sulphur sinks from the ocean, these are typically sulphate evaporites ($\delta^{34}\text{S}$

similar to ocean water) or marine sulphides in sediments (typically negative $\delta^{34}\text{S}$ but variable within the range +15 to -70‰ - Paytan et al. 2012).

Rye (2005) reviews sulphate isotope systematics in magmatic systems and suggests:

- that sulphate minerals (such as jarosite) formed directly by supergene oxidation of sulphides typically have a sulphate $\delta^{34}\text{S}$ similar to the parent sulphide (often around 0‰ in the case of magmatic sulphide).
- isotopically heavier (i.e. positive $\delta^{34}\text{S}$) sulphate can be derived from either admixture with other sulphate sources (e.g. meteoric/marine) or disproportionation of $\text{SO}_2 \rightarrow \text{SO}_4^- + \text{S}$ or H_2S

Nordstrom et al. (2007) reviewed the sulphur isotope chemistry of the acid mine drainage-impacted Animas River catchment in the USA and found that:

- sulphide mineralisation was relatively light $\delta^{34}\text{S} = -7$ to $+2.5$ ‰
- hypogene (hydrothermal) sulphates were typically heavier at around $\delta^{34}\text{S} = +15$ to $+18$ ‰

Nordstrom et al (2007) further state that “*not more than a few ‰ fractionation takes place during oxidation of S_2^{2-} in pyrite to S^{6+} in dissolved sulfate*”. They cite Field (1966) as hypothesising that the $\delta^{34}\text{S}$ of sulphides would change little on oxidation to sulphate and that reported data suggest fractionation effects of -2 to $+3$ ‰.

Bacterial sulphate reduction typically results in a strong depletion in $\delta^{34}\text{S}$ (Habicht & Canfield, 1997) of between -5 and -45 ‰ Canfield and Teske, 1996; Detmers et al., 2015). The strongest isotopic depletions in sulphides may be due to repeated cycles of oxidation of sulphides formed initially from sulphate reduction to sulphur, followed by bacterial disproportionation of the sulphur to sulphate (enriched in $\delta^{34}\text{S}$) and sulphide (depleted in $\delta^{34}\text{S}$) (Canfield & Thamdrup, 1994).

We can summarise the relatively sparse sulphur isotope data from this study as shown in Table 8.1. All of the primary sulphide mineralization samples exhibit a $\delta^{34}\text{S}$ signature that is compatible with primary magmatic sulphide. The sulphate minerals also exhibit negative signatures and thus show no evidence of fractionation due to admixture with other sulphate sources or sulphur/ SO_2 disproportionation. The mine water samples from Sherlovaya Gora also exhibit negative signatures similar to the primary sulphides: they are thus most likely derived from direct oxidation of sulphide minerals (or dissolution of secondary sulphates) and show no clear evidence (at least in the sulphate signatures) of subsequent bacterial sulphate reduction enriching the water in $\delta^{34}\text{S}$ (although this does not preclude bacterial sulphate reduction in niches that are quantitatively insignificant compared with the sulphate reservoir that the water represents).

Sample	Location	Type	$\delta^{34}\text{S}$ (‰)
Primary sulphide minerals			
Shg-A	Sherlovaya Gora	Sulphide (possibly arsenopyrite with some galena) n	-2.1
Shg-B	Sherlovaya Gora	Sulphide	-1.9
Shg-C	Sherlovaya Gora	Probably sphalerite mineralisation	-2.2
Shg-Ei	Novii Akatui	Pyrite/chalcopyrite from tailings area	+3.4
Shg-Eii	Novii Akatui	Sphalerite with small crystals of pyrite	+1.2
Massive sulphate (hydrothermal??)			
Shg-G	Balei	Massive gypsum	-0.2
Secondary sulphate minerals			
SG-14-1-4	Sherlovaya Gora	Possibly epsomite, maybe gypsum	-8.4
Dissolved sulphate in mine water			
Shg-01F	Sherlovaya Gora	Water from borehole 1	-0.4
Shg-03F	Sherlovaya Gora	Water from pond in tailings area	-2.2
Shg-101-F	Sherlovaya Gora	Water from opencast pit lake	-5.8

Table 8.1. Summary of sulphur isotope data from this study

9 REFERENCES

This section contains general references to literature cited in this report only.

Literature sources specific to each sampling locality are cited in the last subsection of each relevant Chapter.

Previous NGU reports resulting from collaboration with Tomsk State University are cited in Chapter 1.

Banks, D., Parnachev, V.P., Frengstad, B., Holden, W., Karnachuk, O.V. & Vedernikov, A.A. (2004). The evolution of alkaline, saline ground- and surface waters in the southern Siberian steppes. *Applied Geochemistry* 19, 1905-1926.

Banks, D. (2014). *A Hydrogeological Atlas of Faryab Province, Northern Afghanistan*. Published by NORPLAN (Asplan VIAK AS, Kristiansand, Norway) for the Ministry of Rural Rehabilitation and Development, Afghanistan and funded by NORAD.

Banks, D., Frank, Y.A., Kadnikov, V.V., Karnachuk, O.V., Watts, M., Boyce, A. (2014). Hydrochemical data report from sampling of two deep abandoned hydrocarbon exploration wells: Byelii Yar and Parabel', Tomsk oblast', western Siberia, Russian Federation. **Nor. Geol. Unders. report** 2014.034.

Canfield, D.E. & Teske, A. (1996). Late Proterozoic rise in atmospheric oxygen concentration inferred from phylogenetic and sulphur-isotope studies. *Nature* **382**, 127-132. doi:10.1038/382127a0

Canfield D.E. & Thamdrup B.T. (1994). The production of ^{34}S -depleted sulfide during disproportionation of elemental sulfur. *Science* **266**: 1973–1975. doi: 10.1126/science.11540246

- Clark, I.D. & Fritz, P. (1997).** *Environmental Isotopes in Hydrogeology*. CRC Press, 352 pp. ISBN: 9781566702492.
- Detmers, J., Brüchert, V., Habicht, K.S. & Kuever, J. (2015).** Diversity of sulfur isotope fractionations by sulfate-reducing prokaryotes. *Appl. Environ. Microbiol.* **67(2)**: 888-894. doi: 10.1128/AEM.67.2.888-894.2001
- Dickson, A.G. & Goyet, C. (eds.) (1994).** *Handbook of methods for the analysis of the various parameters of the carbon dioxide system in sea water; version 2*. U.S. Dept. of Energy, ORNL/CDIAC-74.
- Frengstad, B., Banks, D. & Siewers, U. (2001).** The chemistry of Norwegian groundwaters: IV. The pH-dependence of element concentrations in crystalline bedrock groundwaters. *The Science of the Total Environment* **277**, 101-117. doi: 10.1016/S0048-9697(00)00867-6.
- Frietsch, R., Billström, K. & Perdahl, J.A. (1995).** Sulphur isotopes in Lower Proterozoic iron and sulphide ores in northern Sweden. *Mineralium Deposita* **30**: 275-284.
- Habicht, K.S. & Canfield, D.E. (1997).** Sulfur isotope fractionation during bacterial sulfate reduction in organic-rich sediments. *Geochim. Cosmochim. Acta* **61(24)**: 5351-5361. doi:10.1016/S0016-7037(97)00311-6
- MBARI (2014).** *The MBARI Chemical Sensor Program: Periodic Table of Elements in the Ocean*. Monterey Bay Aquarium Research Institute. Website: <http://www.mbari.org/chemsensor/pteo.htm>. Accessed November 2014.
- Nordstrom, D.K., Wright, W.G., Mast, M.A., Bove, D.J. & Rye, R.O. (2007).** Aqueous-sulfate stable isotopes—a study of mining-affected and undisturbed acidic drainage. Chapter E8 in: Church, S.E., von Guerard, P. & Finger, S.E. (eds.) *“Integrated Investigations of Environmental Effects of Historical Mining in the Animas River Watershed, San Juan County, Colorado”*. U.S. Geological Survey Professional Paper **1651**: 391:416.
- Paytan, A., Gray, E.T., Ma, Z., Erhardt, A. and Faul, K. (2012).** Application of sulphur isotopes for stratigraphic correlation. *Isotopes in Environmental and Health Studies* **48(1)**: 195-206. doi: 10.1080/10256016.2011.625423
- Parnachev, V.P., Banks, D., Berezovsky, A.Y. & Garbe-Schönberg, D. (1999).** Hydrochemical evolution of Na-SO₄-Cl groundwaters in a cold, semi-arid region of southern Siberia. *Hydrogeology Journal*, 7, 546-560.
- Rye, R.O. (2005).** A review of the stable-isotope geochemistry of sulfate minerals in selected igneous environments and related hydrothermal systems. *Chemical Geology* **215**: 5 – 36. doi:10.1016/j.chemgeo.2004.06.034.
- SAHRA (2014).** *Oxygen isotopes*. Sustainability of semi-arid hydrology and riparian areas (SAHRA) website. <http://web.sahra.arizona.edu/programs/isotopes/oxygen.html>. Accessed May 2014.
- Seal, R.R. (2006).** Sulfur isotope geochemistry of sulfide minerals. *Reviews in Mineralogy & Geochemistry* **61**: 633-677. doi: 10.2138/rmg.2006.61.12.
- USGS (2004a).** Resources on isotopes. Fundamentals of stable isotope geochemistry. United States Geological Survey website <http://wwwrcamnl.wr.usgs.gov/isoig/res/funda.html>, last updated January 2004, accessed August 2015.

USGS (2004b). Resources on isotopes. Periodic table - sulfur. United States Geological Survey website http://wwwrcamnl.wr.usgs.gov/isoig/period/s_iig.html, last updated January 2004, accessed August 2015.

10 APPENDIX A: REPORT BY D.A. IVASENKO ON SAMPLING AND ANALYSIS (BY TOMSK STATE UNIVERSITY) BY ICP-MS, SCANNING ELECTRON MICROSCOPE / ENERGY DISPERSIVE X-RAY SPECTROSCOPY (SEM-EDS) AND X-RAY DIFFRACTION (XRD) METHODS

ТОМСКИЙ ГОСУДАРСТВЕННЫЙ УНИВЕРСИТЕТ
КАФЕДРА ФИЗИОЛОГИИ РАСТЕНИЙ И БИОТЕХНОЛОГИИ

TOMSK STATE UNIVERSITY

DEPARTMENT OF PLANT PHYSIOLOGY AND BIOTECHNOLOGY

ГИДРОХИМИЧЕСКИЙ АНАЛИЗ ГРУНТОВЫХ ВОД КАРЬЕРА ДОБЫЧИ МЕТАЛЛОВ
НА ТЕРРИТОРИИ ГОРНО-РУДНЫХ МЕСТОРОЖДЕНИЙ ЗАБАЙКАЛЬСКОГО КРАЯ
РОССИЙСКОЙ ФЕДЕРАЦИИ

*HYDROCHEMICAL ANALYSIS OF GROUNDWATER FROM METAL ORE OPENCASTS IN
THE MINING BELT OF ZABAIBALSK REGION, RUSSIAN FEDERATION*

ЭКСПЕДИЦИЯ В ЗАБАЙКАЛЬСКИЙ КРАЙ. 2014г.

EXPEDITION TO ZABAIBALSK REGION, 2014

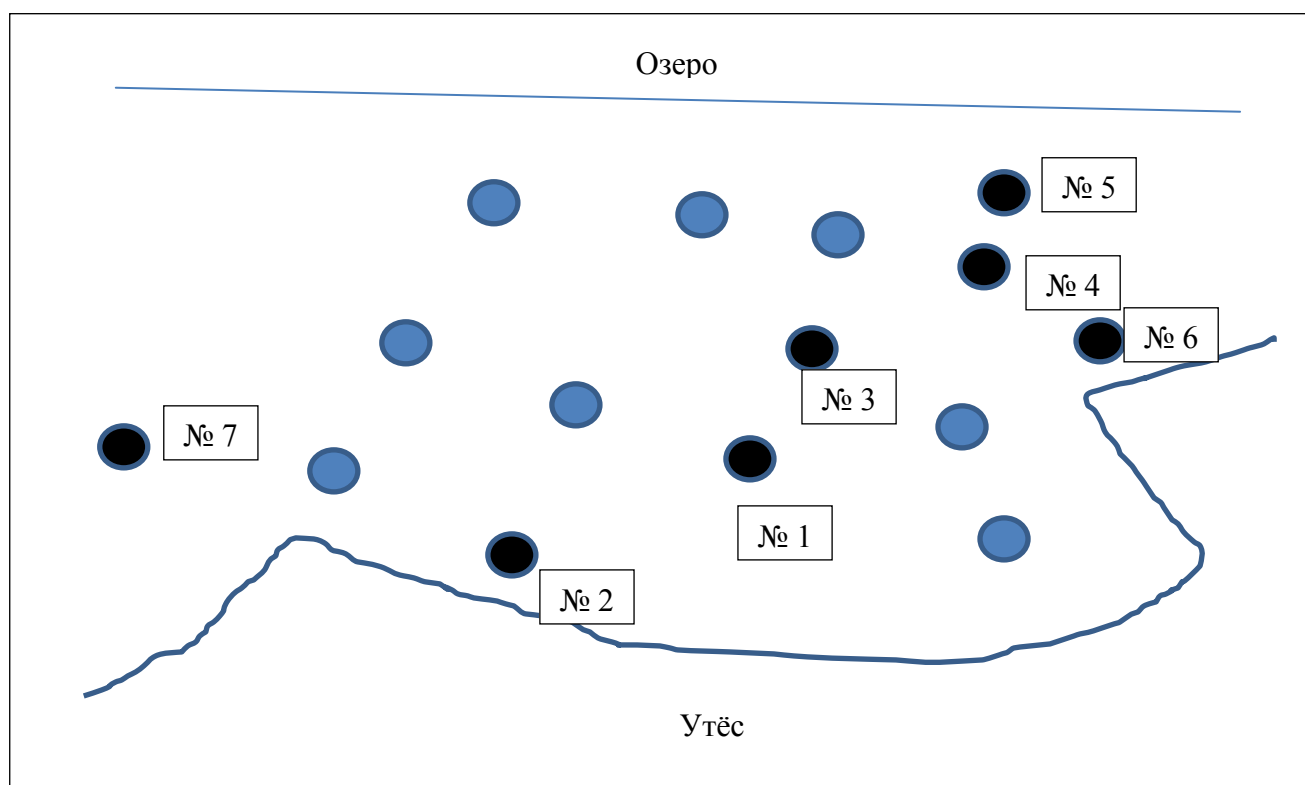
2014



1. ОПИСАНИЕ МЕСТ ОТБОРА ПРОБ (*DESCRIPTION OF SAMPLE LOCALITIES*)

Шерловогорский ГОК (*Sherlovaya Gora*) пгт. Шерловая гора, Борзинский район, Забайкальский край, Россия

Пробы для анализа были отобраны с 27.07.14 по 30.07.14 года на территории карьера и хвостохранилища Шерловогорского ГОК, расположенного рядом с пгт. Шерловая гора Борзинского района, Забайкальского края. С 1932 г. добывалась оловянная руда (касситерит). В 1995 г. в связи с истощением месторождения ГОК был закрыт.

Перечень и описание полученных проб (*Sketch map of sampled boreholes on opencast bench*):



-  - пустая скважина (*dry borehole*)
-  - опытная скважина

1. Образец **ШГ-14-1** - Глубина скважины 7,5 м. Высота водяного столба около 1 м. Цвет воды – интенсивный оранжево-красный.

T = 6,5 – 6,6

pH = 2,58

Eh = + 494 mV

Отобраны: 3 фалькона – посев + ДНК

2 фалькона – профильтрованы через фильтр 0,2 мкм (ICP-MS)
2 мембранных фильтра на посев
Пименов: сульфатредукция, стабильные изотопы, метан
Виталий: метагеном

2. Образец ШГ-14-7

Скважина 6
T = 4,4
Eh = + 365 mV
pH = 3,19
Отбрали:
Мы: 1 фалькон посев/ДНК
Виталий: 10 л метагеном

3. Образец ШГ-14-8

Скважина 7.
T = 6,5
pH = 2,65
Eh = + 447 mV
Цвет светло-желтый
Отбрали:
1 фалькон 50мл на выделение ДНК
2 фалькона ICP-MS
Виталий: 15 л метагеном

4. Образец ШГ-14-2 - (Бывший ШГ-4) под камнем - глинистая влажная порода темно-серого цвета с наслоениями осадка голубого цвета, Отбрано 2 пластиковых фалькона по 50 мл. Взяли на интенсивность сульфат редукции и на посев.

5. Образец ШГ-14-3 (Хвостохранилище)

Вода прозрачная голубовато-зеленоватая, все дно покрыто обрастаниями зеленого цвета, явные стримеры серовато-зеленоватые, слизь.
T = 22
pH = 3,73
Eh = + 430 mV
Отбрали:
Мы: 2 фалькона по 50 мл на ICP-MS
3 фалькона – посев/ДНК/SEM
Отбрали на посев/ДНК – маты + стримеры + осадок под ними, все смешали
Эржена: маты
Виталий: маты/осадок
Пименов: интенсивность

п. Новый Акатуй (*Novii Akatui*) Александрово-Заводского района Забайкальского края
Акатуевское рудное поле расположено на территории одного из старейших рудных районов Забайкалья, изучение которого было начато еще в XVIII веке. С 1993 г. по 2002 г. на Северо-Акатуевском месторождении проводились эксплуатационные работы.

Месторождение располагается на северо-западной окраине п. Новый Акатуй Александрово-Заводского района, площадь участка 12,1 квадратных км.

Месторождение содержит:

- Свинец - запасы балансовые по категории С1 - 7,8 тысячи тонн, С2 - 7,8 тысячи тонн; забалансовые по С1 - 5,6 тысячи тонн; прогнозные ресурсы по Р1 - 24,5 тысячи тонн.
- Цинк - запасы балансовые по С1 - 14,3 тысячи тонн, по С2 - 7,7 тысячи тонн; прогнозные по Р1 - 45,5 тысячи тонн.
- Серебро - запасы балансовые по С1 - 15,4 тонны, по С2 - 1,2 тонны; забалансовые по С1 - 12,7 тонны.
- Золото - балансовые по С1 - 189 кг, забалансовые по С1 - 804 кг.
- Кадмий - запасы балансовые по С2 - 69 тонн.

6. Образец ШГ-14-4

Болото под дамбой. Окисление, рыжие зоны. Железистые стримеры оранжевые + зелёные.

Выход подземной воды.

T = 9,7

pH = 6,7

Eh = + 258 mV

Отобрали:

Мы: 1 фалькон DGGE

2 фалькона на ICP-MS

2 фалькона на щёлочность

1 фалькон ацетат цинка – 5 мл + 2 мл пробы (осадка нет)

Виталий: маты

Пименов: интенсивность

Женя: 1 фалькон – маты

1 фалькон из выхода, где были черные зоны с пленкой серы и интенсивный запах сероводорода.

7. Образец ШГ-14-5

Выход из штольни

T = 2,8

pH = 7,15

Eh = + 271 mV

Массовые зеленые стримеры

Маты на дереве

Мат 2,5-3 мм

Слои:

Зеленый

Желтый

Белый

Черный

Отобрали:

Маты в фалькон

2 фалькона на ICP-MS

Женя: мат

Идея: DGGE мата

8. Образец ШГ-14-6

Ручей идущий в хвостохранилище. Примешивается вода, выходящая из шахты.

T = 16,9

pH = 6,5

Eh = + 435 mV

Отобрали:

Мы: 1 фалькон на посев

2 фалькона на ICP-MS

Карьер.

Идея: посмотреть стабильную изотопию и биоразнообразие в различных скважинах.

Скважина 4 аналогична по pH скважине 1. Скважина 6 более глубокая и менее окисленная, скважина 7 более глубокая с прозрачной водой на заметном отдалении от остальных скважин.

Дэвид: Если температура низкая – должен быть подток подземных вод. В скв. 4 очень мало воды, поэтому решили отобрать из скв.6 и скв.7.

Балей (*Balei*)

город в Забайкальском крае России расположен на реке Унда, в 350 км от Читы. Административный центр Балейского муниципального района.

Основа промышленности города — золотодобыча. До 1917 года это место дало стране около 40 тонн золота, а к 1994 году свыше 400 тонн золота, в последнее время добыча золота официально не ведётся.

9. Образец ШГ-14-9 (у Бэнкса проба 10)

Другое хвостохранилище, не то, которое пробовали в прошлый раз. Много воды, растительность, синий цвет.

Окисление желтое, на дамбе выходы гипса.

T = 25,2

pH = 3,4

Eh = + 468 mV

Жирекенский ГОК (*Zhireken*)

Жирекенское месторождение расположено в Чернышевском районе Забайкальского Края (Восточная Сибирь), в 400 км от г. Читы и 7 км от Транссибирской железнодорожной магистрали. Ближайший аэропорт расположен в г.Чите приблизительно в 400 км от Жирекенского комбината.

«Жирекенский ГОК» входит в состав Управляющей компании «Союзметаллресурс» (SMR).
Основная продукция ООО «Жирикенского ГОК»:

- Концентрат молибденовый;
- Концентрат медный;
- Ферромолибден;
- Нерудные строительные материалы и др.

Доказанные запасы Жирекенского молибденового месторождения составляют 10,6 млн. тонн; прогнозные запасы - 57,3 млн. тонн. Согласно техническому отчету, подготовленному компанией SRK, при объеме переработки в 4,0 млн. тонн в год расчетный срок эксплуатации Жирекенского ГОК составляет 17 лет.

Жирекенское месторождение было открыто в 1958 г.; первые геологоразведочные работы завершены в 1961-1966 гг. группой геологов Читинского геологического управления Министерства геологии РСФСР. Запасы месторождения были утверждены в 1966 г. Строительство Жирекенского комбината началось в 1982 г., и строительство первой очереди обогатительной фабрики было завершено в 1988 г. В период с 1996 по 1999 гг. Жирекенский завод простаивал и был вновь запущен в 2000 г. В 2003 г. был построен и пущен в эксплуатацию опытный завод по производству ферромолибдена с единственной подовой печью. Вторая подовая печь была построена в 2004 г. В 2005 г. для переработки молибденового концентрата в ферромолибден были построены цех обжига, дробильный цех, цех смешения и плавильный.

Однако с началом кризиса мировой экономики в 2008 году рентабельность предприятия стала отрицательной.

На данный момент предприятия законсервировано.

10. Образец ШГ-14-10 (у Бэнкса проба 11)

Хвостохранилище рН 6,4

ГОК молибден, руда молибденит – сульфит Мо. Примеси Se, Re, Fe пирит, халькопирит.

Большое хвостохранилище, вероятно подщелачивают известью.

Сбоку от дамбы хвостохранилища – вода, водоросли, трава.

T = 17,5

pH = 5,6

Eh = + 446 mV



Рис. 1. Место отбора проб ШГ-14-1, ШГ-14-7, ШГ-14-8.



Рис. 2. Место отбора проб ШГ-14-2.



Рис. 3. Место отбора пробы ШГ-14-3.



Рис. 4. Место отбора пробы ШГ-14-4.



Рис. 5. Место отбора пробы ШГ-14-5. Образец мата.



Рис. 6. Место отбора пробы ШГ-14-6.



Рис. 7. Место отбора пробы ШГ-14-9.



Рис. 8. Место отбора пробы ШГ-14-10.

Таблица №1. Результаты масс-спектрального анализа с индуктивно связанной плазмой. (ICP-MS analysis results by Tomsk State Univ.)

№ п/п	Номер пробы	ШГ-14-1	ШГ-14-3	ШГ-14-4	ШГ-14-5	ШГ-14-6	ШГ-14-7	ШГ-14-8	ШГ-14-10
	элемент	содержание, мг/дм ³	Содержание, мг/дм ³	Содержание, мг/дм ³	Содержание, мг/дм ³	Содержание, мг/дм ³	Содержание, мг/дм ³	Содержание, мг/дм ³	Содержание, мг/дм ³
1	Li	1,04	0,74	0,011	0,0033	0,010	0,52	0,39	0,012
2	Be	0,57	0,27	<0,0001	<0,0001	0,0032	0,33	0,14	<0,0001
3	B	<0,002	0,11	0,079	0,074	0,052	0,014	0,064	<0,002
4	Na	5,2	137,1	4,4	2,7	5,9	22,9	1,4	21,4
5	Mg	421	462	33	32	35	365	139	32
6	Al	505	115	0,094	0,11	0,081	19	154	0,022
7	Si	39	28	6,9	7,3	7,4	19	14	0,89
8	P	18,9	0,077	<0,07	<0,07	<0,07	2,0	2,4	<0,07
9	K	0,81	10,9	2,1	1,2	1,7	12,9	0,059	3,5
10	Ca	255	564	188	152	171	377	81	131
11	Sc	0,19	<0,002	<0,002	<0,002	0,010	0,057	0,085	0,019
12	Ti	0,14	0,029	0,019	0,0094	0,012	0,027	0,094	0,0047
13	V	0,0076	<0,002	<0,002	<0,002	<0,002	<0,002	<0,002	<0,002
14	Cr	0,21	0,16	0,27	0,18	0,15	0,30	0,38	0,056
15	Mn	731	253	0,24	0,014	0,18	524	46	0,0029
16	Fe	1916	0,41	0,89	0,46	1,28	305	401	0,95
17	Co	3,1	3,7	0,00061	0,00020	0,00066	3,0	1,2	0,0011
18	Ni	3,7	13,6	0,052	0,079	0,052	3,4	2,0	0,040
19	Cu	98	16	0,0054	0,0040	0,0039	0,95	6,95	0,022
20	Zn	3185	1041	0,56	1,70	1,00	1639	596	<0,002
21	Ga	0,034	0,069	0,00060	<0,0002	0,00037	0,0094	0,0086	0,00035
22	Ge	0,012	0,0033	<0,0002	<0,0002	<0,0002	0,0010	0,0015	<0,0002
23	As	0,143	0,030	0,076	0,074	0,35	0,0081	0,89	0,0021
24	Se	0,067	0,067	0,00062	0,0024	0,0026	0,14	0,10	0,025
25	Br	0,056	0,33	0,11	0,010	0,011	0,014	0,020	0,016
26	Rb	0,033	0,13	0,0030	0,0020	0,0039	0,23	0,010	0,0081

27	Sr	0,73	1,05	0,83	0,49	0,65	2,15	0,24	1,96
28	Y	6,9	3,9	0,0013	0,0011	0,018	2,0	4,2	<0,0001
29	Zr	0,014	0,00068	0,00093	<0,0002	0,00180	0,010	0,0061	0,0022
30	Nb	0,0019	<0,0001	<0,0001	0,00046	<0,0001	<0,0001	<0,0001	0,00015
31	Mo	0,0060	0,0019	0,0057	0,0024	0,0039	<0,0002	<0,0002	0,81
32	Ag	0,0012	0,00065	<0,0001	<0,0001	<0,0001	0,00092	0,00053	<0,0001
33	Cd	18	37	<0,0001	0,0029	0,0035	8,3	38,8	0,0011
34	In	1,01	0,00047	<0,00005	<0,00005	<0,00005	0,0080	0,11	<0,00005
35	Sn	0,072	0,0030	0,0012	<0,0002	<0,0002	0,0070	0,010	0,0011
36	Sb	0,024	0,0018	0,0032	0,0057	0,0064	<0,0001	0,0091	0,010
37	Te	<0,002	<0,002	<0,002	<0,002	<0,002	<0,002	<0,002	<0,002
38	I	0,010	0,0030	0,0017	0,00094	0,0016	0,0014	0,0032	0,0019
39	Cs	0,012	0,022	0,00017	0,00051	0,00050	0,024	0,0068	0,00052
40	Ba	0,042	0,048	0,035	0,0078	0,019	0,0055	0,0044	0,025
41	La	2,94	0,32	0,000077	0,00011	<0,00005	0,31	0,28	<0,00005
42	Ce	701	101	<0,00005	0,00018	<0,00005	0,79	0,77	<0,00005
43	Pr	0,82	0,2	<0,00005	<0,00005	<0,00005	0,092	0,11	<0,00005
44	Nd	3,09	0,93	<0,00005	<0,00005	<0,00005	0,38	0,44	<0,00005
45	Sm	0,76	0,39	<0,00005	<0,00005	<0,00005	0,94	0,19	<0,00005
46	Eu	0,082	0,014	<0,00005	<0,00005	<0,00005	0,017	0,017	<0,00005
47	Gd	0,95	0,54	<0,00005	<0,00005	<0,00005	0,17	0,34	<0,00005
48	Tb	0,17	0,11	<0,00005	<0,00005	<0,00005	0,033	0,086	<0,00005
49	Dy	1,07	0,70	<0,00005	<0,00005	<0,00005	0,24	0,62	<0,00005
50	Ho	0,22	0,13	<0,00005	<0,00005	<0,00005	0,054	0,13	<0,00005
51	Er	0,69	0,39	<0,00005	<0,00005	<0,00005	0,16	0,40	<0,00005
52	Tm	0,1	0,051	<0,00005	<0,00005	<0,00005	0,022	0,054	<0,00005
53	Yb	0,64	0,30	<0,00005	<0,00005	0,000056	0,13	0,33	<0,00005
54	Lu	0,093	0,039	<0,00005	<0,00005	<0,00005	0,019	0,047	<0,00005
55	Hf	0,0049	0,0040	<0,00005	<0,00005	<0,00005	0,0013	0,0030	<0,00005
56	Ta	0,028	0,00075	0,00021	<0,00005	<0,00005	0,00054	0,0012	0,000034
57	W	0,0075	0,0011	0,000051	0,00011	0,00020	0,0011	0,0024	0,00019
58	Au	<0,00005	<0,00005	<0,00005	<0,00005	<0,00005	<0,00005	<0,00005	<0,00005
59	Hg	0,00074	0,00075	<0,00005	<0,00005	<0,00005	<0,00005	<0,00005	0,00069

60	Tl	0,00038	0,0058	<0,00005	<0,00005	0,00005	0,0033	0,00021	<0,00005
61	Pb	0,32	2,20	0,00060	0,0029	0,014	0,32	0,46	0,0014
62	Bi	0,0099	<0,00005	0,000089	<0,00005	<0,00005	<0,00005	0,00014	0,00043
63	Th	2,79	0,0018080	<0,00005	<0,00005	<0,00005	0,0716589	0,2690608	<0,00005
64	U	2,35	0,73	0,0083	0,0037	0,0056	0,30	1,37	0,052
65	S	5373	2121	137		116	2210	1233	136

Для полученных проб воды и осадков изучены физико-химические параметры и определены концентрации растворенных металлов методом масс-спектрального анализа с индуктивно связанной плазмой.

Пробы ШГ-14-1, ШГ-14-3, ШГ-14-7, ШГ-14-8 характеризовались низким значением рН – 2,58; 3,73; 3,19; 2,65 соответственно. Основными металлами и металлоидами для этих проб были: натрий, магний, алюминий, железо, цинк, мышьяк, кроме того выявлено наличие лантаноидов.

Высокие концентрации серы свидетельствуют об активном протекании процесса окисления, что приводит к понижению уровня рН и выведению металлов в раствор. Наиболее вероятная форма серы в водной фазе – сульфат.

3. РЕЗУЛЬТАТЫ АНАЛИЗА ОБРАЗЦОВ МЕТОДОМ РАСТРОВОЙ ЭЛЕКТРОННОЙ МИКРОСКОПИИ (*SEM-EDS RESULTS*)

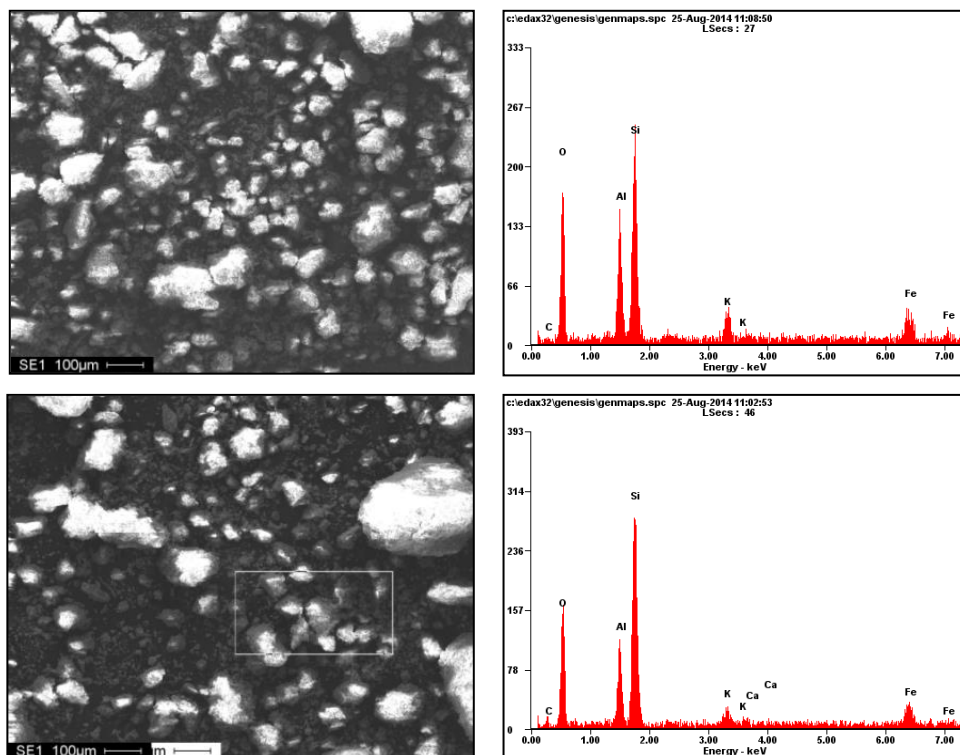


Рис. 9. Микрофотографии (SEM 515) осадков ШГ-14-2 и соответствующие им ЭДС на разном увеличении.

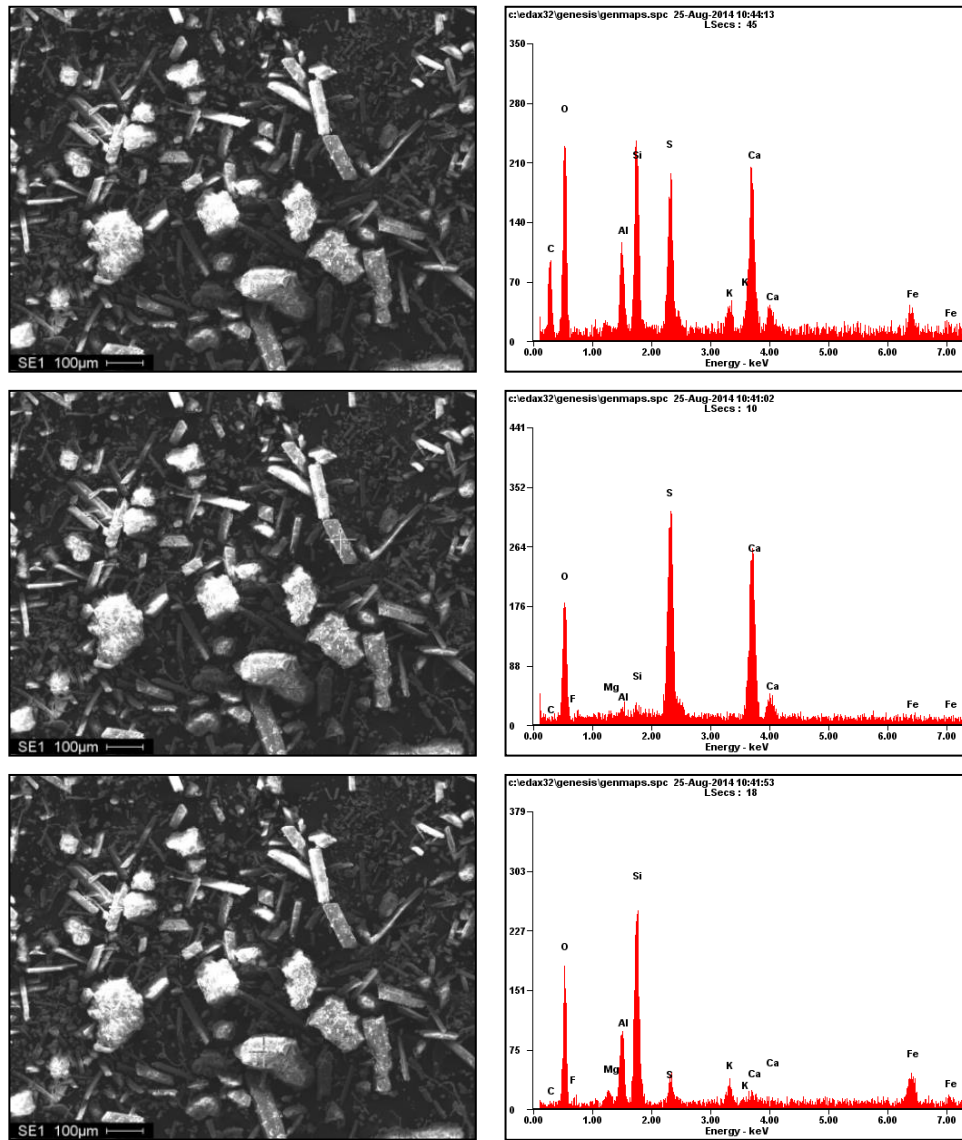


Рис. 10. Микрофотографии (SEM 515) осадков ШГ-14-3 и соответствующие им ЭДС на разном увеличении.

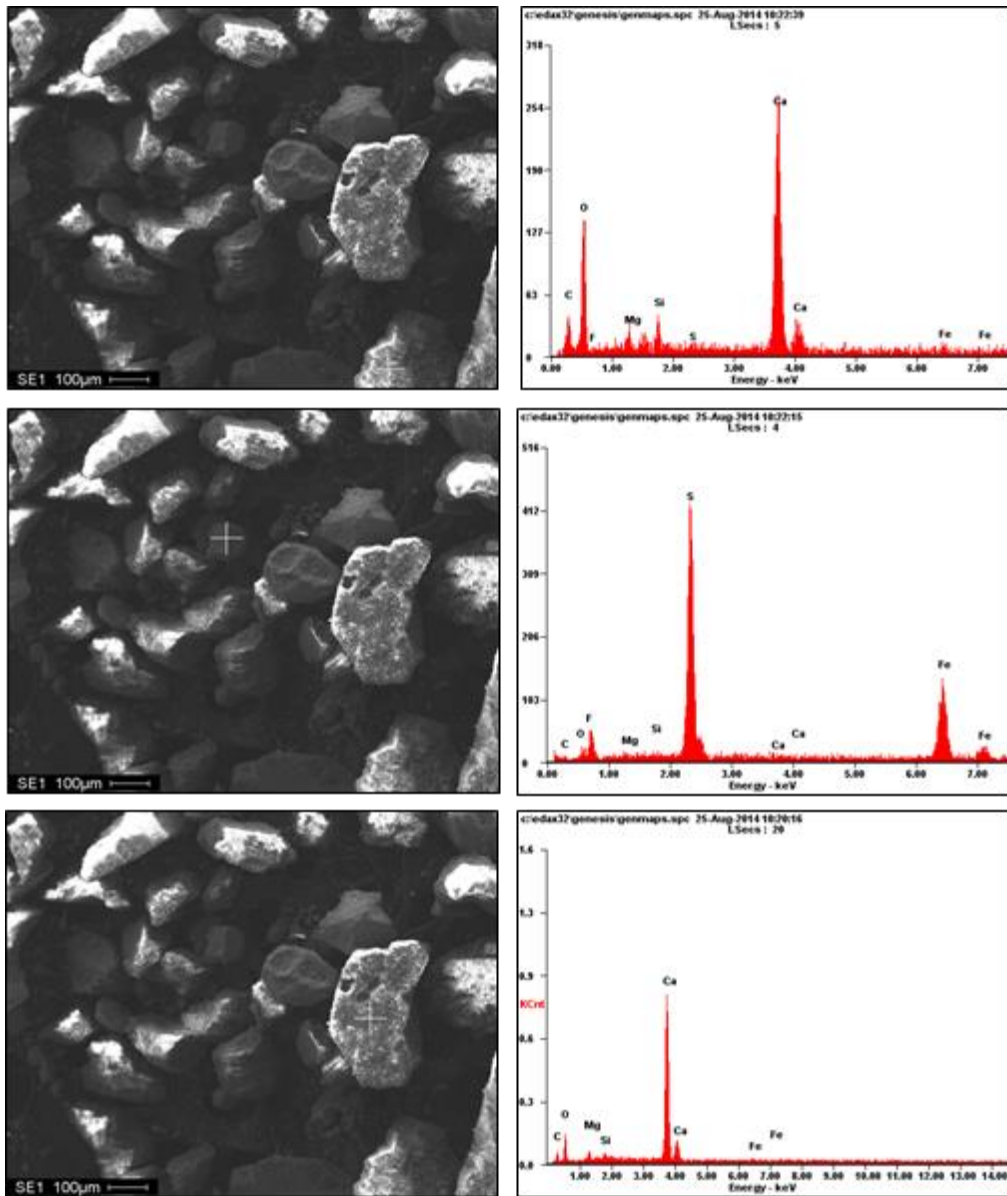


Рис. 11. Микрофотографии (SEM 515) осадков ШГ-14-6 и соответствующие им ЭДС на разном увеличении.

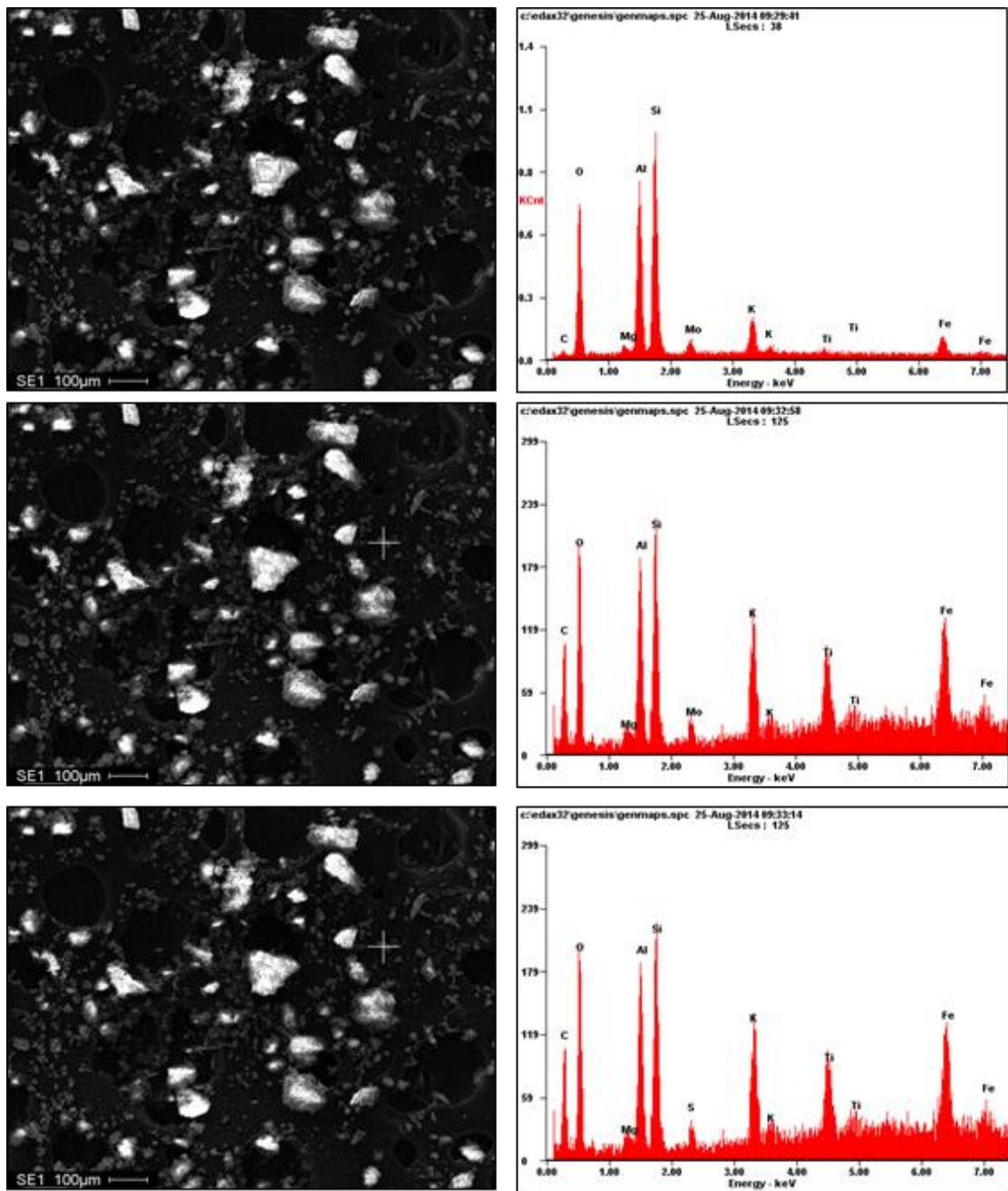


Рис. 12. Микрофотографии (SEM 515) осадков ШГ-14-9 и соответствующие им ЭДС на разном увеличении.

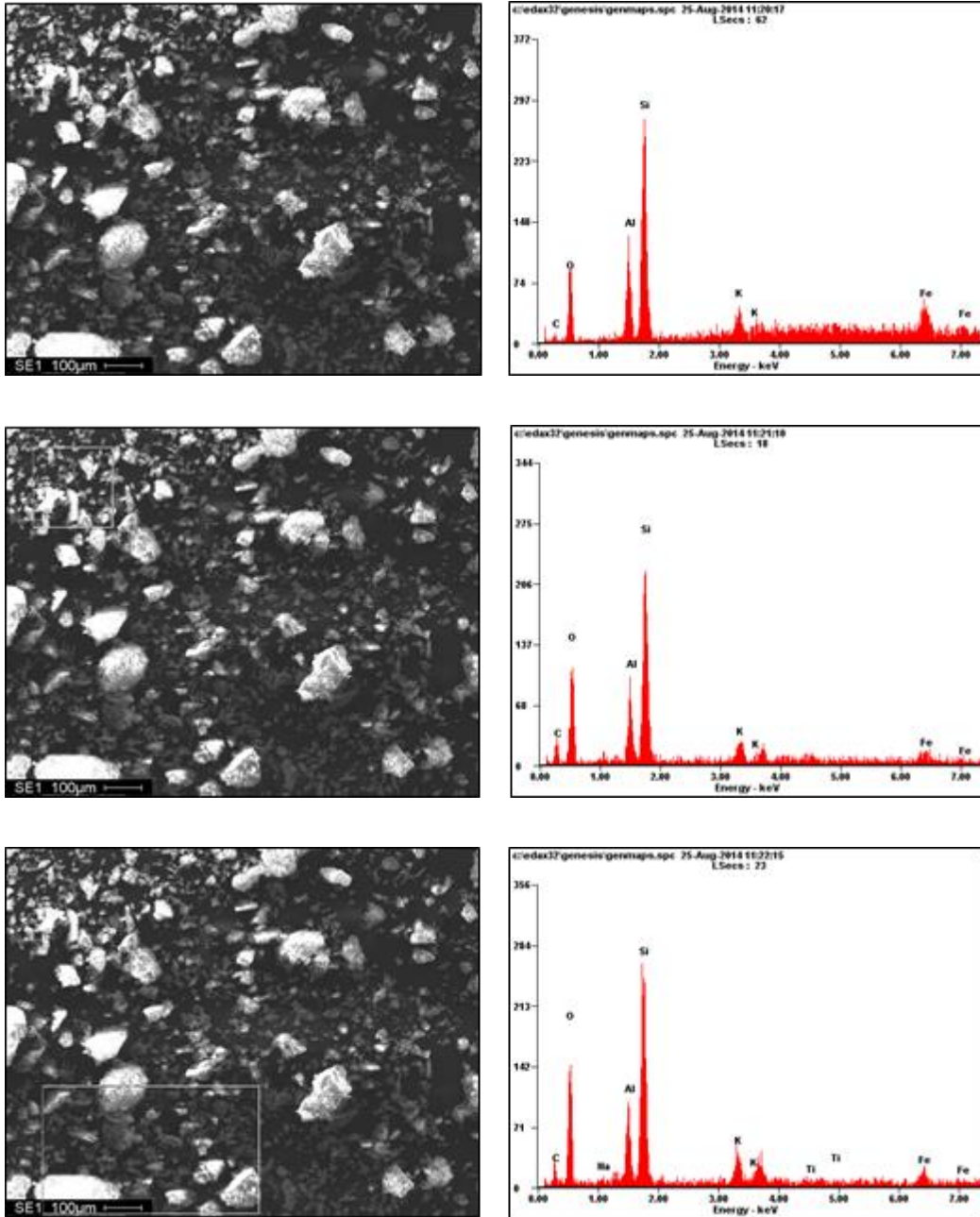


Рис. 13. Микрофотографии (SEM 515) осадков ШГ-14-10 и соответствующие им ЭДС на разном увеличении.

Таблица 2 – Весовая и атомная доля элементов, обнаруженных в осадках (не пересчитаны по углероду)

Элемент	ШГ-14-2		ШГ-14-3		ШГ-14-6		ШГ-14-9		ШГ-14-10	
	Весовая доля (Wt %)	Атомная доля (At %)	Весовая доля (Wt %)	Атомная доля (At %)	Весовая доля (Wt %)	Атомная доля (At %)	Весовая доля (Wt %)	Атомная доля (At %)	Весовая доля (Wt %)	Атомная доля (At %)
<i>C</i>	14,77	22,80	37,37	49,27	22,16	34,19	09,93	16,02	16,76	27,00
	06,57	10,77	00,00	00,00	09,36	20,06	37,42	51,74	31,15	42,32
			07,36	12,12	19,20	29,97	38,12	52,09	24,42	34,64
<i>O</i>	45,34	52,54	40,41	40,00	36,26	42,00	46,52	56,34	35,40	42,79
	49,05	60,39	65,38	80,53	08,23	13,25	33,58	34,86	41,98	42,81
			44,50	54,96	44,02	51,60	33,62	34,49	44,54	47,42
<i>F</i>	-	-	-	-	05,04	04,92	-	-	-	-
	-	-	00,00	00,00	16,10	21,81	-	-	-	-
			04,08	04,24	-	-	-	-	-	-
<i>Mg</i>	-	-	-	-	02,55	01,94	00,79	00,63	-	-
	-	-	00,44	00,36	01,89	02,00	00,77	00,52	-	-
			02,11	01,71	03,43	02,65	00,77	00,52	-	-
<i>Na</i>	-	-	-	-	-	-	-	-	-	-
	-	-	-	-	-	-	-	-	-	-
			-	-	-	-	-	-	00,84	00,62
<i>Al</i>	08,72	05,99	03,22	01,89	01,29	00,88	13,51	09,70	10,20	07,31
	12,39	09,05	01,17	00,85	-	-	06,34	03,90	06,05	03,66
			08,55	06,26	-	-	06,35	03,86	06,77	04,27
<i>Si</i>	24,33	16,06	06,35	03,58	06,65	04,39	20,60	14,21	27,34	18,83
	23,17	16,25	00,78	00,55	00,75	00,69	07,10	04,20	16,98	09,86
			22,04	15,51	01,71	01,14	07,12	04,16	18,43	11,18
<i>Mo</i>	-	-	-	-	-	-	02,54	00,51	-	-
	-	-	-	-	-	-	01,64	00,28	-	-
			-	-	-	-	-	-	-	-
<i>S</i>	-	-	04,65	02,03	07,57	04,37	-	-	-	-
	-	-	15,81	09,72	37,17	29,84	-	-	-	-
			02,84	01,75	-	-	00,85	00,44	-	-
<i>K</i>	01,95	00,93	00,95	00,39	-	-	02,99	01,48	03,41	01,69
	02,87	01,45	-	-	-	-	03,34	01,42	01,85	00,77
			01,83	00,93	-	-	03,30	01,39	02,46	01,07
<i>Ca</i>	00,42	00,20	05,23	02,07	09,04	04,18	-	-	-	-
	-	-	15,84	07,79	00,78	00,50	-	-	-	-
			01,09	00,54	30,44	14,24	-	-	-	-
<i>Fe</i>	04,46	01,48	01,81	00,51	09,45	03,14	02,63	00,91	06,89	02,39
	05,95	02,10	00,57	00,20	25,72	11,85	06,62	01,97	01,99	00,58
			05,58	01,98	01,21	00,41	06,67	01,96	02,19	00,67
<i>Ti</i>	-	-	-	-	-	-	00,47	00,19	-	-
	-	-	-	-	-	-	03,19	01,11	-	-
			-	-	-	-	03,20	01,09	00,36	00,13

4. ДИФРАКЦИОННЫЙ АНАЛИЗ ОСАДКОВ (*XRD ANALYSES OF PRECIPITATES*)

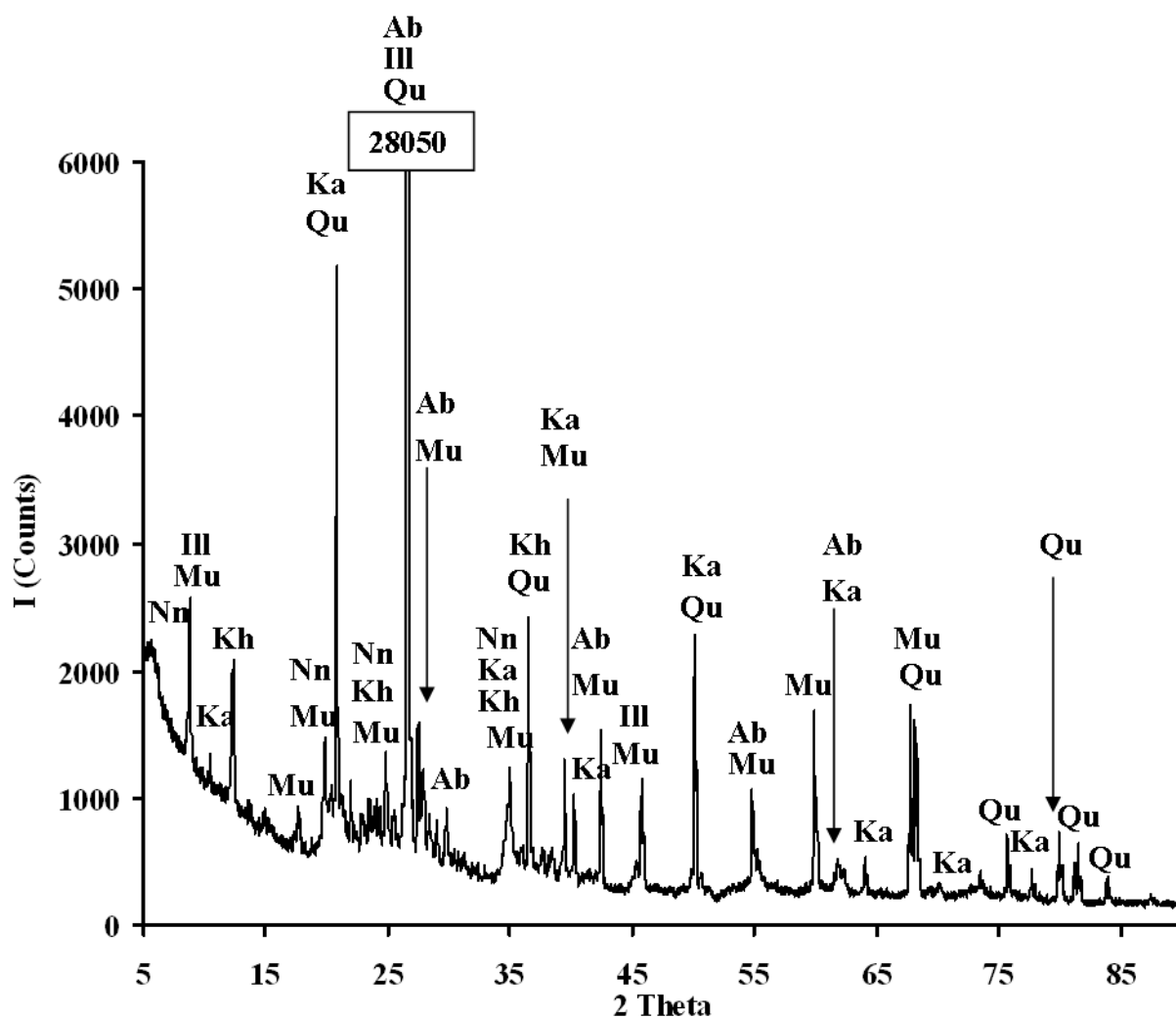


Рис.14. – ШГ-14-2.

Обозначения на дифрактограмме:

Mu – мусковит, $KAl_2(AlSi_3O_{10})(OH)_2$

Kh – клинохлор, $(Mg,Fe,Al)_6(Si,Al)_4O_{10}(OH)_8$

Qu - кварц, SiO_2

Ab – альбит, $(Na,Ca)Al(Si,Al)_3O_8$

Nn – Нонтронит, $(Na,Ca)_{0.3}Fe_2(Si,Al)_4O_{10}(OH)_2 \cdot H_2O$

Ill – иллит, $(K_{0.71}Ca_{0.01}Na_{0.01})(Al_{1.86}Mg_{0.15}Fe_{0.04})((Si_{3.27}Al_{0.73})O_{10}(OH)_2)$

Ka - каолинит, $Al_2Si_2O_5(OH)_4$

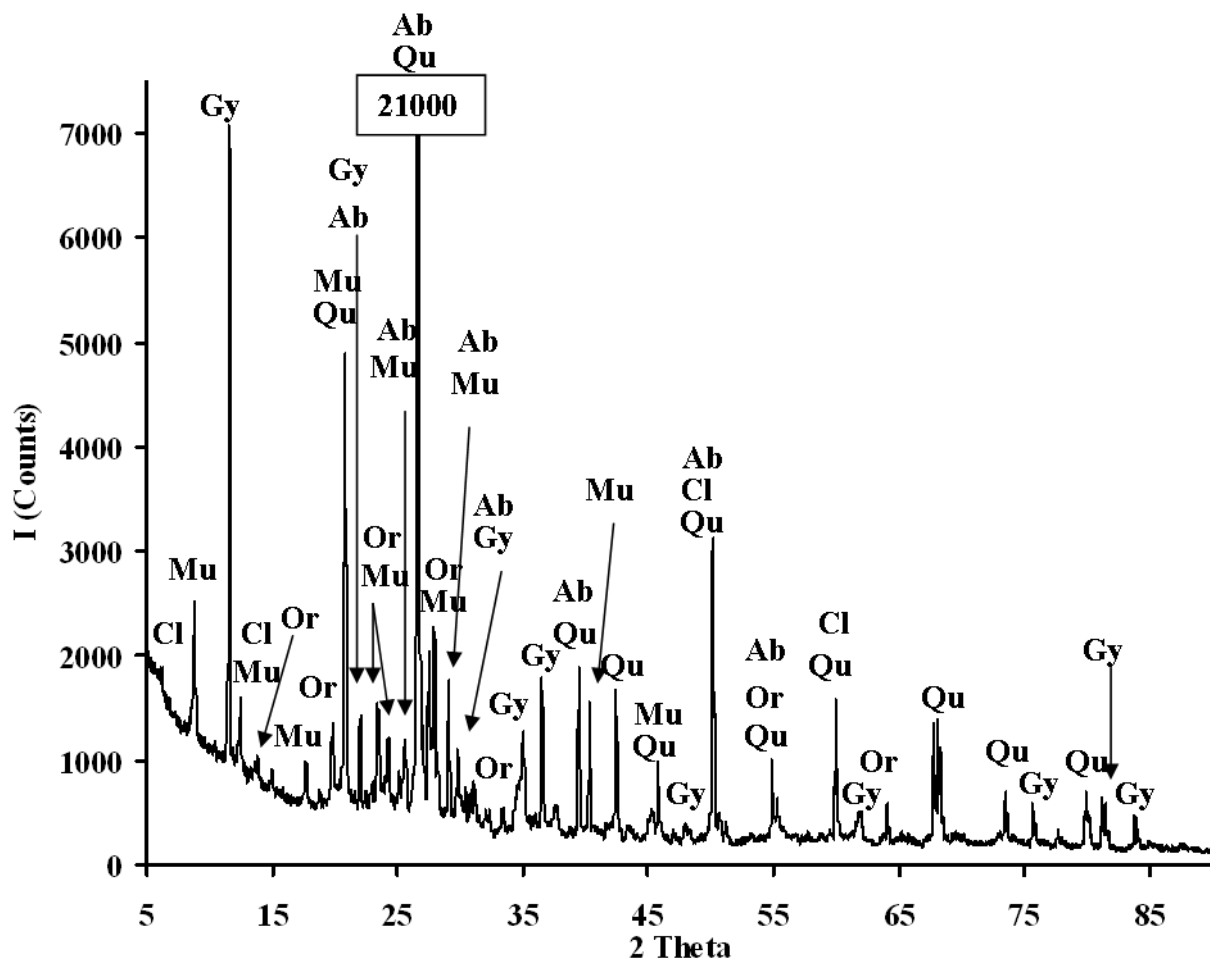


Рис. 15. – ШГ-14-3.

Обозначения на дифрактограмме:

Cl – хлорит (клинохлор), $Mg_{2.5}Fe_{1.65}Al_{1.5}Si_{2.2}Al_{1.8}O_{10}(OH)_8$

Qu - кварц, SiO_2

Ab – альбит, $(Na,Ca)Al(Si,Al)_3O_8$

Gy – гипс, $Ca(SO_4)(H_2O)_2$

Mu – мусковит, $KAl_2(AlSi_3O_{10})(OH)_2$

Or – ортоклаз, $K(AlSi_3)O_8$

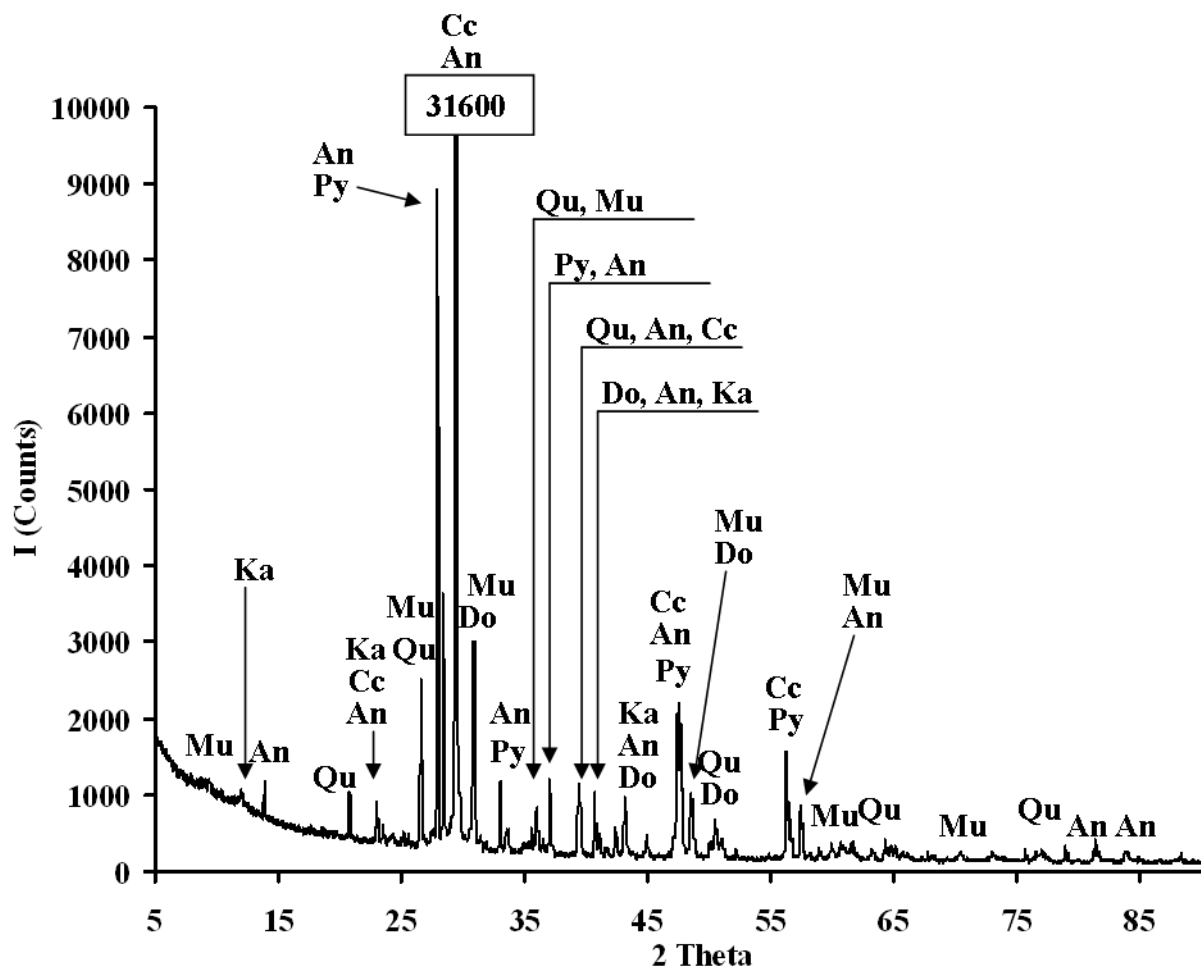


Рис.16. – ШГ-14-6.

Обозначения на дифрактограмме:

Qu - кварц, SiO_2

Ka - каолинит, $\text{Al}_2\text{Si}_2\text{O}_5(\text{OH})_4$

Py – пирит, FeS_2

Do – доломит, $\text{CaMg}(\text{CO}_3)_2$

An – анортит, $\text{CaAl}_2\text{Si}_2\text{O}_8$

Cc – кальцит, CaCO_3

Mu – мусковит, $\text{KAl}_2(\text{AlSi}_3\text{O}_{10})(\text{OH})_2$

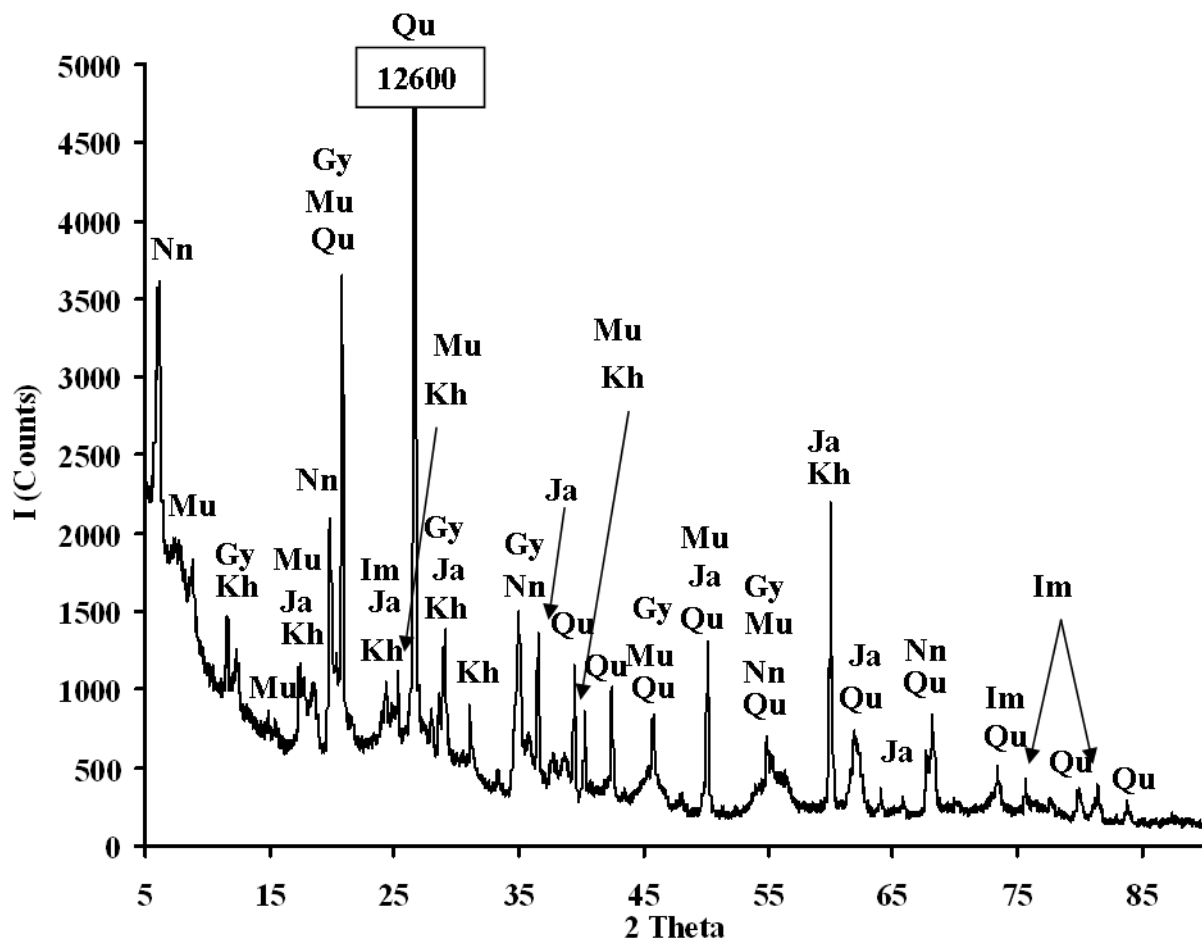


Рис.17. – ШГ-14-9.

Обозначения на дифрактограмме:

Ja – Ярозит, $\text{KFe}_3(\text{SO}_4)_2(\text{OH})_6$

Nn – Нонтронит, $(\text{Na},\text{Ca})_{0.3}\text{Fe}_2(\text{Si},\text{Al})_4\text{O}_{10}(\text{OH})_2 \cdot \text{H}_2\text{O}$

Kh – клинохлор, $(\text{Mg},\text{Fe},\text{Al})_6(\text{Si},\text{Al})_4\text{O}_{10}(\text{OH})_8$

Qu – кварц, SiO_2

Gy – гипс, $\text{Ca}(\text{SO}_4)(\text{H}_2\text{O})_2$

Mu – мусковит, $\text{KAl}_2(\text{AlSi}_3\text{O}_{10})(\text{OH})_2$

Im – ильменит, $\text{Fe}(\text{TiO}_3)$

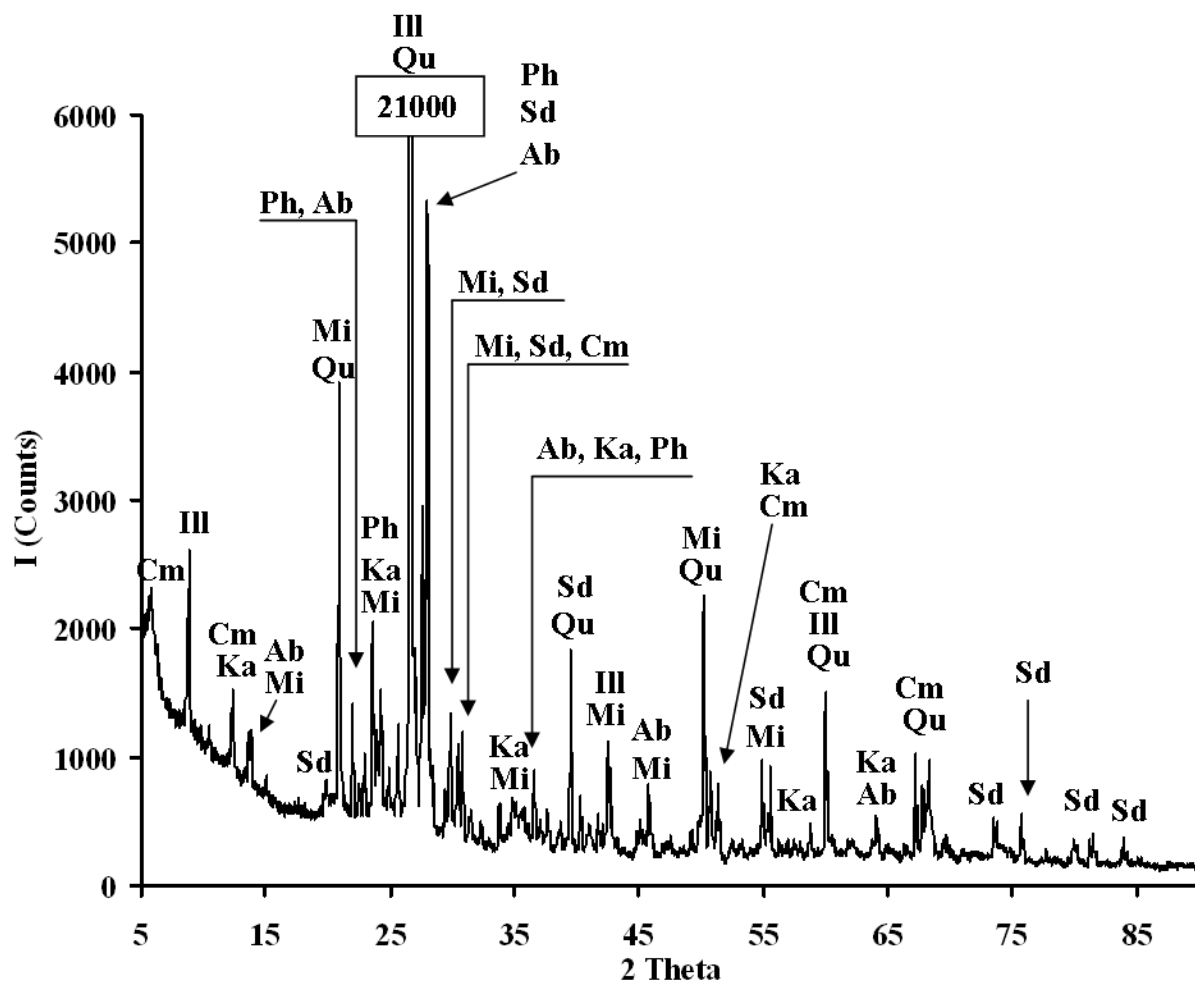


Рис. 18.– ШГ-14-10.

Обозначения на дифрактограмме:

Ph – филлипсит, $\text{Ca}_{1.64}\text{K}_2\text{Si}_{10.67}\text{Al}_{5.33}\text{O}_{32}(\text{H}_2\text{O})_{12}$

Sd – санидин, $(\text{K}_{0.86}\text{Na}_{0.14})(\text{AlSi}_3\text{O}_8)$

Cm – шамозит, $(\text{Fe,Al,Mg})_6(\text{Si,Al})_4\text{O}_{10}(\text{OH})_8$

Qu - кварц, SiO_2

Mi – Микролин, $\text{K}_{0.94}\text{Na}_{0.06}\text{Al}_{0.95}\text{Si}_{3.05}\text{O}_8$

Ab – альбит, $(\text{Na,Ca})\text{Al}(\text{Si,Al})_3\text{O}_8$

Ka - каолинит, $\text{Al}_2\text{Si}_2\text{O}_5(\text{OH})_4$

Ill – иллит, $(\text{K}_{0.71}\text{Ca}_{0.01}\text{Na}_{0.01})(\text{Al}_{1.86}\text{Mg}_{0.15}\text{Fe}_{0.04})((\text{Si}_{3.27}\text{Al}_{0.73})\text{O}_{10}(\text{OH})_2)$

5. ОПИСАНИЕ МИНЕРАЛОВ (*DESCRIPTIONS OF MINERALS*)

Mi – Микролин, $K_{0.94}Na_{0.06}Al_{0.95}Si_{3.05}O_8$

Cl – хлорит (клинохлор), $Mg_{2.5}Fe_{1.65}Al_{1.5}Si_{2.2}Al_{1.8}O_{10}(OH)_8$

Ja – Ярозит, $KFe_3(SO_4)_2(OH)_6$

Nn – Нонтронит, $(Na,Ca)_{0.3}Fe_2(Si,Al)_4O_{10}(OH)_2 \cdot H_2O$

Sd – санидин, $(K_{0.86}Na_{0.14})(AlSi_3O_8)$

Cm – шамозит, $(Fe,Al,Mg)_6(Si,Al)_4O_{10}(OH)_8$

Do – доломит, $CaMg(CO_3)_2$

An – анортит, $CaAl_2Si_2O_8$

Cc – кальцит, $CaCO_3$

Kh – клинохлор, $(Mg,Fe,Al)_6(Si,Al)_4O_{10}(OH)_8$

Qu - кварц, SiO_2

Ab – альбит, $(Na,Ca)Al(Si,Al)_3O_8$

Gy – гипс, $Ca(SO_4)(H_2O)_2$

Mu – мусковит, $KAl_2(AlSi_3O_{10})(OH)_2$

Ill – иллит, $(K_{0.71}Ca_{0.01}Na_{0.01})(Al_{1.86}Mg_{0.15}Fe_{0.04})((Si_{3.27}Al_{0.73})O_{10}(OH)_2)$

Ка - каолинит, $Al_2Si_2O_5(OH)_4$

Or – ортоклаз, $K(AlSi_3)O_8$

Im – ильменит, $Fe(TiO_3)$

Sd – санидин, $(K_{0.86}Na_{0.14})(AlSi_3O_8)$

Санидин (англ. Sanidine) — минерал, формула $K(AlSi_3)O_8$, типичные примеси Fe,Ca,Na,H₂O, молекулярный вес 274,30. Происхождение названия — от греческого sanis — «табличка» и idos — «вид», из-за его таблитчатого **габитуса**

Цвет минерала — бесцветный, белый, серый, желтовато-белый, красновато-белый, цвет черты — белый, прозрачный или полупрозрачный, блеск — стеклянный. Точное разделение между санидином, микроклином, анортоклазом и ортоклазом можно провести исходя из оптических свойств и результатов рентгено-структурного анализа.

Санидин типичен для экскурзивных изверженных пород, где происходит быстрое остывание породы. Санидин -высокотемпературный КПШ. Его структура стабильна

при 900° С и выше. При 500 - 900° С стабильна структура ортоклаза , а при температуре меньшей 400° С стабилен мироклин . Структуры отличаются только степенью упорядочения атомов алюминия и кремния. С повышением температуры степень упорядочения уменьшается - структура санидина самая разупорядоченная.

В природе санидин встречается в виде таблитчатых кристаллов светло-серого, серого цвета, реже бесцветные. Санидин обычно образуют уплощенные кристаллы. Санидин не образует волокнистого двойникования, характерного для другого КПШ - мироклина .

Санидин - довольно распространенный минерал, но ювелирные разновидности редки. Прозрачные образцы санидина гранят и используются для вставок в ювелирные изделия.

Ст – шамозит, $(\text{Fe,Al,Mg})_6(\text{Si,Al})_4\text{O}_{10}(\text{OH})_8$

Минерал из группы слоистых силикатов. Подгруппа высокожелезистых хлоритов. Кристалло-химическая формула $\text{Fe}_4^{+2}\text{Al}[\text{Si}_3\text{AlO}_{10}](\text{OH})_6$. Состав: $\text{SiO}_2 = 25 \div 28\%$, $\text{Al}_2\text{O}_3 = 15 \div 20\%$, $\text{FeO} = 35 \div 40\%$, Fe_2O_3 до 5%, H_2O до 5%. Растворим в горячей HCl . На термограммах имеется эндотермический эффект при 580 — 600°; второй эндотермический эффект (~900°) часто плохо выражен. Экзотермическая реакция при 920 — 950°. В очень небольших количествах распространен во многих п.: тундровых, дерново-подзолистых, серых лесных и т. п. Имеются указания на присутствие шамозитоподобных минералов в латеритах и ферраллитных п., развитых на продуктах изменения основных пород. Возможно, что здесь шамозит является новообразованным минералом.

Шамозит может иметь самое различное происхождение - хемогенно-осадочное, гипергенное, гидротермальное, метасоматическое.

Шамозит осадочного происхождения встречается в глинистых отложениях и в осадочных (оолитовых) железных рудах, формирующихся в прибрежных зонах морских бассейнов, преимущественно в условиях дефицита кислорода.

Гипергенный шамозит распространён в очень небольших количествах во многих почвах: тундровых, дерново-подзолистых, серых лесных, а также в латеритах и ферраллитных почвах, развитых на продуктах изменения [основных пород](#).

Вместе с тем, шамозиты являются характерными жильными минералами ряда гидротермальных месторождений, а также входят в состав околорудных метасоматитов.

Do – доломит, $\text{CaMg}(\text{CO}_3)_2$

Доломит — минерал из класса карбонатов химического состава $\text{CaCO}_3 \cdot \text{MgCO}_3$; доломитом называют также осадочную карбонатную горную породу, состоящую из минерала доломита на 95 % и более. Получил название в честь французского инженера и геолога Деода де Доломьё (1750—1801), описавшего признаки доломитовых пород.

Состав минерала близок к теоретическому. Кристаллы ромбоэдрические. Обычно массивные, от грубо- до тонкозернистых и фарфоровидных, агрегаты. Цвет — бесцветный или белый, желтоватый, буроватый (за счёт примеси гидроксидов железа и глинистых частиц). Блеск стеклянный до матового и перламутрового. Хрупкий. Спайность совершенная. Твёрдость 3,5-4,0. Излом ступенчатый до раковистого (в фарфоровидных агрегатах). Черта белая. С HCl реагирует слабо (однако бурно вскипает в горячей HCl). Вскипает под действием 1%-го раствора соляной кислоты в порошке (в царапине).

Отличить доломит от других карбонатов непросто. Более того, он часто ассоциируется с кальцитом, обладающим сходными диагностическими признаками, прежде всего ромбоэндрическим обликом кристаллов. В полевых условиях для определения этих минералов обычно используют соляную кислоту. Кусочек минерала размером со спичечную головку кладут на стекло и капают на него HCl . Кальцит бурно «вскипает» в холодной кислоте с выделением углекислого газа, тогда как доломит реагирует очень медленно, неохотно, а растворяется только при нагревании.

Сс – кальцит, CaCO_3

Кальцит, известковый шпат — минерал CaCO_3 из группы карбонатов, одна из природных форм карбоната кальция. Исключительно широко распространён на поверхности Земли, породообразующий минерал. Кальцитом сложены известняки, меловые породы, мергели, карбонатиты. Кальцит — самый распространённый биоминерал: он входит в состав раковин и эндоскелета большинства

скелетных беспозвоночных, а также покровных структур некоторых одноклеточных организмов.

Карбонат кальция имеет и другие полиморфные модификации — арагонит (ромбической сингонии) и фатерит (гексагональной сингонии).

Название предложено Гайдингером в 1845 году и происходит, как и название химического элемента, от лат. *calx* (род.п. *calcis*) — известь.

В чистом виде кальцит белый или бесцветный, прозрачный (исландский шпат) или просвечивающий, — в зависимости от степени совершенства кристаллической структуры. Примеси окрашивают его в разные цвета. Ниокрашивает в зелёный; кобальтовые, марганцевые кальциты — розовые. Тонкодисперсный пирит окрашивает в синеватый и зеленоватый цвет. Кальцит с примесью железа — желтоватый, буроватый, красно-коричневый; с примесью хлорита — зелёный. Угlistое вещество часто придает кальциту неравномерную чёрную окраску. Известны кристаллы с многочисленными включениями битуминозного вещества, они имеют жёлтый или бурый цвет.

Черта белая, плотность 2,6-2,8, излом ступенчатый, твёрдость по шкале Мооса 3, спайность совершенная по основному ромбоэдру, блеск стеклянный до перламутрового. Вскипает при взаимодействии с разбавленной соляной кислотой (HCl). Характерно многообразие двойников срастания и прорастания по многочисленным законам, а также деформационные двойники. Прозрачные кристаллы обладают двупреломлением света, особо хорошо наблюдаемым сквозь поверхности спайности в ромбоэдрических выколках или толстых пластинах.

Ап – анортит, $\text{CaAl}_2\text{Si}_2\text{O}_8$

Анортит (др.-греч. ἄνωρος — косо́й) — минерал из группы полевых шпатов (плагноклазов). По составу относится к алюмосиликатам со структурой каркасного типа.

Химическая формула чистого анортита: $\text{CaAl}_2\text{Si}_2\text{O}_8$, где CaO — 20,1 %, Al_2O_3 — 36,7%, SiO_2 — 43,2 %. Бесцветный или белый, серый, иногда желтоватый, красноватый. Блеск стеклянный, излом неровный. Прозрачный до полупрозрачного.

Твёрдость 6 — 6,5. Плотность 2,76 г/см³. Анортит образует в основном зернистые агрегаты. Кристаллы призматические, реже вытянуты. Образует сплошные зернистые массы.

Сингония триклинная. Характерный для основных интрузивных и эффузивных магматических пород. Находится вместе с магнезио-железистыми силикатами, а также в метеоритах. Используется в керамической промышленности.

Чистый анортит редок. Породообразующий минерал таких магматических пород, как базальт, габбро, норит; встречается в местах контактов магматических пород с известняками, в амфиболитах. Анортит встречается в Карелии, на Урале, на Украине. Является также одной из основных пород лунного реголита (Наряду, с пироксеном, оливином и ильменитом).

Ja – Ярозит, $KFe_3(SO_4)_2(OH)_6$

Ярозит (от названия местности Jaroso — Харосо в Испании, где впервые был найден ярозит) — минерал, основной сульфат калия и железа; химический состав: $KFe(III)_3(SO_4)_2(OH)_6$, зачастую содержит примеси натрия.

Твёрдость по шкале Мооса: 2,5 — 3,5 (гипс — кальцит), плотность: 2,9 — 3,3 г/см³. Кристаллизуется в тригональной (пирамидальной) системе. Ярозит встречается с прозрачностью от просвечивающего до полностью непрозрачного. Блеск стеклянный либо тусклый. Цвет — коричневый, жёлтый.

Очень часто ярозит путают с лимонитом, гётитом, с которыми он часто встречается в железных шляпах. По сути, ярозит — железосодержащий аналог алунита.

Минерал ярозит образует мелкие ромбоэдрические кристаллы; агрегаты тонкокристаллические, сплошные зернистые, реже землистые.

Охристо-жёлтый цвет; невысокая твердость; кристаллическое состояние; совершенная спайность; алмазный блеск на плоскостях спайности (яркие проблески в кристаллических агрегатах); жирный на ощупь; растворяется в HCl; сильный пирозлектрик.

Минерал ярозит встречается в ассоциации с алунитом, пиритом.

Минерал ярозит формируется в экзогенных условиях при начальных стадиях развития зон окисления сульфидных месторождений, возникает при окислении пирита. В поверхностных условиях неустойчив, гидратируется, переходя в гётит и гидрогётит. Сохранению ярозита благоприятствуют условия сухого жаркого климата.

Nn – Нонтронит, $(Na,Ca)_{0,3}Fe_2(Si,Al)_4O_{10}(OH)_2 \cdot H_2O$

Нонтронит (от назв. г. Нонтрон, Nontron во **Франции** — места первой находки " а. nontronite; н. Nontronit; ф. nontronite, graminite; и. nontronita) — **минерал** подкласса слоистых силикатов группы смектитов (монтмориллонита), $(\text{Fe}, \text{Mg})_2[\text{Si}_4\text{O}_{10}](\text{OH})_2 \cdot n\text{H}_2\text{O}$. Содержит изоморфные примеси Al, Mg, Ni, Co, Cu, Zn (до целых%). Сингония моноклинная. Кристаллическая структура слоистая. Встречается в виде землистых и **плотных** (опалоподобных) **агрегатов**, жирных на ощупь. Окраска зеленовато-жёлтая, оливковая, буроватая. Излом раковистый. **Твёрдость** 1-2. Плотность 1700-1900 кг/м³. Обладает высокой анион-катионной обменной (80-90 мг/экв. на 100 г) и сорбционной способностью, набухаемостью в присутствии **воды**. Образуется при **выветривании** серпентинитов. При дальнейшем выветривании замещается гидроксидами **железа**. Входит в состав **руд Ni**.

Im – ильменит, Fe(TiO₃)

Ильменит (титанистый железняк) — **минерал** общей химической формулы $\text{FeO} \cdot \text{TiO}_2$ или FeTiO_3 (36,8 % **Fe**, 31,6 % **O**, 31,6 % **Ti**), состав непостоянен. Редкий минерал, сложный оксид, внешне похожий на ильменит, называется «кричтонитом». Ильменит был впервые описан в 1827 году А.Т. Купффером.

Ильменит кристаллизуется в тригональной сингонии, образуя сложные ромбоэдрические или пластинчатые кристаллы, преимущественно искаженного облика. Агрегаты - зернистые массы и сплошные скопления. Непрозрачен; цвет черный с ярким металлическим блеском. Твёрдость 5-6; удельный вес 4,72. В чистом виде при обычной температуре ильменит немагнитен, что имеет важное значение при его промышленном извлечении. Кристаллы, содержащие более 25 % Fe_2O_3 в виде **твёрдого раствора**, магнитны. Ильменит и **титаномагнетит** являются ценной рудой для получения титана и его производных (оксида **титана**, **ферротитана** и других).

Крупные месторождения ильменита находятся в **России** на **Южном Урале**, где этот минерал был впервые открыт в **Ильменских горах**. Ильменит встречается во многих месторождениях **Норвегии**, **Швеции**, **Финляндии**, в рудах **Бушвельдского комплекса** в **ЮАР** и рудного района **Садбери** в **Канаде**, кроме того ильменитом богата **лунная почва**.

Qu - кварц, SiO₂

Кварц (нем. Quarz) — один из самых распространённых минералов в земной коре, породообразующий минерал большинства магматических и метаморфических пород. Свободное содержание в земной коре 12 %. Входит в состав других минералов в виде смесей и силикатов. В общей сложности массовая доля кварца в земной коре более 60 %. Химическая формула: SiO_2 (диоксид кремния).

Му – мусковит, $\text{KAl}_2(\text{AlSi}_3\text{O}_{10})(\text{OH})_2$

Мусковит — минерал, калиевая слюда $\text{KAl}_2(\text{AlSi}_3\text{O}_{10})(\text{OH})_2$. Используют в электро- и радиотехнике, для изготовления смотровых оконцев в котлах, печах и др. Кристаллы таблитчатые моноклинной системы. Спайность по базису весьма совершенная. Мусковит легко расщепляется на тончайшие листочки, что обуславливается его кристаллической структурой, сложенной 3-слойными пакетами из 2 листов кремне- и алюмоокислородных тетраэдров, соединённых через слой, составленный из октаэдров, в центре которых расположены ионы Al, окруженные 4 ионами кислорода и 2 группами OH; 1/3 октаэдров не заполнена ионами Al. Пакеты соединены между собой ионами калия.

Материал обладает очень высокими электрическими свойствами: Нагревостойкость 500—600 °C; Удельное объемное сопротивление 1012–1014 Ом/м; Тангенс угла потерь 0.0003; Относительная диэлектрическая проницаемость 6-8.

Ка - каолинит, $\text{Al}_2\text{Si}_2\text{O}_5(\text{OH})_4$

Каолинит — глинистый минерал из группы водных силикатов алюминия. Химический состав $\text{Al}_4[\text{Si}_4\text{O}_{10}](\text{OH})_8$; содержит 39,5 % Al_2O_3 , 46,5 % SiO_2 и 14 % H_2O . Образует землистые массы, в которых при больших увеличениях под электронным микроскопом обнаруживаются мелкие шестигранные кристаллы. Кристаллизуется в моноклинной сингонии. В основе кристаллической структуры каолинита лежат бесконечные листы из тетраэдров Si—O₄, имеющих три общих кислорода и связанных попарно через свободные вершины алюминием и гидроксидом. Эти листы соединены между собой слабыми связями, что обуславливает весьма совершенную спайность каолинита и возможность различного наложения одного слоя на другой, что, в свою очередь, ведёт к некоторому изменению симметрии всей кристаллической постройки.

Слоистая структура каолинита придаёт минералам на его основе (глинам и каолинам) свойство пластичности. Твёрдость по минералогической шкале 1; плотность

2540—2600 кг/м³; жирен на ощупь. При нагревании до 500—600 °С каолинит теряет воду, а при 1000—1200 °С разлагается с выделением тепла, давая вначале **силлиманит**, а затем **муллит**; реакция эта составляет основу керамического производства.

Каолинит — основной компонент многих **глин**. Образуется при **каолинизации** (выветривании и гидротермальном изменении полевошпатовых пород). Около 50 % от всего добываемого каолинита используется при производстве бумаги для мелования и в качестве наполнителя. В керамической промышленности он используется для создания **ангоба** и **глазури**. Каолинит также применяется в фармацевтике, в качестве **пищевой добавки**, в зубных пастах (в качестве лёгкого абразивного материала), в косметике (под названием «белая глина») и многих других областях.

Ог – ортоклаз, $K(AlSi_3)O_8$

Ортоклаз — широко распространённый **породообразующий минерал** из класса силикатов, одна из разновидностей полевых шпатов (калиевый **полевой шпат**). В состав ортоклаза входят **оксид калия** (K_2O) — 16,9 %, **оксид алюминия** (Al_2O_3) — 18,4 %, **диоксид кремния** (SiO_2) — 64,7 %, также часто присутствует несколько процентов оксида натрия (Na_2O). Может содержать **Изоморфные** примеси: Na, Ba, Rb, Fe^{2+} , Ca и др. Ортоклаз, как и другие кали-натриевые полевые шпаты, встречается главным образом в кислых, иногда в средних по кислотности изверженных породах.

Применяется как сырьё для производства фарфора и электрокерамики. Большого значения как ювелирный и поделочный материал не имеет. Прозрачные, бесцветные или жёлтые ортоклазы иногда подвергают огранке как любопытную **коллекционную редкость**.

Ка - каолинит, $Al_2Si_2O_5(OH)_4$

Каолинит — **глинистый минерал** из группы водных силикатов **алюминия**. Химический состав $Al_4[Si_4O_{10}](OH)_8$; содержит 39,5 % Al_2O_3 , 46,5 % SiO_2 и 14 % H_2O . Образуется землястые массы, в которых при больших увеличениях под электронным микроскопом обнаруживаются мелкие шестигранные кристаллы. Кристаллизуется в моноклинной сингонии. В основе кристаллической структуры каолинита лежат бесконечные листы из **тетраэдров** $Si—O_4$, имеющих три общих кислорода и связанных попарно через свободные вершины алюминием и гидроксидом. Эти листы соединены между собой слабыми связями, что обуславливает весьма совершенную спайность

каолинита и возможность различного наложения одного слоя на другой, что, в свою очередь, ведёт к некоторому изменению симметрии всей кристаллической постройки.

Слоистая структура каолинита придаёт минералам на его основе (глинам и каолинам) свойство пластичности. Твёрдость по минералогической шкале 1; плотность 2540—2600 кг/м³; жирен на ощупь. При нагревании до 500—600 °С каолинит теряет воду, а при 1000—1200 °С разлагается с выделением тепла, давая вначале силлиманит, а затем муллит; реакция эта составляет основу керамического производства.

Каолинит — основной компонент многих глин. Образуется при каолинизации (выветривании и гидротермальном изменении полевошпатовых пород). Около 50 % от всего добываемого каолинита используется при производстве бумаги для мелования и в качестве наполнителя. В керамической промышленности он используется для создания ангоба и глазури. Каолинит также применяется в фармацевтике, в качестве пищевой добавки, в зубных пастах (в качестве лёгкого абразивного материала), в косметике (под названием «белая глина») и многих других областях.

Py – пирит, FeS₂

Пирит – серный колчедан, железный колчедан — минерал, дисульфид железа химического состава FeS₂ (46,6 % Fe, 53,4 % S). Нередки примеси Co, Ni, As, Cu, Au, Se и др. Пирит кристаллизуется в кубической сингонии, образуя кубические, пентагондодекаэдрические (режеоктаэдрические) кристаллы; на гранях кристаллов характерна грубая штриховка, параллельная рёбрам куба. Но распространён преимущественно в виде сплошных масс, мелкозернистых агрегатов, прожилков, а в осадочных горных породах — желваков и стяжений различной формы. Цвет на свежем сколе светлый латунно-жёлтый до золотисто-жёлтого, со временем меняется до тёмно-жёлтого, часто с побежалостью, за счёт образования поверхностной окисной плёнки. Имеет металлический блеск. Обладает проводниковыми свойствами.

Твёрдость по шкале Мооса 6—6,5 (уменьшается при повышении содержания никеля); плотность 4,9—5,2 г/см³, теплопроводность = 47,8±2,4 Вт/(м К) при T=300 К; температура плавления 1177—1188 °С. Нерастворим в воде. Парамагнетик.

Пирит — один из самых распространённых в Земной коре сульфидов. Большие его залежи сосредоточены в месторождениях гидротермального происхождения, особенно в серноколчеданных залежах, осадочных метаморфических породах. В осадочных породах пирит образуется в закрытых морских бассейнах, подобных

Чёрному морю, в результате осаждения сероводорода. Кроме того, пирит в небольших количествах образуется при магматических процессах. Он часто образует псевдоморфозы по органическим остаткам (по древесине и различным остаткам организмов). На земной поверхности неустойчив, и со временем кристаллы пирита разрушаются, окисляясь до лимонита.

Gy – гипс, $\text{Ca}(\text{SO}_4)(\text{H}_2\text{O})_2$

Гипс — минерал из класса сульфатов, по составу $\text{CaSO}_4 \cdot 2\text{H}_2\text{O}$. Волокнистая разновидность гипса называется селенитом, а зернистая — алебастром. Блеск стеклянный или шелковистый (у волокнистых разновидностей), спайность весьма совершенная в одном направлении (расщепляется на тонкие пластинки). Цвет белый, серый, иногда красноватый, при наличии примесей имеет серую, желтоватую, розоватую, бурую окраску. Волокнистые разновидности дают занозистый излом. Черта белая. Система моноклинная. Плотность — 2,3 г/см³, твёрдость по шкале Мооса — 2. Текстура — массивная. Гипс является типичным осадочным минералом.

Ill – иллит, $(\text{K}_{0.71}\text{Ca}_{0.01}\text{Na}_{0.01})(\text{Al}_{1.86}\text{Mg}_{0.15}\text{Fe}_{0.04})(\text{Si}_{3.27}\text{Al}_{0.73})\text{O}_{10}(\text{OH})_2$

Иллит (синонимы: гидромусковит, монотермит, грундит, гешвитцит) — минерал из группы гидрослюд структурного типа листовые силикаты класса Силикаты. В большинстве случаев иллит — продукт частичного гидролиза мусковита, в ряде случаев при этом появляются смешанно слойные иллит-мусковитовые образования, к которым в большинстве случаев и применяется название гидромусковит. В некоторых случаях — продукт изменения при превращении полевых шпатов в каолинит. Выделяется в чешуйчатых и тонкопластинчатых белых массах, жирных на ощупь, в составе глин, обычно в смеси с каолинитом и другими минералами, часто в почвах.

Эмпирическая формула: $(\text{K}_{0.75}(\text{H}_3\text{O})_{0.25})\text{Al}_2(\text{Si}_3\text{Al})\text{O}_{10}((\text{H}_2\text{O})_{0.75}(\text{OH})_{0.25})_2$; цвет — белый, бледно-желтый, бледно-зеленый; блеск — перламутровый; спайность — очень слабая; сингония — моноклинная; твердость — 1-2 (шкала Мооса). Наряду с каолинитом, используется в производстве керамогранита, придавая смесям повышенную пластичность.

Kh – клинохлор, $(\text{Mg,Fe,Al})_6(\text{Si,Al})_4\text{O}_{10}(\text{OH})_8$

(или $\text{Mg}_{4.54}\text{Al}_{0.97}\text{Fe}_{0.46}\text{Mn}_{0.03}(\text{Si}_{2.85}\text{Al}_{1.15}\text{O}_{10})(\text{OH})_8$)

Клинохлор - минерал, листовой алюмосиликат железа и магния, наиболее распространённый член группы хлоритов. Образует серию твёрдых растворов со своим железистым аналогом шамозитом. Цвет клинохлора изменяется от травяно-зелёного до бледного оливково-зелёного, жёлтого, иногда белого (лейхтенбергит) с сероватым, розовым, фиолетовым (у хромсодержащих разновидностей) и другими оттенками. В тонких листочках прозрачный или просвечивает. Блеск на плоскостях спайности перламутровый. Маложелезистая бесцветная разновидность называется лейхтенбергитом, а с примесью хрома - кочубеитом (фиолетово-розовый). Под п. тр. не плавится. Полностью разлагается только в концентрированной серной кислоте. **Метаморфический** минерал в сланцах и мраморах, как гидротермальный минерал в кварцевых жилах и жилах альпийского типа. Характерный продукт гидротермального изменения амфиболов, пироксенов и биотита. **Породообразующий** минерал хлоритовых сланцев. Встречается в различных метаморфических породах, возникая за счёт изменения пироксенов, амфиболов, гранатов, магнезиально-железистых слюд. Также в контактово-метасоматических породах -скарнах и в изменённых зальбандах и боковых породах гидротермальных жил.

Ab – альбит, $(\text{Na,Ca})\text{Al}(\text{Si,Al})_3\text{O}_8$

Альбит — один из наиболее распространенных породообразующих минералов, белый натриевый полевой шпат магматического происхождения класса силикатов, алюмосиликат группы плагиоклазов. Альбит с иризацией, серо-голубого, сине-голубого или бледно-фиолетового цвета на плоскостях назван беломоритом. Также он называется перистеритом (от Перистерии). Кристаллы таблитчатые, встречаются сдвойникованные кристаллы, полисинтетические двойники. Состав (%): Na_2O — 11,67; Al_2O_3 — 19,35; SiO_2 — 68,44. Примеси: K, Ca, Rb, Cs. Плавится с трудом, слабо растворим в кислотах. Образование часто связано с метасоматическими процессами. Агрегаты плотные, лучистые, в форме зёрен.

Используют в керамическом производстве. Для украшений чаще используются образцы с оптическим эффектом иризации, которые обычно обрабатываются шлифовкой в форме плоских кабошонов. В научных исследованиях применяется для определения степени метаморфизма. Популярный коллекционный камень.

Ph – филлипсит, $\text{Ca}_{1,64}\text{K}_2\text{Si}_{10,67}\text{Al}_{5,33}\text{O}_{32}(\text{H}_2\text{O})_{12}$

Филлипсит — минерал, каркасный силикат из группы цеолитов. Филлипсит, как и большинство других цеолитов, имеет достаточно сложный химический состав. Встречается в виде одиночных призматических кристаллов, а также их сростков, часто крестообразных. Образуется преимущественно в трещинах эффузивных пород из постмагматических термальных растворов, а также за счёт изменения палагонита в условиях медленного осадконакопления.

Типичное местонахождение этого минерала - миндалины в базальтах, где его и обнаруживают иногда совместно с шабазитом. Встречается также в пустотах других изверженных пород и некоторых осадочных породах в виде одиночных призматических кристаллов, а также их сростков, часто крестообразных. Чистый филлипсит бесцветен, но может быть окрашен примесями в светло-серые или желтовато-серые оттенки. Блеск стеклянный. Кристаллы филлипсита прозрачные, полупрозрачные или просвечивающие.

Mu – мусковит, $KAl_2(AlSi_3O_{10})(OH)_2$

Мусковит — минерал, калиевая слюда $KAl_2(AlSi_3O_{10})(OH)_2$. Используют в электро- и радиотехнике, для изготовления смотровых оконцев в котлах, печах и др. Кристаллы таблитчатые моноклинной системы. Спайность по базису весьма совершенная. Мусковит легко расщепляется на тончайшие листочки, что обуславливается его кристаллической структурой, сложенной 3-слойными пакетами из 2 листов кремне- и алюмоокислородных тетраэдров, соединённых через слой, составленный из октаэдров, в центре которых расположены ионы Al, окруженные 4 ионами кислорода и 2 группами OH; 1/3 октаэдров не заполнена ионами Al. Пакеты соединены между собой ионами калия.

Материал обладает очень высокими электрическими свойствами: Нагревостойкость 500—600 °C; Удельное объемное сопротивление 10¹²–10¹⁴ Ом/м; Тангенс угла потерь 0.0003; Относительная диэлектрическая проницаемость 6-8.

6. ПОЛУЧЕНИЕ НАКОПИТЕЛЬНЫХ КУЛЬТУР ИЗ ОБРАЗЦОВ ПРОБ

(ENRICHMENT CULTURES FROM SAMPLES)

Название пробы	Дата Посева	Дата начала роста	Условия культивирования	Результаты микроскопирования
ШГ14-1	19.08.2014	08.09.2014	Ср.Виddeля+фруктоза рН(среды)=2,3	В поле зрения 20-25 клеток. Из них примерно 90% подвижные палочки, а 10% крупные палочки со спорой. Кроме того, встречаются единичные слегка изогнутые палочки



Norges geologiske undersøkelse
Postboks 6315, Sluppen
7491 Trondheim, Norge

Besøksadresse
Leiv Eirikssons vei 39, 7040 Trondheim

Telefon 73 90 40 00
Telefax 73 92 16 20
E-post ngu@ngu.no
Nettside www.ngu.no

*Geological Survey of Norway
PO Box 6315, Sluppen
7491 Trondheim, Norway*

*Visitor address
Leiv Eirikssons vei 39, 7040 Trondheim*

*Tel (+ 47) 73 90 40 00
Fax (+ 47) 73 92 16 20
E-mail ngu@ngu.no
Web www.ngu.no/en-gb/*